Neuronal Protection by a Novel C-terminal Hsp90 Modulator

Heather Menchen

Submitted to the graduate degree program in Pharmacology and Toxicology and the Graduate Faculty of the University of Kansas in partial fulfillment of the requirements for the degree of Doctor of Philosophy.

_____
Chairperson: Dr. Mary Lou Michaelis

_____
Dr. Elias Michaelis

_____
Dr. ShiDu Yan

_____
Dr. Rick Dobrowsky

_____
Dr. Brian Blagg

Date Defended: June 28, 2012

The Dissertation Committee for Heather Menchen
certifies that this is the approved version of the following dissertation:

Neuronal Protection by a Novel C-terminal Hsp90 Modulator

_____
Chairperson Dr. Mary Lou Michaelis

Date approved: June 28, 2012

ABSTRACT

Alzheimer's disease (AD), like most neurodegenerative disorders, is characterized by accumulation of misfolded and aggregated proteins, indicating that the protein quality control machinery is compromised. Enhancing the activity of molecular chaperones such as the 'heat shock' proteins (Hsp's) that re-fold or signal degradation of damaged proteins may help remove protein oligomers/aggregates and prevent cell death. The goal of our studies was to characterize a novel, non-toxic Hsp90 modulator, KU-32, which protects primary cortical neurons against $A\beta_{1-42}$, a toxic peptide found in AD brain. Pharmacokinetic studies indicated that KU-32 is blood brain barrier permeable and orally bioavailable. Using two AD mouse models, JNPL3 and rTg4510, which both contain the P301L *Tau* mutation and develop aberrant *Tau* tangles as well as cognitive impairments, we assessed KU-32 treatment *in vivo*. The JNPL3 mice were treated with 20 mg/kg of KU-32 or with 12.5% Captisol® (vehicle) five times a week for six months. Immunohistochemical studies indicated significant decreases of hyperphosphorylated Tau in the cortical region. The rTg4510 mice were treated with 60 mg/kg of KU-32 or with vehicle (5% Captisol®) twice a week for 10 weeks. Immunofluorescent analyses demonstrated significant protection against dendritic pathology and neuronal death in KU-32-treated *vs* vehicle-treated rTg4510 mice. Further studies were conducted to examine the potential mechanisms of drug action. We hypothesized that KU-32 activated the heat shock response leading to an increase in molecular chaperones involved in protein quality control such as Hsp70. Our data suggest that KU-32 is not acting through this mechanism, and further studies are

needed to elucidate the mechanism. Overall, our *in vivo* results suggest that the novel Hsp90 modulator, KU-32, may have therapeutic potential for treatment of AD.

ACKNOWLEDGEMENTS

First and foremost, I would like to thank Dr. Mary Lou Michaelis for her guidance throughout my graduate career. She has been an understanding and supportive mentor, from whom I have learned more that I ever thought I could. I would also like to thank Dr. Elias Michaelis for his constant support and guidance. The remaining members of my committee: Drs. Rick Dobrowsky; ShiDu Yan; and Brian Blagg, thank you for your help and suggestions. Thank you to the NIH for the support from the U01 grant, AG-031106, and Barbara Johnson Bishop for the Johnson-Bishop Scholarship.

The “lab ladies” have made my graduate experience as easy and wonderful as possible. I have been lucky to work with such a strong, intelligent, and supportive group of women. Jennifer Bean, thanks for all of the cell preps and your ears during stressful times. Dr. Lei Jiang, you have been extremely influential in my experimental development, as well as the respect I have gained in myself as a scientist. Misty Bechtel, for your constant support, help, and gels! Cynthia Leary, for being there for me when I needed someone most, and never letting me give up.

To the members of Dr. Elias Michaelis’s lab: Drs. Ranu Pal, Dongwei Hui, Xinkun Wang and Abdul Baki Agbas. Ranu took me under her wing when I first started in the lab, and helped me develop important immunofluorescent techniques. Dongwei taught me everything I know about molecular biology, and transfections. Xinkun performed the microarray analysis, and helped analyze the data. Baki helped me with dissections, as well as how important it is to respect your neighbor. Finally, Laura Anguiano, I cannot thank you enough for just being you, and being my friend.

Graduate school would not have been possible without the help and support from the graduate students. Thank you all so much for listening, and letting me listen. I have learned a lot from you all. I wish you the best of luck in your future endeavors.

Finally, I would like to thank my parents George and Robin Menchen, as well as my sister and brother-in-law, Megan and Nick Tiesmann. None of this would have been possible without their guidance and support. To my friends, Dr. Derek Oien, Chanel Li, Jade Franklin, and Liang Zhang, thanks! Last, but not least, Jesse Allen for accepting my craziness and loving me for it.

TABLE OF CONTENTS

List of Tables and Figures

CHAPTER ONE: Novel Modulators of Hsp90 as a Therapeutic Approach for Alzheimer's Disease

1. PATHOLOGICAL CHARACTERISTICS OF NEURODEGENERATIVE DISEASES

Most neurodegenerative disorders are characterized by the accumulation of aggregated proteins. These aberrant proteins manifest in areas of the brain that regulate cognitive and motor functions. The deposition of these 'misfolded' proteins is cytotoxic, causing improper cell function and ultimately death. Some of these diseases include: Huntington's disease (HD) with mutant huntingtin; Parkinson's disease (PD) with accumulated α-synuclein; amyotropic lateral sclerosis (ALS) containing mutant superoxide dismutase-1 (SOD1) and TAR DNA-binding protein-43 (TDP-43) deposits; and spinal and bulbar muscular atrophy (SBMA) with mutant androgen receptor aggregates (Muchowski and Wacker, 2005).

The most common age-related dementia, Alzheimer's disease (AD), is characterized by the development of lesions made of two misfolded protein aggregates; senile plaques (SPs) comprised of the β-amyloid peptide and neurofibrillary tangles (NFTs) made up of hyperphosphorylated Tau, a microtubule stabilizing protein. These lesions are deposited in cortical and limbic regions of the brain leading to devastating cognitive and memory impairments. Although AD has been studied extensively, promising therapeutic candidates that slow progression of the disease and ameliorate these toxic aggregates are proving difficult to develop.

Prevalence of Alzheimer's Disease (AD)

Presently, AD is the sixth leading cause of death in the United States with an estimated 5.4 million individuals living with the disease in 2012 (Alzheimer's, 2012). One in eight people over the age of 65 have AD (5.2 million) (Hebert et al., 2003). As the baby boomer generation ages, the proportion of individuals over 65 with AD is expected to rapidly increase. In this particular population, more women than men have AD. Approximately, 3.4 of the 5.2 million people over age 65 with AD are women while 1.8 million are men (Seshandri et al., 1997). This difference is attributed to the fact that women live longer than men (Hebert et al., 2001). However, as individuals age the likelihood of developing AD is much greater with an estimated 46% of people over 85 living with AD (Hebert et al., 2003).

The development of AD in an aging population places a tremendous burden on caregivers. It is estimated that 80% of caregivers are unpaid, and provide care in their homes, at the expense of their careers, income, and emotional state (Institutes of Medicine, 2008). In 2011, the unpaid hours provided by an AD caregiver was estimated at $17.4 billion. Healthcare costs attributed to AD are expected to be about $200 billion in 2012 (Alzheimer's Association, 2012).

Sadly, the diagnosis of AD is difficult, though new strategies are becoming available. Most individuals are diagnosed when symptoms develop, which occurs relatively late in disease progression. Many of the earliest, sometimes neglected symptoms include: difficulty remembering names, places, or recent events. Individuals with AD become apathetic or depressed. As the disease advances people begin to have motor problems such as difficulty swallowing, walking, or speaking. Prominent

behavioral changes are accompanied by disorientation, confusion, and impaired judgment (Alzheimer's Association, 2012). AD progression is insidious, and the disease ultimately leads to death.

Although AD is difficult to detect, there have been significant strides in developing better diagnostic tools. First, is the development of clinical diagnosis criteria including the DSM IV Clinical Criteria and the NINDS ADRDA Criteria. Individuals with cognitive decline are given various memory and physiological tests. The results of these tests determine which level of cognitive decline the patient is currently exhibiting (Psychiatric Association, 2000, Dubois et al., 2007). The physiological tests given include PET scans to measure neuronal metabolism (Mosconi et al., 2008), MRI scans to determine brain atrophy (Jack et al., 2000), Pittsburgh Compound-B (PIB) which labels amyloid aggregates in the brain (Mathis et al., 2008), and cerebral spinal fluid (CSF) measurements of phosphorylated Tau and Aβ peptides (Andreasen et al., 2001, Reimenschneider et al., 2001). These tests help positively diagnose individuals with mild to moderate AD as well as distinguish AD from other misfolded protein diseases; however there are still many patients with early cognitive impairments that are overlooked (Gabriela-Fita et al., 2001). Even though these breakthroughs in the diagnosis of AD have improved overall detection in humans, a more accurate measure is still desired.

Pathological Characteristics of AD

The amyloid plaques and neurofibrillary tangles were first described in 1907 by the German neuropathologist Alois Alzheimer. He discovered the lesions after

performing silver staining on brain tissue from his patient, Auguste Deter, who died at age 51 with severe memory and cognitive dysfunctions. Before this discovery by Alzheimer, doctors and non-scientific members of the community thought dementia was an inherent part of aging. The implications of this discovery were not appreciated until nearly 100 years later. This concept that there was a neuropathological phenotype associated with dementia, led to an explosion of scientific research dedicated to determining the origins of the lesions and their characteristics. This disease was named for the neuropathologist who discovered it, i.e. Alzheimer (Selkoe, 2001).

In 1984, Glenner and Wong isolated the amyloid peptide from the plaques in the brains of patients with Alzheimer-like dementia. The peptide was sequenced and further studies determined that this 40 to 42 amino acid peptide was the main component of SPs (Masters et al., 1985, Miller et al., 1993). It was not until 1986 that the protein in NFTs was characterized and revealed as the microtubule associated protein Tau (Grundke-Iqbal et al., 1986a). Since the discovery of the composition of the pathological proteins associated with AD, there has been a plethora of scientific research undertaken to elucidate the causes of the disease in hopes of developing interventions to stop disease progress. Unfortunately, two problems still remain; the complexity of AD diagnosis, and the lack of promising disease-reversal therapeutics.

Genetic Causes and Risk Factors for AD

Many risk factors are associated with AD although the exact cause of the majority of cases remains unknown. AD presents itself in three different forms: early onset FAD, late-onset familial Alzheimer's dementia, familial AD (FAD), and a sporadic

late-onset, nonhereditary form. Sporadic, late onset AD is the most common, and represents about 95% of AD patients (Alzheimer's Association, 2012).

Early onset FAD is associated with mutations in three different genes: amyloid precursor protein (APP) on chromosome 21, Presenilin 1 (PSEN1) on chromosome 14, and Presenilin 2 (PSEN2) on chromosome 1. PSEN1 mutations are the predominant genetic determinants of FAD; however, taken together the PSEN1 and PSEN2 mutations are responsible for about 90% of FAD mutations (Ho and Shen, 2011). Late onset, FAD is linked with apolipoprotein 4 (APOE4), and represents susceptibility more than a genetic determinant. Sporadic AD has multiple environmental causes with aging being the greatest risk factor. In the next set of subsections, the different forms of AD will be discussed in greater detail.

Early onset FAD

Amyloid precursor protein (APP) is a transmembrane protein and, although its role in AD has been well characterized, the normal biological function of this protein is not well understood. A group of enzymes called secretases are responsible for processing APP. The enzymes within this group are designated as α, β, and γ-secretases.

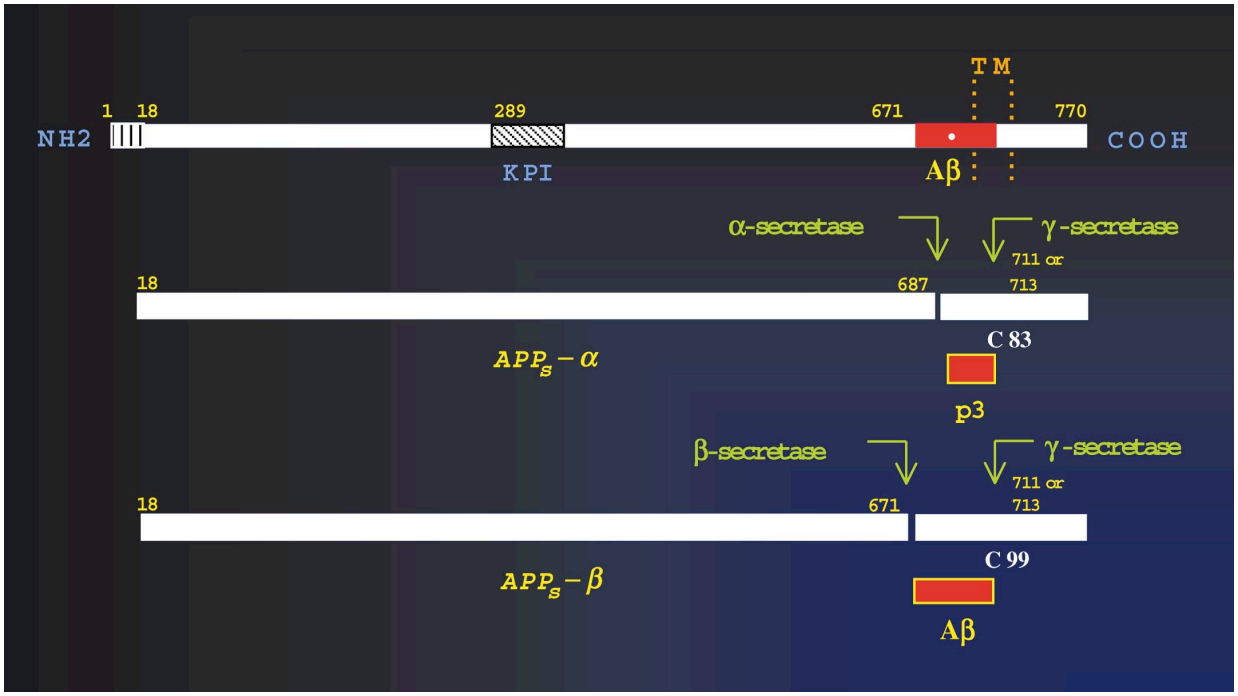

'with permission' Selkoe, DJ. (2001). Alzheimer's Disease: Genes, Proteins, and Therapy. *Physiological Reviews, 81*(2), 741-766

Figure 1.1: Proteolytic processing of APP.
Amyloid precursor protein (APP) exists as an integral membrane protein in neurons. Full length APP is drawn at the top of the schematic, which consists of 770 amino acids. Three enzymes cleave APP: α-,β-, and γ-secretases. The second APP illustration in the schematic demonstrates subsequent cleavage by α- and γ-secretase, which produces sAPPα and a soluble fragment termed p3. This pathway is called the non-amyloidogenic pathway. The third APP representation shows cleavage by β- and γ-secretase, which generates sAPPβ and a 40 to 42 amino acid peptide called Aβ. This pathway is referred to as the amyloidogenic pathway as it produces the toxic Aβ peptides that aggregate into senile plaques (SPs).

As demonstrated in Figure 1.1, proteolytic processing of APP by the secretases can occur through two different pathways, the non-amyloidogenic or the amyloidogenic pathway. The non-amyloidogenic pathway begins with α-secretase. This enzyme cuts within the Aβ sequence, thereby preventing the formation of toxic Aβ peptides. Cleavage by α-secretase produces a soluble form of APP (sAPPα) that can be released and a C-terminal fragment (C83) that retains association with the membrane. This C-terminal fragment is further processed by γ-secretase that generates a soluble fragment called p3 (Haass et al., 1992, Haass et al., 1993).

The amyloidogenic pathway involves APP cleavage by both β- and γ-secretases. First, β-secretase cuts APP outside the Aβ sequence. Proteolysis results in a soluble fragment called sAPPβ, and a C-terminal fragment (C99) that stays within the membrane (Marlow et al., 2003). The C-terminal fragment produced by β cleavage, is then processed by the enzyme γ-secretase. When γ-secretase cleavage of C99 occurs, the product is toxic Aβ peptides ranging from 39 to 43 amino acids in sequence (Yu et al., 2001). The most abundant, less toxic form is $A\beta_{1-40}$, which represents about 80-90% of the amyloid-β peptides, and the longer form $A\beta_{1-42}$ is only about 10% of the secreted peptides. However, the longer $A\beta_{1-42}$ variant is the main component of senile plaques associated with AD (Jarrett et al., 1993). Mutations within the APP determine whether the amyloidogenic or non-amyloidogenic pathway is followed. For example, the APP Swedish mutation stimulates more β-secretase processing of APP leading to greater production of toxic Aβ peptides (Sinha et al., 1999).

As mentioned previously, early onset FAD is also caused by mutations in the presenilin proteins. Presenilin is one of four transmembrane proteins that comprise the γ-secretase complex (Figure 1.2). These proteins play an important functional role in γ-secretase activity as well as in biological functions outside the complex (De Strooper et al., 2012).

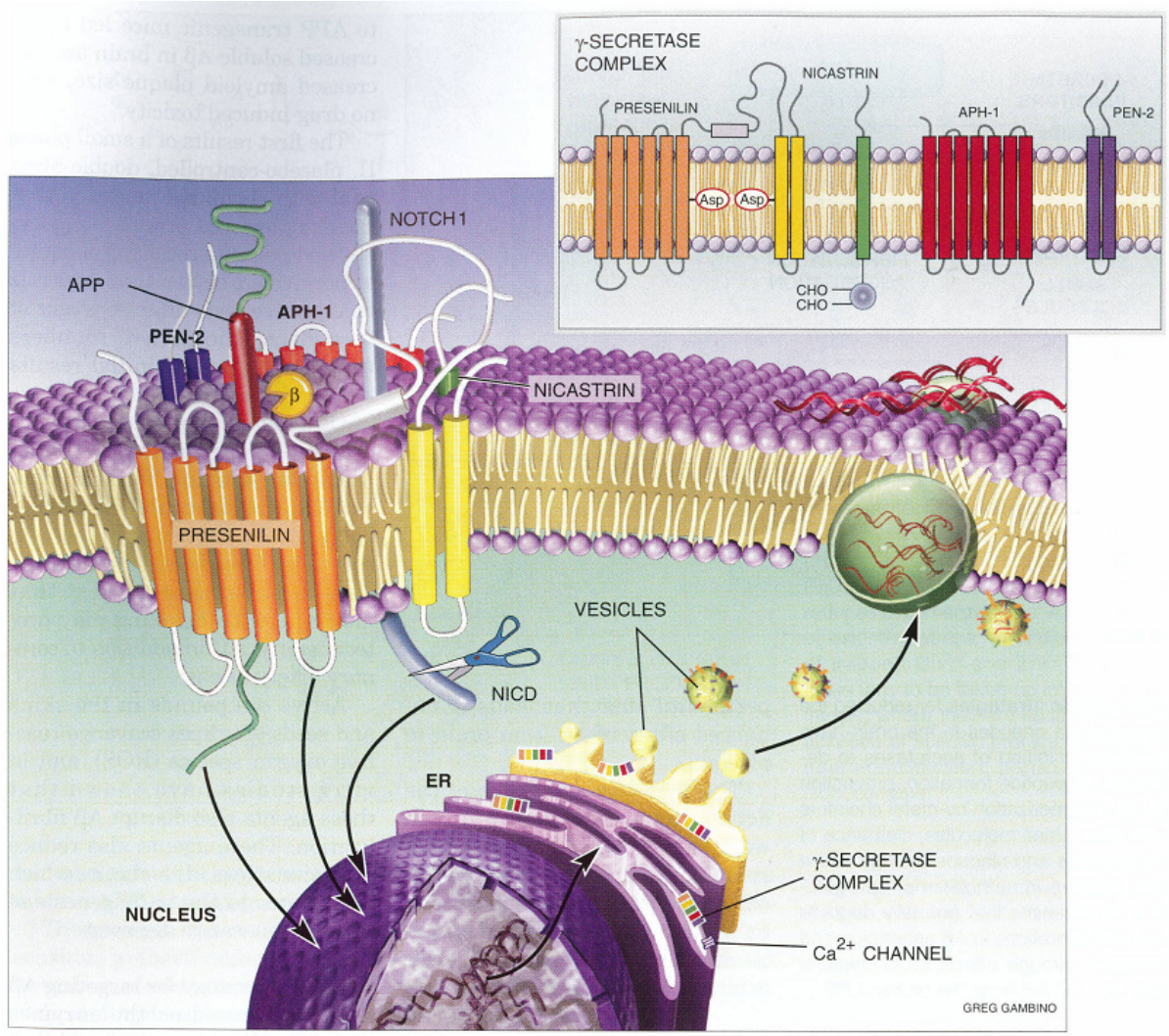

Michaelis, ML. (2003). Drug discovery and neuronal degeneration in Alzheimer's disease. *Science and Medicine, 9*(4), 214-223.

Figure 1.2: The γ-secretase complex. This complex is comprised of four proteins: Presenilin 1 (PSEN1); nicastrin; APH-1; and PEN-2. These proteins function together in order to cleave APP and Notch1. The Notch intracellular domain (NICD), which is formed by Notch1 cleavage, translocates to the nucleus and regulates transcription of genes important in synaptic plasticity.

It has been elucidated that the presenilins have critical, functional connections with γ-secretase activity. De Strooper and colleagues discovered that PSEN1 was crucially involved in the production of Aβ (De Strooper et al., 1998). It has been suggested that presenilin is a protease (Li et al., 2000), and essentially the catalytic subunit of γ-secretase (Wolfe et al., 1999). Presenilins also direct the γ-secretase

cleavage of a protein involved in embryogenesis and development called Notch (De Strooper et al., 1999). Before this discovery, γ-secretase inhibitors were thought to be a promising potential AD therapeutic, but inhibition of the enzyme led to a decrease in APP processing as well as blocked the cleavage of Notch. Therefore, use of these inhibitors as a therapeutic intervention would lead to detrimental side effects in AD patients.

Late onset FAD

Late onset FAD is more closely linked to the apolipoprotein E (APOE) gene on chromosome 19. APOE is a glycoprotein that exists in three different isoforms: E2, E3, and E4, separated by single amino acid substitutions. Alleles, ε2, ε3, and ε4 that code for these isomers are present within the general population (Cedazo-Menguez and Cowburn, 2001). Each person has 2 of the 3 possible alleles. Prevalence rates for these alleles differ where 7% to 8% of individuals have the ε2 allele, 75% to 80% have the ε3 allele, and 14% to 15% have the ε4 allele (Zannis et al., 1993). It has been demonstrated that heterozygous or homozygous expression of the ε4 allele leads to problems with membrane repair, steroid homeostasis, as well as the promotion of activities that lead to β-amyloid aggregation in AD brain (Schipper, 2011).

Some researchers believe this genetic defect is more akin to susceptibility for AD than genetic determination. Regardless, others believe as the population ages, people with symptoms of dementia should undergo genetic screening for presence of the APOE ε4 allele. The likelihood of developing AD markedly increases with the expression of one or both copies of the ε4 allele (Hsiung and Sadovnick, 2007). The

lifetime risk of developing AD may increase from 9% in an ε4-negative individual to 29% for carriers of a single ε4 allele (Seshandri et al., 1995). Also, the presence of an ε4 allele may hasten the appearance of AD symptoms by one to two decades when compared with non-carriers of the ε4 allele (Corder et al., 1993).

Sporadic, late onset AD

Although research has uncovered genetic mutations causing AD, much less progress has been made in identifying the factors that cause sporadic, late-onset AD. Most of the factors linked to sporadic AD are environmental, and "modifiable," meaning one can prevent AD development by controlling certain aspects of his/her life. For instance, there is an association between AD and cardiovascular disease. The causes of cardiovascular disease are physical inactivity, diabetes, smoking, obesity, and high cholesterol (Kivipelto et al., 2005, Hendrie et al., 2006, Anstey et al., 2007, Yaffe, 2007, Whitmer et al., 2008, Wu et al., 2008, Pendlebury and Rothwell, 2009, Solomon et al., 2009, Raji et al., 2010, Rusanen et al., 2010, Yaffe et al., 2011). Therefore, one can decrease the likelihood of developing AD by changing daily habits such as increasing physical activity to improve cardiovascular health.

Individuals that have experienced traumatic brain injury, head injury, and/or head trauma have demonstrated an increased risk for developing AD. Reports have shown that people with moderate head injuries have double the risk of developing AD, while patients experiencing severe head trauma are 4.5 times more likely to develop AD than non-head injury individuals. Moderate head injury is classified as a loss of consciousness for about 30 minutes, and severe is when the loss of consciousness

lasts 24 hours or more (Lye and Shores, 2000, Plassman et al., 2000). People with careers in which repeated head injuries are common such as boxers, football players, and combat veterans have an increased risk of developing dementia, and have a greater chance of late-life cognitive impairments, as brains from a number of these individuals present post-mortem Tau tangles (Roberts et al., 1990, Groswasser et al., 2002, Guskiewicz, 2005).

Reports have also revealed that remaining mentally and socially active later in life (Hall et al., 2009) as well as eating a diet low in saturated fats may promote brain health (Polidori et al., 2009). Unfortunately, there are not many studies that strongly support these conclusions, and the current investigations involve a small number of participants. In the end, the greatest risk factor for AD is advancing age (Alzheimer's Association, 2012).

Taken as a whole, the risk factors leading to AD are multi-faceted. Familial forms due to genetics are involved in AD development, as well as non-genetic associations. The realization that there are many causes of AD has made the discovery and development of therapeutic interventions extremely challenging.

Current Treatments for AD

Currently, there are no therapeutic agents available that slow or reverse the progression of neurodegeneration in AD. Available therapeutics only help to alleviate symptoms or maintain brain function for a short time before the inevitable cognitive decline. At this time, there are five FDA-approved drugs on the market available for AD

patients. These drugs can be classified into two categories, the cholinesterase modifiers and the glutamate antagonists.

The first class of drugs, the cholinergic system modifiers, include 4 of the 5 FDA approved AD therapeutics (Health, 2010). One of the most well known is the cholinesterase inhibitor Aricept (donepizel). As cholinergic neurons degenerate throughout AD progression, there is a loss of cholinergic activity. The cholinesterase inhibitors prevent degradation of acetylcholine by the enzyme acetylcholinesterase, which is thought to help cholinergic activity by increasing the concentration of synaptic acetylcholine, thereby making more neurotransmitter available to activate cholinergic receptors. This class of inhibitors helps delay the loss of cognition, but it does not stop the neurons from degenerating. After an average of 6 to 12 months of treatment, the cholinergic neuronal loss progresses to a point at which the cholinesterase inhibitors are no longer effective (Alzheimer's, 2011).

A second class of FDA-approved AD therapeutics is the glutamate antagonists. This class only contains one drug, Namenda (memantine). Namenda binds to glutamatergic NMDA receptors, and prevents their activation. It has been demonstrated that overactivity of the glutamatergic system in AD brain leads to neuronal damage. This drug reduces the activity of this system, which decreases the potential for neuronal loss. At this time, Namenda is available to treat patients with moderate to severe AD symptoms (Health, 2010).

Currently, there is a wide array of novel therapeutics involved in clinical trials for AD treatment. At this time, there are over 90 drugs undergoing clinical testing as potential AD therapeutics (Health, 2009). Most have been unsuccessful at various

points in the clinical trial process. For example, passive immunotherapeutics targeted to Aβ plaques demonstrated clearance of the peptides; however, 6% of the clinical trial participants developed sterile meningoencephalitis, which terminated the clinical trial (Orgogozo et al., 2003). Later monoclonal antibodies raised against Aβ plaques, like bapineuzumab, demonstrated decreases in Aβ plaques in the brain, although no cognitive improvements were exhibited (Rinne et al., 2010).

Other drugs, which target Tau aggregates such as Rember, have also been investigated for therapeutic potential. This compound is a methylene blue derivative that has been proposed as an inhibitor of Tau aggregation (Atamna et al., 2008). Preliminary results from a Phase IIB clinical trial in the United Kingdom and Singapore demonstrate that Rember slowed AD progression by about 81% while patients given the placebo experienced cognitive decline. A phase III clinical trial began in 2009, but the results from this study are not yet available (Bulic et al., 2008).

Since the drug treatments described above have had little to no success in truly modifying the disease process, there is still a need to find some other means of targeting the pathology and ultimate degeneration of neurons. Interestingly, promising targets have been found in currently FDA approved therapeutics for cancer. For example, the N-terminal Hsp90 ATPase inhibitors, like geldanamycin (GA), have demonstrated promise in mouse models of AD, in which decreases in Tau aggregates were observed (Dou et al., 2003a, Luo et al., 2007). More recently a group from Case Western Reserve University School of Medicine discovered that an FDA approved drug for skin cancer, bexarotene, led to the clearance of 50% of Aβ plaques from a mouse model of AD in 72 hours (Cramer et al., 2012). The mechanisms of these potential

therapeutics improve overall cellular function by targeting systems that lead to AD pathology development. The compounds stimulate cellular activities such as the protein quality control machinery, as opposed to focusing specifically on removing the characteristic protein aggregates associated with AD. Therefore, focusing on developing therapeutics that enhance cellular activities may prove to be better AD treatments.

2. TAU PATHOLOGY IN NEURODEGENERATION

As discussed earlier, neurodegeneration is caused by the accumulation of aberrant, misfolded proteins in or around neurons leading to synaptic dysfunction and subsequent cell death. There are several neurodegenerative diseases, each characterized by aggregates of a specific protein. For example, mutant huntingtin is the protein that accumulates in Huntington's disease (HD), alpha-synuclein in Parkinson's disease (PD), amyotrophic lateral sclerosis (ALS) is due to accumulation of misfolded SOD1 and TDP-43, and prion protein aggregates are present in prion diseases. Interestingly, the most common form of dementia, Alzheimer's disease is characterized by two proteinaceous hallmarks: senile plaques (SPs) comprised of amyloid-β and neurofibrillary tangles (NFTs) produced by aggregation of Tau protein. Most efforts for AD therapy have focused on Aβ rather than Tau, but recently Tau has gained much attention as a target, even though Tau is not mutated in AD.

Physiological Function of Tau

The microtubule-associated protein, Tau, is believed to be highly soluble, unstructured, heat stable, and hydrophilic (Barghorn and Mandelkow, 2002). In mammalian brains, the major physiological function of the Tau protein is to promote assembly and stability of microtubules (Weingarten et al., 1975). Tau binding to microtubules is dynamic, i.e., equilibrium is maintained between Tau bound to microtubules and Tau dissociated from microtubules. This equilibrium is controlled by the degree of Tau phosphorylation (Lindwall and Cole, 1984, Alonso et al., 1994, Iqbal et al., 1994, Khatoon et al., 1995). It has been suggested that this dynamic relationship may be essential for proper axonal transport (Ballatore et al., 2007).

Multiple post-translational modifications occur on different epitopes throughout the Tau protein. As mentioned earlier, Tau binding to microtubules is controlled by phosphorylation, which occurs on serine/threonine residues and is directed to proline containing regions (Mazanetz and Fischer, 2007). Other post-translational modifications such as glycosylation are thought to have an effect on Tau binding to microtubules (Arnold et al., 1996, Liu et al., 2004, Li et al., 2006), but phosphorylation is the most prominent mechanism (Mazanetz and Fischer, 2007). Tau can have other post-translational modifications such as ubiquitination (Cripps et al., 2006), nitration (Mailliot et al., 2002), sumoylation (Dorval and Fraser, 2006, 2007), and glycation (Münch et al., 2002). However, the role of these modifications in physiological Tau regulation or development of pathological forms of Tau have not been well characterized.

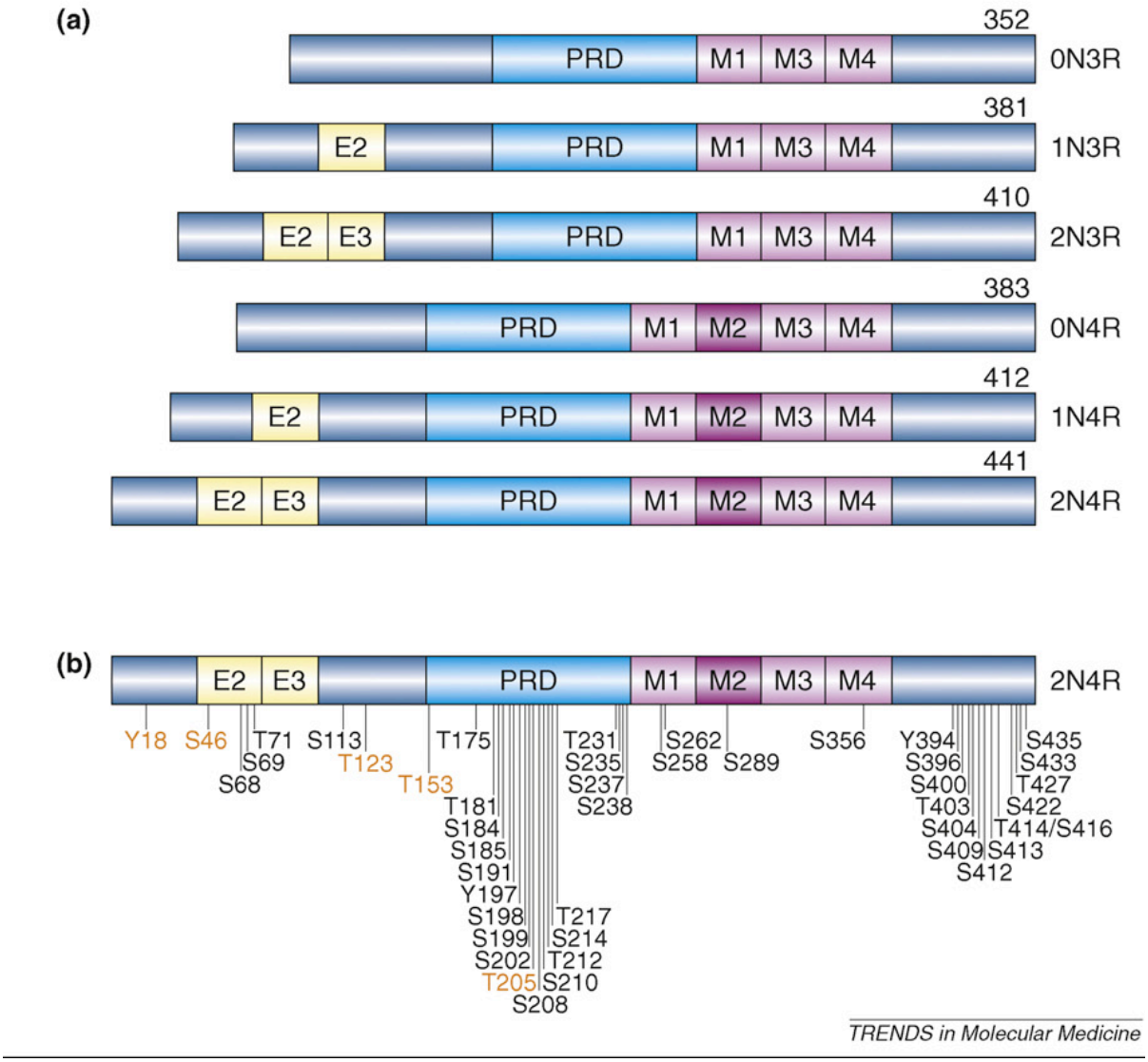

'with permission ' Hanger, DP, Anderton, BH, and Noble, W. (2009). Tau phosphorylation: the therapeutic challenge for neurodegenerative disease. *Trends in Molecular Medicine, 15*(3), 112-119.

Figure 1.3: Tau isoforms in the CNS and Tau phosphorylation sites. (a) Six isoforms of Tau exist in human brain, where exons 2, 3, and 10 are alternatively spliced. Exons 2 and 3 (E2 and E3) code for two 28 amino acid inserts at the N-terminal portion of Tau. When E2 and E3 are absent from Tau, it is designated as 0N. When only E2 is present, it gives rise to 1N Tau isoforms. If E2 and E3 are present in the protein, it results in 2N Tau isoforms. M1-M4 denote the four microtubule binding repeat domains, and M2 is encoded by exon 10. Absence of M2 results in 3R Tau and presence of M2 leads to 4R Tau isoforms. At the center of Tau is the proline –rich domain (PRD). Tau isoforms can range in size from 352-441 amino acids as a result of alternative splicing. (b) Approximately 45 phosphorylation sites have been identified on Tau. Most sites are present in the PRD and in the C-terminal region, with few sites found in the microtubule-binding domain. Sites labeled in orange indicate that identification occurred through phospho-specific antibody labeling, while the remaining sites were discovered through mass spectrometry and/or Edman degradation.

Tau protein is located on chromosome 17 and contains 16 exons, of which 8 are alternatively spliced. These include exons 2, 3, 4A, 6, 8, 10, 13, and 14 (Goedert et al., 1989a, Goedert et al., 1989b, Himmler, 1989, Wei and Andreadis, 1998, Gao et al., 2000). Six isoforms of Tau are present in adult brains, and all are derived from the same gene, *MAPT*, through alternative splicing. The basic structure of Tau includes an N-terminal 'projection domain' that is followed by a proline-rich region. Following the proline-rich domain is the C-terminal region, which contains the microtubule-binding domain. This domain consists of either 3 or 4 repeats of a highly conserved tubulin-binding motif (Lee et al., 1989).

The six isoforms of Tau differ from each other in two ways. First, is by the number of microtubule binding motifs present at the C-terminal end of the protein. There can be either three or four repeats present, designated as 3R or 4R isoforms. The 3R and 4R isoforms are present in a one-to-one ratio in normal adult brains (Hong et al., 1998). Secondly, they can differ by the absence or presence of two 29-amino acid-long sequences at the N-terminal region, which does not affect microtubule binding (Binder et al., 1985). These two sequences are exons 2 and 3, and their absence or presence is indicated by -2-3 or +2+3. However, one can be present without the other and this combination is designated -2+3 or +2-3. The precise function of these multiple isoforms has not been established, although it has been discovered that the isoforms are differentially expressed throughout development (Ballatore et al., 2007).

Pathogenic Tau

One of the classic markers of neurodegeneration in Tauopathies is a decrease in Tau bound to microtubules leading to an increase in free, unbound Tau. It is believed that increases in the cytosolic unbound Tau enhance the probability of conformational changes in Tau, eventually leading to aggregation and neurofibrillary tangle (NFT) formation (Kuret et al., 2005b). Development of large NFTs from Tau is considered to be a multi-step process that first begins with the dissociation of Tau from the microtubules. Abnormal dissociation of Tau is caused by various processes such as a decrease in dephosphorylation and/or an increase in phosphorylation. The overall result is an increase in the free cytosolic Tau. As the concentration of unbound Tau increases, small 'pretangle' deposits form, which lead to paired helical filaments (PHFs), and eventually NFTs (Ross and Poirier, 2004, Kuret et al., 2005a, Kuret et al., 2005b). 'Pretangle' formation is not detectable by β-sheet dyes, unlike NFTs (Galvan et al., 2001, Maeda et al., 2006, Maeda et al., 2007).

Importantly, increases in pathological Tau correlate with clinical manifestations of dementia, which is not the case with Aβ plaques (Alafuzoff et al., 1987, Arriagada et al., 1992). It has been discovered that individuals without clinical AD have as much Aβ plaque formation as age-matched individuals with AD, except the non-AD tissue lacks dystrophic neurites and NFTs present in the AD brains (Dickson et al., 1988, Katzman et al., 1988, Dickson et al., 1992). Also, there is a group of diseases termed Tauopathies, which have AD-like neurofibrillary tangles without the presence of β-amyloid plaques. These are all due to specific mutations in the Tau gene discussed below. Tauopathies are characterized by dementia and include frontal temporal

dementia with parkinsonism-linked to chromosome 17 (FTDP-17), progressive supranuclear palsy, Pick's disease, and corticobasal degeneration (Hutton et al., 1998, Poorkaj et al., 1998, Spillantini et al., 1998). Therefore, dementia can occur without β-amyloid plaques further substantiating studies demonstrating that NFTs more closely correlate with neuronal loss than β-amyloid plaques.

Multiple stimuli are suspected of directly or indirectly influencing Tau aggregation. Mutations in Tau clearly lead to fibrillization, but aberrant kinase and phosphatase activities are also possible culprits. Some data also suggest NFT formation occurs downstream from β-amyloid deposition as assumed by the β-amyloid cascade hypothesis.

Mutations in Tau protein

One of the most direct causes of abnormal Tau activity is the presence of mutations in the gene for Tau, *MAPT*. Several research groups have carried out numerous genetic studies to demonstrate that mutations within *MAPT* lead to the development of FTDP-17 and other Tauopathies. The FTDP-17 Tauopathy is characterized by the presence of hyperphosphorylated Tau that assembles into filaments (von Bergen et al., 2001, Goedert and Jakes, 2005). Currently, there are over 30 different mutations of the Tau gene identified in families with FTDP-17(Goedert and Jakes, 2005).

Mutations within Tau cause many functional abnormalities, and there are multiple hypotheses advanced to explain how these mutations lead to abnormal Tau activity. It has been suggested that certain mutations, i.e. the P301L mutation, increases Tau self-

interaction, which predisposes Tau for filament assembly leading to rapid fibrillization (Nacharaju et al., 1999). Other groups have demonstrated that mutated Tau is more easily phosphorylated and/or less susceptible to dephosphorylation (Alonso et al., 2004) than normal Tau. Dayanandan and colleagues reported that Tau mutations led to impairments in the microtubule binding capabilities of the protein, thereby facilitating depolymerization of microtubules (Hong et al., 1998, Dayanandan et al., 1999).

Intronic *MAPT* mutations, coding mutations in exon 10 (i.e. N279K), or missense mutations (i.e. P301L) may lead to changes in alternative splicing of Tau. These changes could disrupt the one to one ratio of 3R to 4R Tau isoforms, causing an increase in the concentration of the 4R isoform. Absence or presence of exon 10 also disrupts this ratio, and it has been demonstrated that the 4R Tau isoform is more susceptible to hyperphosphorylation (Alonso et al., 2004, Bhaskar et al., 2005). Lastly, mutations within or adjacent to exon 10 hasten the formation of Tau filaments as these mutations are found within the microtubule binding domain of Tau (Nacharaju et al., 1999).

Kinases associated with Tau hyperphosphorylation

Under physiological conditions Tau contains 2 to 3 moles of phosphate per mole of protein (Kopke et al., 1993). In AD, Tau becomes abnormally hyperphosphorylated (Iqbal et al., 1986) and forms the pathological PHFs and NFTs characteristic of the disease (Grundke-Iqbal et al., 1986a, Grundke-Iqbal et al., 1986b, Iqbal et al., 1989, Lee et al., 1991). Interestingly, individuals with AD have the same amount of normal Tau as age-matched controls; however, there is a 4 to 8-fold increase of

hyperphosphorylated Tau in AD brains (Khatoon et al., 1992, 1994). Up to 40% of this aberrantly phosphorylated Tau occurs in the cytosol unassociated with PHFs or NFTs (Kopke et al., 1993). As the hyperphosphorylated Tau increases, it begins to sequester normal Tau, further disrupting microtubule stability (Alonso et al., 1994, Alonso et al., 1996).

Over 38 serine/threonine residues on Tau are phosphorylated in AD (Morishima-Kawashima et al., 1995, Hanger et al., 1998). Multiple kinases have been implicated in the hyperphosphorylation of Tau including: glycogen synthase kinase-3β (GSK3β); cyclin-dependent kinase-5 (cdk5); microtubule-affinity-regulating kinase (Dokmanovic et al.); protein kinase A (PKA); casein kinase-1 (CK-1); mitogen-activated protein kinase (MAPK); and calcium and calmodulin-dependent protein kinase-II (CaMKII) (Pei et al., 2003, Iqbal et al., 2005).

GSK3β and cdk5 phosphorylate several of sites on Tau, and the majority of these sites are shared between the two kinases (Wang et al., 1998, Anderton et al., 2001). Both of these enzymes have high expression levels in the brain (Woodgett, 1990, Lew et al., 1994) and have been involved in all areas of NFT formation (Pei et al., 1998, Pei et al., 1999). Transgenic mice overexpressing GSK3β have an increase in hyperphosphorylated Tau, which can be attenuated with GSK3β inhibition by lithium chloride (Perez et al., 2003, Tatebayashi et al., 2004).

In order for cdk5 to be active, it requires a small fragment p35 or its proteolytic product p25, which results from calpain cleavage of p35 (Kushakawa et al., 2000). The production of p25 significantly increases the activity of cdk5. A transgenic mouse model

overexpressing p25 demonstrates increases in hyperphosphorylated Tau as a result of abnormal cdk5 activity (Cruz et al., 2003, Noble et al., 2003).

Phosphatases have also been implicated in the development of hyperphosphorylated Tau, including protein phosphatase-2A (PP-2A) and protein phosphatase-1 (PP-1). It has been demonstrated that their activity is decreased by about 20% in AD brain (Gong et al., 1993, Gong et al., 1995). These enzymes are responsible for dephosphorylating about 90% of the serine/threonine sites in mammals (Oliver and Shenolikar, 1998).

β-amyloid cascade hypothesis and Tau pathology

The β-amyloid Cascade Hypothesis is one of the most accepted models of AD progression. It states that Aβ generation is the primary pathological event leading to NFT formation and dementia (Hardy and Higgins, 1992, Hardy and Selkoe, 2002). Many studies substantiate this hypothesis, in particular, studies on the triple transgenic (3xTgAD) mouse model, which contains the APP Swedish, PSEN1, and P301L Tau mutations (APPswe-PS1M146V-TauP301L) (Oddo et al., 2003b). This model develops Aβ pathology before the deposition of Tau tangles, and the 3xTgAD model had more NFT pathology than the double transgenic model (Tg2x). This model contains the PSEN1 and P301L mutations, but not the Aβ producing APP-Swedish mutation (Oddo et al., 2003a). A second study that supports the Amyloid Cascade Hypothesis involved intracerebral injections of Aβ into a P301L transgenic mouse model. Injections of the aggregated Aβ exacerbated the Tau pathology in the mutant Tau mouse model (Gotz et al., 2001). P301L transgenic mice crossed with mice containing the APP-Swedish plus

the London mutations also developed more prominent Tau pathology than mice expressing the P301L mutation alone (Lewis et al., 2000).

A third experimental procedure that supports the Amyloid Cascade Hypothesis is the use of Aβ peptides to induce toxicity in cellular models. The addition of Aβ peptides also stimulates Tau phosphorylation in cell culture (Li et al., 2003, Blurton-Jones and LaFerla, 2006, Oddo et al., 2006, Seyb et al., 2007).

Unfortunately, results from mouse and cell culture studies do not correlate with human data. First, individuals without AD develop Aβ plaques similar to individuals with AD, and the former group does not show neurofibrillary pathology (Katzman et al., 1988). Secondly, higher levels of Aβ burden are observed in hereditary cerebral hemorrhage with amyloid pathology, Dutch type, but Tau pathology does not develop with the disease (Levy et al., 1990). Third, as mentioned before, individuals affected with the Tauopathies exhibit a demented phenotype, but only produce neurofibrillary pathology (Hutton et al., 1998). Finally, cultured cells expressing the PSEN1 mutation do not regenerate Aβ peptides after levels of Aβ peptides were depleted (Shioi et al., 2007).

Overall, studies examining the β-amyloid Cascade Hypothesis are still a matter of some controversy. Although some studies support the idea that Aβ leads to Tau pathology, the human studies do not substantiate these conclusions. At this point in time, AD research certainly makes it clear that this disease is multi-faceted, and the β-amyloid Cascade Hypothesis may be too simplistic to describe disease progression.

3. MOLECULAR CHAPERONES AND THERAPEUTICS FOR PROTEIN MISFOLDING DISEASES

Molecular chaperones are families of highly conserved proteins that mediate the folding of nascent proteins, or re-folding of misfolded proteins, but are not part of the final product (Muchowski and Wacker, 2005a). These proteins are essential for numerous cellular processes such as proteasomal degradation, lysosomal autophagy, signal transduction, and protein transport (Hartl and Hayer-Hartl, 2002). When stressful cellular events occur such as temperature elevation, pH changes, or reactive oxygen species (ROS) generation, the cell stimulates the production of a subset of molecular chaperones called the heat shock proteins (HSPs). The HSPs are essential in recovering proteins damaged from cellular stress (Lindquist, 1986). Six different families of HSPs exist, and they are classified by their molecular weight in kilodaltons (kDa). These families include: Hsp100, Hsp90, Hsp70, Hsp60, Hsp40, and HSPs that weigh less than 40 kDa called the small HSPs (sHSPs) (Muchowski, 2002). There are many isoforms within each of these families, some of which are constitutively expressed and some are inducible.

In addition to the molecular chaperones, there are groups of proteins called co-chaperones that assist the primary molecular chaperones in refolding or clearing the targeted protein. Through their interactions with the molecular chaperone, they can help determine the fate of the faulty protein, i.e., whether it will be removed from the cell through degradation or whether it will be re-folded into its native conformation. There are many different co-chaperones, and in our studies we will only focus on three such proteins: BAG1, BAG2, and CHIP.

Heat Shock Proteins and the Heat Shock Response

As previously mentioned, the heat shock proteins play an important role in the ability of the cell to respond to cellular stresses like increases in temperature, changes in pH, or oxidative insults. When these cell stresses occur, a cytosolic transcription factor, heat shock factor-1 (HSF-1), is released from its binding partner, Hsp90. Upon release, HSF-1 becomes phosphorylated, trimerizes, and enters the nucleus. Once inside the nucleus, HSF-1 binds to the heat shock response element (HSRE) on several genes, and increases the transcription of mRNA for additional proteins involved in protein folding or protein degradation such as Hsp90, Hsp70, and Hsp40. These HSPs form complexes with other proteins and provide assistance in refolding denatured proteins and targeting non-repairable proteins for degradation (Ferrarini et al., 1992).

Hsp90 family

The Hsp90 family of molecular chaperones makes up 1-2% of all cytosolic proteins in a typical cell. This family consists of four isoforms that control the activity of a vast array of signaling proteins. These proteins refold and stabilize misfolded proteins (Muchowski and Wacker, 2005b) as well as signal the ubiquitination and degradation of proteins beyond repair (Ferrarini et al., 1992). These four isoforms include: Hsp90α, the inducible form found in the cytosol; Hsp90β, the constitutive form also found in the cytosol; 94kDa glucose-regulated protein (Grp94) localized in the endoplasmic reticulum; and Hsp75/tumor necrosis factor receptor associated protein-1 (TRAP-1) confined to the mitochondrial matrix (Maloney and Workman, 2002).

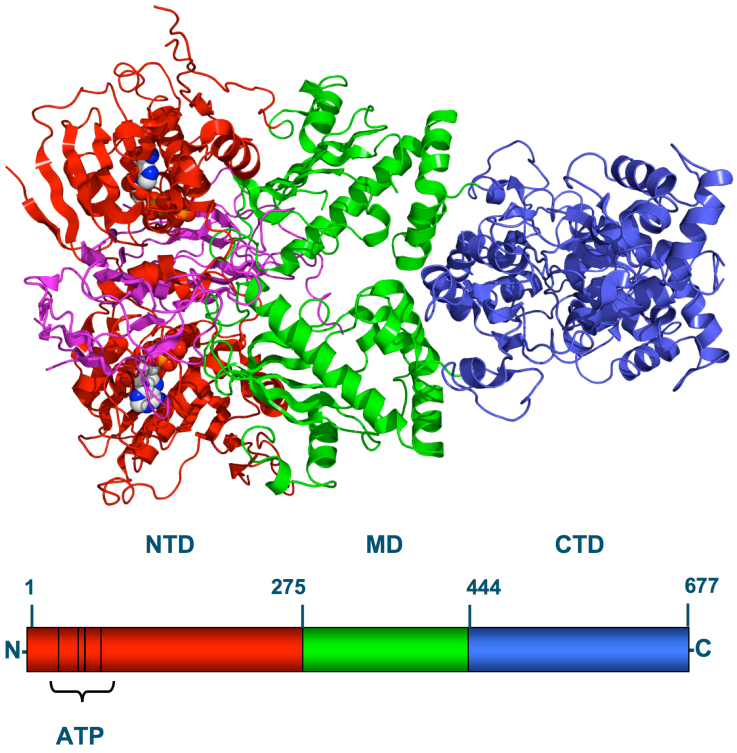

Figure 1.4: Structure of Hsp90. The Hsp90 protein consists of 677 amino acids and contains three different domains: N-terminal domain (NTD; red); the middle domain (MD; green); and the C-terminal domain (CTD; blue). An ATP binding site is located at the NTD, and is represented by white and blue balls. Hsp90 functions as a dimer with client proteins. Client proteins interact with the dimeric protein at the MD. The protein dimer forms through interactions at the CTD.

In its active form, Hsp90 exists as a dimer. As shown in Figure 1.4, Hsp90 is composed of three different domains: an N-terminal domain (NTD), which contains an ATP binding site; the middle domain (MD) where client binding occurs; and the C-terminal domain (CTD), which is the site of dimerization (Pearl and Prodromou, 2006). Each of these regions performs important roles in the activity of Hsp90.

Within the NTD is the nucleotide-binding pocket, which is highly conserved across species (Bergerat et al., 1997). Binding and hydrolysis of ATP at this site results in multiple conformational changes in Hsp90. These conformations permit the Hsp90

to bind and interact with a sizeable group of structurally diverse client proteins, as well as large complexes that contain other molecular chaperones and co-chaperones (Krukenberg et al., 2011).

Client protein binding to Hsp90 occurs at the MD. This region contains a catalytic loop, which is critical in the hydrolysis of ATP at the NTD. The activity of co-chaperones that hydrolyze ATP can also be increased by the catalytic loop of the MD (Meyer et al., 2003b).

Not only is the CTD of Hsp90 the portion where dimerization occurs, it also plays an important role in regulating activities at the NTD. There is a C-terminal motif (MEEVD) that promotes co-chaperone binding. Co-chaperones that bind at this motif regulate Hsp90 activity. The type of co-chaperone that binds determines the outcome. These co-chaperones can aid in client folding, modulate Hsp90 ATPase activity, determine recruitment of specific client proteins, and stimulate maturation of substrates (Krukenberg et al., 2011). For example, when the co-chaperone Tom70 binds to Hsp90, Tom70 stimulates Hsp90 to assist in mitochondrial transport (Wandinger et al., 2008).

Hsp70 family

This family of 70kDa proteins is the most evolutionarily conserved (Hunt and Morimoto, 1985). There have been eleven members of the Hsp70 family identified, each encoded in a different gene (Brocchieri et al., 2008), and these homologs exhibit tissue specific expression levels and differences in sub-cellular localization (Tavaria et al., 1996). Most Hsp70 homologs contain an ATPase domain, a peptide binding

domain, and a middle region containing protease sensitive sites (Bukau et al., 2006, Brocchieri et al., 2008). The expression level of the Hsp70 proteins differs depending on the cellular situation. Most Hsp70 proteins are constitutively expressed, while a few are inducible forms with increased expression occurring during cellular stress events (Daugaard et al., 2007). Hsp70 proteins are critical for many cellular functions: degradation of faulty or 'misfolded' proteins; nascent folding of proteins and refolding of abnormal proteins; and maintenance of cellular homeostasis by controlling proteins during stress events such as high pH levels, ischemia, high temperature, or inflammation (Lindquist and Craig, 1988).

The ATPase domain of Hsp70 is responsible for substrate binding and release. Hsp70 is bound to a substrate with low affinity when it is in its ATP binding state, and the substrate binds to Hsp70 with high affinity when it is in the ADP state. This ATPase switching is mediated by co-chaperones that regulate the duration of the Hsp70-substrate bound complex (Erbse et al., 2004). These co-chaperones play a very important role in targeting Hsp70 to sites involved in specific cellular functions at multiple regions in the cells.

Hsp70 proteins never work alone. In order for it to be fully active, Hsp70 requires a co-chaperone. These co-chaperones include Hsp40 and nucleotide exchange factors (NEFs) such as the Bcl-2-associated athanogene (BAG) proteins. The type of co-chaperone bound to Hsp70 will determine the ultimate outcome (Kampinga and Craig, 2010) such as BAG2 association with Hsp70, which will lead to ubiquitin independent degradation of client proteins (Carrettiero et al., 2009).

Hsp60 family

Hsp60 is generally found in the mitochondria; however, recent evidence suggests that some Hsp60 also resides in the cytosol (Chandra et al., 2007). Within the mitochondria, Hsp60 interacts with Hsp10, an sHSP, to regulate nascent polypeptide folding into native conformations (Naylor and Hartl, 2001, Ranford and Henderson, 2002, Meyer et al., 2003a). Hsp60 also interacts with mitochondrial Hsp70, also called mortalin, to regulate apoptosis (Wadhwa et al., 2005, Deocaris et al., 2006, Kaul et al., 2006). In addition to regulating protein folding, Hsp60 also plays a role in protein trafficking (Deocaris et al., 2006) and peptide-hormone signaling (Czarnecka et al., 2006). Cytosolic Hsp60 and mitochondrial Hsp60 function in pro-apoptotic and pro-survival pathways depending on the cellular conditions (Chandra et al., 2007). For example, Hsp60 controls key pathways involved in tumor cell development, which provides an attractive protein for cancer therapy (Cappello et al., 2008).

Hsp40 family

The Hsp40 family of proteins is characterized by the presence of a highly conserved 70 amino acid region called the 'J domain'. The primary function of this domain is to regulate the ATPase activity of Hsp70 (Craig et al., 2006, Hageman and Kampinga, 2009). There are about 41 different Hsp40 proteins that bind to the ATPase domain of Hsp70 (Kampinga and Craig, 2010). The Hsp40 that interacts with Hsp70 directly determines which client protein is present in the complex (Craig et al., 2006, Hageman and Kampinga, 2009). For example, the ribosome-associated J protein DnaJ

subfamily C member 2 (DNAJC2) recruits Hsp70 to the endoplasmic reticulum (ER) in order to assist in later stages of polypeptide formation (Hundley et al., 2005).

Small HSPs family

The small heat shock proteins (sHSPs) are considered “housekeeping” proteins as they play essential roles in regulating cellular functions. Hsp27 has been demonstrated to promote protein folding as well as to regulate apoptosis. For example, Hsp27 blocks cytochrome c release from the mitochondria by interacting with phosphatidylinositol 3 kinase (PI3K) eventually leading to the phosphorylation of Bcl-2-associated-X protein (BAX) (Havasi et al., 2008). Hsp22 prevents protein aggregation and participates in apoptosis. Another sHSPs, Hsp20 displays chaperone activity and regulates contraction of smooth muscle cells (Mymrikov et al., 2011).

Molecular Co-Chaperones

Co-chaperones are non-client proteins that bind to Hsp70 or Hsp90 and regulate their cellular actions. Many proteins bind to the nucleotide-binding site present on both Hsp70 and Hsp90, and regulate client binding. Others structurally link Hsp70 or Hsp90 to their desired client protein. For example, Aha1 interacts with Hsp90 and stimulates the ATPase activity of Hsp90 (Panaretou et al., 2002).

Although there are over 100 different co-chaperones, almost all can be placed into one of two different categories based on their structural features. There are the Hsp40 proteins (J proteins) that only interact with Hsp70, or the TRP binding proteins

that can interact with both Hsp70 and Hsp90 (Caplan, 2003). In this section, three co-chaperones will be discussed in their relationship to Hsp70: BAG1, BAG2, and CHIP.

BAG proteins

One family of co-chaperones that interacts with Hsp70 is the Bcl-2-associated athanogene (BAG) group. The BAG family of proteins consists of 6 different members, 4 of which have been shown to associate with Hsp70 (Takayama and Reed, 2001). These proteins share a BAG domain that consists of a conserved sequence of about 110 amino acids located at the C-terminal region; this region interacts with the Hsp70 ATPase domain (Takayama et al., 1999). BAG proteins can induce the release of a bound substrate from Hsp70 by mediating nucleotide-exchange (Sonderman et al., 2001). These proteins also assist in Hsp70-dependent protein degradation (Takayama and Reed, 2001). Here, two BAG proteins will be discussed, with regard to in their relationship with Hsp70 and its client protein Tau.

BAG1

There are three human and two mouse BAG1 isoforms (Takayama et al., 1998). It has been demonstrated that BAG1 interacts with Hsp70 and Tau (Luders et al., 2000), and increases Hsp70 refolding activity in neurons (Liman et al., 2005). BAG-1 is crucial in the formation and maintenance of neurons (Gotz et al., 2005). Conversely, it has also been reported that BAG1 binding to Hsp70/substrate complexes suppresses the refolding activity of Hsp70 (Takayama et al., 1997). It has been shown in mouse models of Alzheimer's disease that BAG1 is highly expressed in neurons where Tau

tangles reside. This increased expression of BAG1 does not prevent ubiquitination, but it can inhibit Tau degradation via the 20S proteasome (Elliott et al., 2007).

BAG1 is different from the other BAG proteins in that it has an ubiquitin-like domain. This domain is present at the N-terminus of the protein and is correlated with ubiquitin-dependent degradation of proteins (Demand et al., 2001). BAG1 and the ubiquitin-ligase, carboxy terminus of Hsc70-binding protein (CHIP), simultaneously bind to Hsp70 to ubiquitinate client proteins and target them for degradation in the proteasome (Hartl and Hayer-Hartl, 2002, Gamerdinger et al., 2011).

BAG2

Another member of the BAG family, BAG2, has been reported to play a critical role in mediating a highly efficient mode of Tau degradation through ubiquitin-independent mechanisms. It has been demonstrated that the BAG2/Hsp70 complex can tether hyperphosphorylated Tau from microtubules to the proteasome for degradation without the ubiquitination of Tau (Carrettiero et al., 2009). Lukiw and colleagues have shown that expression of BAG2 is inhibited by miR-128, a microRNA that is up-regulated in Alzheimer's disease (Lukiw, 2007), thereby preventing BAG2 associated removal of aggregated Tau.

Although there are not many studies demonstrating the roles of BAG proteins in relation to Tau, it cannot be denied that there is some evidence suggesting an interaction between the BAG proteins and HSP70 in the context of Alzheimer's disease.

CHIP

One Hsp70 co-chaperone that has been widely studied in relation to Tau pathology is the carboxy terminus of Hsc70-binding protein (CHIP). This protein has a tetratricopeptide repeat (TPR) domain that associates with Hsp70 protein (Ballinger et al., 1999) and a U-box domain that has E3, or ubiquitin-ligase activity. The E3 enzymes catalyze the third and final step of substrate recognition by the proteasome (Hatakeyama et al., 2004). CHIP interacts with Hsp70, Hsp90, and Tau, although its most prominent effect is observed through Hsp70 (Grelle et al., 2006). CHIP binding to Hsp70 abrogates the ATPase refolding activity of HSP70 (Ballinger et al., 1999).

CHIP levels are elevated in human Alzheimer's disease tissue (Sahara et al., 2005) suggesting that CHIP plays a part in the formation of Tau tangles. This ubiquitin-ligase protein mediates ubiquitination of Tau and somehow increases Tau aggregation (Petrucelli et al., 2004a). CHIP also associates with BAG1 and controls crosstalk between the ubiquitin-proteasome system and chaperone proteins (Luders et al., 2000). Intriguingly, BAG2 inhibits CHIP activity by preventing E3 ligase activation (Arndt et al., 2005). Dickey and colleagues used an *in vitro* model demonstrating that CHIP is a critical modulator of hyperphosphorylated Tau levels when HSF-1 is absent (Dickey et al., 2007).

Based on current knowledge, the co-chaperones are essential in regulating the activity of molecular chaperones. The way these proteins interact with the molecular chaperone complexes is multi-faceted, and appears to depend on what proteins are present in the complex. The complexity of these interactions not withstanding, a better

understanding of the role these proteins play in maintaining the quality of proteins will help in the development of efficacious therapeutics for AD.

4. HSP90 MODULATION AS A POTENTIAL THERAPEUTIC FOR AD

As previously mentioned, many neurodegenerative diseases are characterized by the accumulation of aberrant proteins. Tauopathies, such as FTDP-17 and AD, have neuronal loss due to the presence of hyperphosphorylated Tau protein. Hyperphosphorylated Tau is unable to properly associate with microtubules, and disrupts the critical process of exoplasmic transport. In addition, the dissociated Tau begins to form aggregates, the NFTs, and forces the cell to try to function in the presence of these aggregated proteins.

One possible culprit responsible for NFT development may be ineffective chaperones. For example, reduced expression or activity of molecular chaperones would be expected to lead to Tau fibrils. Some groups have shown that the protein degradation systems, particularly the proteasome that would normally remove these toxic aggregates are overburdened or functioning improperly. This dysregulation of the proteasome is a part of aging (Layfield et al., 2003) and thus the proteins of the degradation pathway cannot keep up with the need to clear aggregated Tau. Also reported are increased levels of the ubiquitin-ligase, CHIP, in AD brains (Sahara et al., 2005). An increase of CHIP, in conjunction with a decrease in proteasome activity, supports the finding that Tau aggregates are poly- and mono-ubiquitinated, but are not cleared (Cripps et al., 2006). One group has shown a decrease in Hsp70 and Hsp90

protein levels in cellular, rodent, and human disease models of 'Tauopathies' (Dou et al., 2003b).

Hsp90 Inhibition in Cancer

Hsp90 inhibitors were first designed as cancer treatments. Proteomic studies revealed that many tumor types overexpress HSPs, thereby using this system to fold nascent client proteins required for proliferation. In order to stop the proliferation of cancer cells, researchers designed therapeutic agents to modulate the folding of these molecules (Khalil et al., 2011). In fact, early stages of HSP-designed cancer therapy used hyperthermia as an effective intervention (Lindquist, 1986).

The classic HSP family involved in cancer is HSP90 (Sreedhar et al., 2004). It is believed that cancer cells take control of the protein quality control machinery to start producing cancer cell polypeptides (Pockley, 2001). Several small molecule inhibitors demonstrate strong anti-tumor capabilities in multiple malignancies (Taldone et al., 2008). These inhibitors prevent the cells from folding the proteins contributing to malignancy. Currently, there are 14 Hsp90 inhibitors in clinical trials to be used as single agents or in combination therapy to treat cancer (Porter et al., 2010). These clinical trials include the Hsp90 inhibitor 17-allylamino-17-demethoxygeldanamycin (17-AAG), a derivative of the ansamycin antibiotic geldanamycin (GA). 17-AAG has already demonstrated promising results in various Phase I and Phase II clinical trials (Banerji et al., 2005, Goetz et al., 2005, Grem et al., 2005, Heath et al., 2005, Ramanathan et al., 2005).

Cancer Therapeutics Transition to AD

Similar to cancer, overexpression of HSPs is demonstrated in multiple neurodegenerative disorders, including AD, possibly as a compensatory response to the misfolded protein aggregates (Perez et al., 1991, Anthony et al., 2003). This overexpression of HSPs in neurodegenerative diseases led researchers to design a group of novel drugs that could modulate the activity of Hsp90 and activate the protein folding or clearance cascade. At this time there are two different domains within Hsp90 where drugs are being targeted; agents designed to inhibit the N-terminal ATPase activity of Hsp90 or agents to modulate the C-terminal region of Hsp90.

Although Hsp90 inhibitors are designed against different domains of the protein, the hypothetical effect of the drug on modulating the activity of molecular chaperones by activating the heat shock response is considered similar. The schematic in Figure 1.5 shows the theoretical outcome of Hsp90 inhibition. For instance, when an Hsp90 inhibitor enters the cytosol of the cell, it blocks Hsp90, which releases proteins bound in the complex including the transcription factor, HSF-1. With HSF-1 being free from Hsp90, it can be phosphorylated, trimerized, and translocated to the nucleus. Once in the nucleus, it binds to the heat shock response element (HSRE) and up-regulates transcription of molecular chaperones important to maintaining protein quality. Concurrently, other molecular chaperones i.e. Hsp70 and Hsp40 originally bound to the Hsp90 complex are also free to assist faulty proteins.

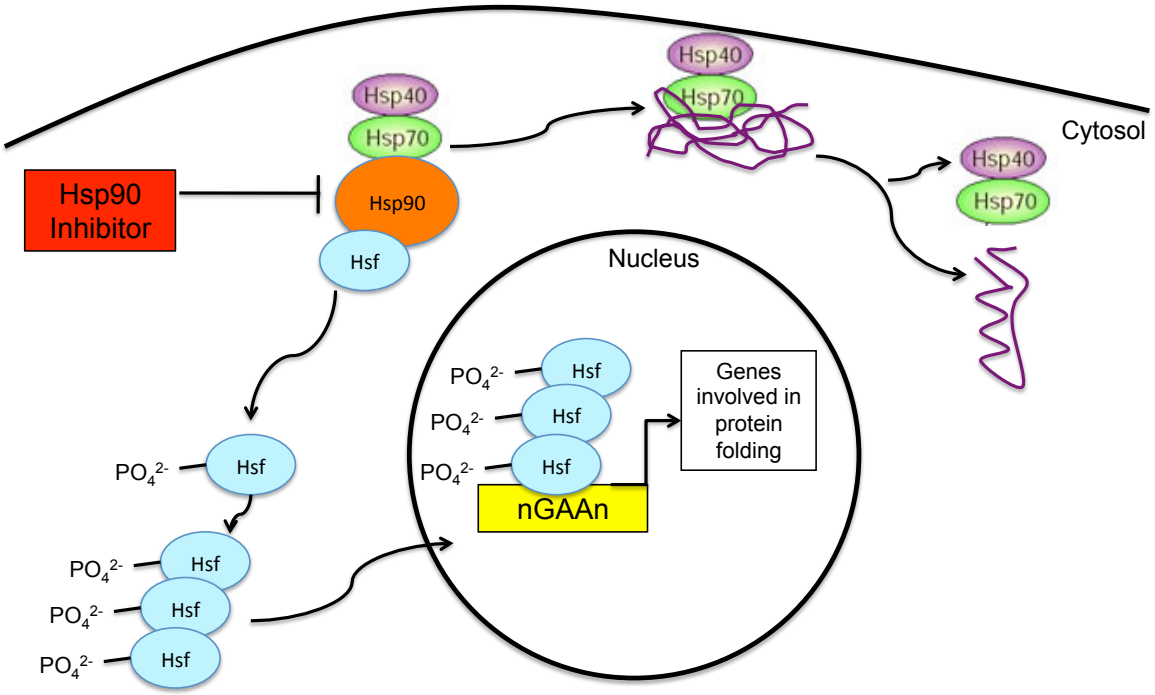

Figure 1.5: A hypothetical schematic of Hsp90 inhibition. An Hsp90 inhibitor enters the cell where it dissociates the Hsp90 complex, freeing the transcription factor, HSF-1. Once free, HSF-1 is phosphorylated, trimerized, and translocated to the nucleus where it binds to the heat shock response element (nGAAn). This stimulates an increase in transcription of molecular chaperones involved in protein folding and degradation. Subsequently, the Hsp90 inhibitor frees other molecular chaperones in the Hsp90 complex i.e. Hsp70 and Hsp40, which allows them to interact with faulty proteins and return them to their native conformation.

In the next two sections, compounds designed against the N-terminal and C-terminal portions of Hsp90 will be described in their relation to neurodegeneration, specifically AD.

N-terminal Hsp90 Inhibition in Neurodegeneration

The factors that lead to the deposition of SPs and NFTs in the affected AD brain, first develop as cellular dysfunctions (Chui et al., 1999, Hsia et al., 1999, Moechars et al., 1999, Kumar-Singh et al., 2000). Since the HSPs play an important role in

maintaining proper cellular function, and there are promising reports of Hsp90 inhibitors as cancer therapeutics, it is logical to propose similar roles for Hsp90 inhibitors in neurodegenerative diseases (Luo et al., 2008).

The best known Hsp90 inhibitor is geldanamycin (GA), an ansamycin antibiotic that was first used as an antifungal medication (DeBoer et al., 1970). Greengard's group used *in vitro* cell models transfected with abnormal Tau, and treated them with GA to demonstrate dose dependent decreases of insoluble Tau, as well as dose dependent increases in Hsp70 and Hsp90 protein levels. GA treatment decreased the levels of hyperphosphorylated Tau induced by okadaic acid (OA), a PP2A inhibitor (Dou et al., 2003). Interestingly, a microtubule-binding assay showed that GA increased the association of Tau with microtubules while simultaneously decreasing levels of aggregated Tau (Dou et al., 2003). These findings support the idea that Hsp90 inhibitors are potential candidates for AD treatment.

Further studies with GA were continued in other labs studying neurodegenerative diseases. Petrucelli and colleagues used GA and the addition of pure HSF-1 protein to reveal increases in Hsp70 levels in a human neuroblastoma cell line expressing endogenous Tau. These results demonstrated that the increases in Hsp70 occur through an HSF-1 mediated pathway. This group also revealed that CHIP mediated ubiquitination of Tau, but the presence of Hsp70 prevented CHIP from ubiquitinating Tau. Overexpression of Hsp70 in a mouse model at 30 months of age demonstrated a decrease in Tau when compared to age matched mice without the Hsp70 transgene (Petrucelli et al., 2004). Overall, the results from Greengard's and Petrucelli's groups

validate the idea that Hsp90 inhibitors stimulate the heat shock response to assist cells in clearing aggregated proteins.

Although a potent modulator of the heat shock response, GA is hepatotoxic (Supko et al., 1995). This led to the development of the derivatives, such as 17-AAG, which demonstrates the same biological behaviors as GA (Schulte and Neckers, 1998), but is less toxic to the liver (Page et al., 1997). Using 17-AAG, and PU24Cl, a synthetic derivative of GA, Greengard's group demonstrated dose-dependent increases in Hsp70 protein levels as well as dose-dependent decreases in hyperphosphorylated Tau epitopes in COS-7 cells containing mutant P301L Tau (Luo et al., 2007). A blood brain barrier (BBB) permeable derivative of GA, PU-DZ8, also displayed decreases of hyperphosphorylated Tau in a mouse model expressing mutant P301L Tau (Luo et al., 2007).

Other groups have also developed non-toxic, small molecule inhibitors of Hsp90. Dickey and colleagues developed a BBB permeable Hsp90 inhibitor called EC-102. This compound displayed robust increases in Hsp70, Hsp40 and Hsp27 levels in CHO cells transfected with mutant P301L Tau. Using the same transfected P301L Tau cell model, this group also demonstrated decreases in hyperphosphorylated and total Tau levels. These changes were the same or similar to cells treated with 17-AAG (Dickey et al., 2006).

In 2007, Dickey's group published results regarding the small molecule inhibitor of Hsp90, EC102. EC102 increased Hsp70 levels in CD-1 mouse brains while concurrently decreasing hyperphosphorylated Tau levels in HeLa cells transfected with mutant Tau. A cell model with siRNA directed against CHIP prevented EC102 mediated

decreases in phospho-Tau. Hsp40 knockdown also prevented EC102 decreases in phospho-Tau (Dickey et al., 2007). These results suggest that EC102 requires CHIP and Hsp40 to modulate the removal of hyperphosphorylated Tau.

As the compounds discussed here are all derivatives of the two well-described N-terminal Hsp90 inhibitors, GA and 17-AAG, it is possible that although these agents show promise with acute treatment in animal models, there is potential for toxicity with chronic treatment. In order for a neurodegenerative therapeutic to be effective, the drug will most likely need to be administered for years. Therefore, it is necessary to develop a compound that will stimulate the heat shock response, but will remain non-toxic over long periods of treatment. Keeping this in mind, Hsp90 inhibitors directed at the C-terminus of the protein were developed and assessed for their efficacy as a treatment for AD.

C-terminal Hsp90 Inhibition in Neurodegeneration

Given that N-terminal Hsp90 inhibitors are toxic at low doses, researchers searched for other methods to modulate Hsp90 activity. In 2000, a group demonstrated that novobiocin (Figure 1.6), an inhibitor of bacterial DNA gyrase, bound to the C-terminus of Hsp90 with low affinity (Marcu et al., 2000a, Marcu et al., 2000b). Derivatives for novobiocin were developed in order to increase potency, as well as to assess the ability of these analogs to provide protection in models of AD.

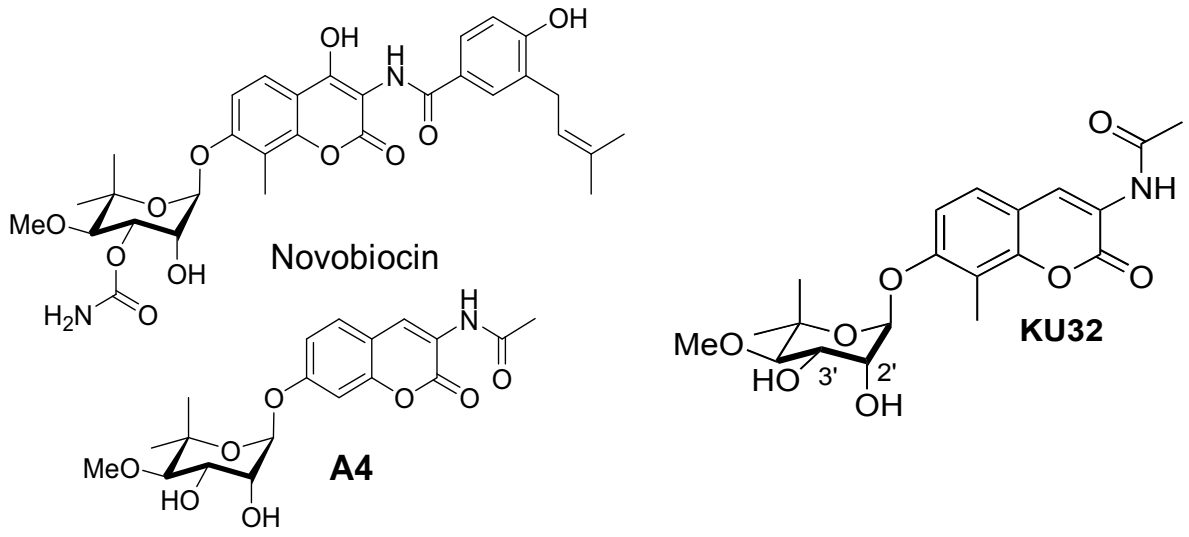

Figure 1.6: Structure of Novobiocin and the Novobiocin derivatives, A4 and KU-32

One of the first non-toxic novobiocin derivatives with high affinity binding to the C-terminus of Hsp90 was A4 (Figure 1.6). This compound dose-dependently protected primary rat neurons from Aβ induced toxicity, and dose dependently increased levels of Hsp70 similar to GA. Most importantly, this analog was not toxic to primary neurons at concentrations up to 10 μM, whereas the same concentration of GA induced 80% cell death (Ansar et al., 2007).

As more derivatives of novobiocin were developed, a second potent analog was discovered, designated KU-32 (Figure 1.6). Early results regarding this compound demonstrated that it was protective against Aβ-toxicity in undifferentiated and differentiated neuroblastoma cells (Lu et al., 2008). Further studies involving KU-32 show that it dose-dependently increased Hsp70 levels in MCF7 cells, and provided dose-dependent protection against demyelination and glucose toxicity in peripheral neurons. However, the most promising results from this study indicate that KU-32

requires Hsp70 for neuroprotection. Chronic KU-32 treatment of mice deficient in the inducible form of Hsp70 did not reveal protection against streptozotocin (STZ)-induced diabetic peripheral neuropathy (DPN) while mice with inducible Hsp70 demonstrated protection against DPN upon KU-32 administration (Urban et al., 2010). These studies support that C-terminal Hsp90 inhibitors modulate the heat shock response similarly to N-terminal Hsp90 inhibitors; however, the C-terminal inhibitors are much less toxic.

As revealed in the preceding studies, C-terminal inhibitors are a promising potential agent for neurodegenerative disorders, but further studies are needed to demonstrate efficacy in models of AD. The major focus of this dissertation is to examine the neuroprotective capabilities of KU-32 in cellular and animal models of AD. Our hypothesis is that KU-32 protects primary neurons from Aβ-induced death, as well as decreases hyperphosphorylated Tau in transgenic models of AD, and protects the mouse brains from neuronal loss and neuritic dystrophy. We addressed the *in vivo* effect of KU-32 on only Tau phosphorylation as this pathological entity most closely correlates with the neurodegenerative phenotype (Spillantini et al., 1998).

Overall, the studies performed here demonstrate that KU-32 is a potent neuroprotective agent in animal and cellular models of AD. KU-32 decreases hyperphosphorylated Tau species and improves cognitive behavior in a transgenic mouse model of AD. These experiments reveal that KU-32 is an efficacious compound for the treatment of AD as it improves cognition, decreases Tau pathology and can be tolerated at high doses for long periods of administration. This drug may be a beneficial

addition to the current treatments of AD and warrants further investigation into its therapeutic effects.

5. References

Alafuzoff I, Iqbal K, Friden H, Adolfsson R, Winblad B (1987) Histopathological criteria for progressive dementia disorders: clinical-pathological correlation and classification by multivariate data analysis. Acta Neuropathologica 74:209-225.

Alonso A, Grundke-Iqbal I, Iqbal K (1996) Alzheimer's disease hyperphosphorylated Tau sequesters normal Tau into tangles of filaments and disassembles microtubules. Nature Medicine 2:783-787.

Alonso A, Mederlyova A, Novak M, Grundke-Iqbal I, Iqbal K (2004) Promotion of hyperphosphorylation by frontotemporal dementia Tau mutations. Journal of Biological Chemistry 279:34873-34881.

Alonso A, Zaidi T, Grundke-Iqbal I, Iqbal K (1994) Role of abnormally phosphorylated Tau in the breakdown of microtubules in Alzheimer disease. Proceedings of the National Academy of Sciences 91:5562-5566.

Alzheimer's Association (2011) Current Alzheimer's Treatments. alz.org.

Alzheimer's Association (2012) 2012 Alzheimer's disease facts and figures. Alzheimer's and Dementia 8:1-72.

American Psychiatric Association (2000) Diagnostic and statistical manual of mental disorders. Washington DC: American Psychiatric Publisher.

Anderton B, Betts J, Blackstock W, Brion J, Chapman S, Connell J, Dayanandan R, Gallo J, Gibb G, Hanger D, Hutton M, Kardalinou E, Leroy K, Lovestone S, Mack

T, Reynolds C, Van Slegtenhorst M (2001) Sites of phosphorylation in Tau and factors affecting their regulation. Biochemical Society Symposia 73-80.

Andreasen N, Minthon L, Davidsson P, Vanmechelen E, Vanderstichele H, Winblad B, Blennow K (2001) Evaluation of CSF-Tau and CSF-Abeta42 as diagnositc markers for Alzheimer disease in clinical practice. Archives of Neurology 58:373-379.

Ansar S, Burlison JA, Hadden MK, Yu XM, Desino KE, Bean J, Neckers L, Audus KL, Michaelis ML, Blagg BS (2007) A non-toxic Hsp90 inhibitor protects neurons from Abeta-induced toxicity. Bioorganic and Medicinal Chemistry Letters 17:1984-1990.

Anstey K, von Sanden C, Salim A, O'Kearney R (2007) Smoking as a risk factor for dementia and cognitive decline: A meta-analysis of prospective studies. American Journal of Epidemiology 166:367-378.

Anthony S, Schipper H, Tavares R, Hovanesian V, Cortez S, Stopa E, Johanson C (2003) Stress protein expression in the Alzheimer-diseased choroid plexus. Journal of Alzheimer's Disease 5:171-177.

Arndt V, Daniel C, Nastainczyk W, Alberti S, Hohfeld J (2005) BAG-2 acts as an inhibitor of the chaperone-associated ubiquitin ligase CHIP. Molecular Biology of the Cell 12:5891-5900.

Arnold C, Johnson G, Cole R, Dong D, Lee M, Hart G (1996) The microtubule-associated protein Tau is extensively modified with O-linked-N-acetylglucosamine. Journal of Biological Chemistry 271:28741-28744.

Arriagada P, Growdon J, Hedley-Whyte E, Hyman B (1992) Neurofibrillary tangles but not senile plaques parallel duration and severity of Alzheimer's disease. Neurology 42:631-639.

Atamna H, Nguyen A, Schultz C, Boyle K, Newberry J, Kato H, Ames B (2008) Methylene blue delays cellular senescence and enhances key mitochondrial biochemical pathways. FASEB 22:703-712.

Bagatell R, Paine-Murrieta G, Taylor C, Pulcini E, Akinaga S, Benjamin I, Whitesell L (2000) Induction of a heat shock factor-1 dependent stress response alters the cytotoxic activity of hsp90-binding agents. Clinical Cancer Research 6:3312-3318.

Ballatore C, Lee V, Trojanowski J (2007) Tau-mediated neurodegeneration in Alzheimer's disease and related disorders. Nature Reviews Neuroscience 8:663-672.

Ballinger C, Connell P, Wu Y, Hu Z, Thompson L, Yin L, Patterson C (1999) Identification of CHIP, a novel tetratricopeptide repeat-containing protein that interacts with heat shock proteins negatively regulates chaperone functions. Molecular and Cellular Biology 19:4535-4545.

Banerji U, O'Donnell A, Scurr M, Pacey S, Stapleton S, Asad Y, Simmons L, Maloney A, Raynaud F, Campbell M, Walton M, Lakhani S, Kaye S, Workman P, Judson I (2005) Phase I pharmacokinetic and pharmacodynamic study of 17-allylamino, 17-demethoxygeldanamycin in patients with advanced malignancies. Journal of Clinical Oncology 23:4152-4161.

Barghorn S, Mandelkow E (2002) Toward a unified scheme for the aggregation of Tau in Alzheimer paired helical filaments. Biochemistry 41:14885-14896.

Bergerat A, de Massy B, Gadelle D, Varoutas P, Nicolas A, Forterre P (1997) An atypical topoisomerase II from Archaea with implications for meitotic recombination Nature 386:414-417.

Bhaskar K, Yen S, Lee G (2005) Disease-related modifications in Tau affect the interaction between Fyn and Tau. Journal of Biological Chemistry 280:35119-35125.

Binder L, Frankfurter A, Rebhun L (1985) The distribution of Tau in the mammalian central nervous system. Journal of Cellular Biology 101:1371-1378.

Blurton-Jones M, LaFerla F (2006) Pathways by which Aβ facilitates Tau pathology. Current Alzheimer Research 3:437-448.

Brocchieri L, Conway de Macario E, Macario A (2008) *hsp70* genes in the human genome: Conservation and differentiation patters predict a wide array of overlapping and specialized functions. BMC Evolutionary Biology 8:19.

Bukau B, Weissman J, Horwich A (2006) Molecular Chaperones and Protein Quality Control. Cell 125:443-451.

Bulic B, Pickhardt M, Schmidt B, Mandelkow E, Waldmann H, Mandelkow E (2008) Development of Tau aggregation inhibitors for Alzheimer's disease. Angewandte Chemie International Edition 48:1740-1752.

Caplan A (2003) What is a co-chaperone? Cell Stress and Chaperones 8:105-107.

Cappello F, Conway de Macarlo E, Marasa L, Zummo G, Macario A (2008) Hsp60 expression, new locations, functions and perspectives in cancer diagnosis and therapy. Cancer Biology and Therapy 7:801-809.

Carrettiero D, Hernandez I, Neveu R, Papagiannakopoulos T, Kosik K (2009) The co-chaperone BAG2 sweeps paired helical filament-insoluble Tau from the microtubule. Journal of Neuroscience 29:2151-2161.

Cedazo-Menguez A, Cowburn R (2001) Apolipoprotein E. a major piece in the Alzheimer's disease puzzle. Journal of Cellular and Molecular Medicine 5:254-266.

Chandra D, Choy G, Tang D (2007) Cytosolic accumulation of HSP60 during apoptosis with or without apparent mitochondrial release: evidence that its pro-apoptotic or pro-survival functions involve differential interactions with caspase-3. Journal of Biological Chemistry 282:31289-31301.

Chui D-H, Tanahashi H, Ozawa K, Ikeda S, Checler F, Ueda O, Suzuki H, Araki W, Inoue H, Shirotani K, Takahashi K, Gallyas F, Tabira T (1999) Transgenic mice with Alzheimer presenilin 1 mutations show accelerated neurodegeneration without amyloid plaque formation. Nature Medicine 5:560-564.

Corder E, Saunders A, Strittmatter W, Schmechel D, Gaskell P, GW S, Roses A, Haines J, Pericak-Vance M (1993) Gene dose of apolipoprotein E type 4 allele and the risk of Alzheimer's disease in late onset families. Science 261:921-923.

Craig E, Huang P, Aron R, Andrew A (2006) The diverse roles of J-proteins, the obligate Hsp70 co-chaperone. Reviews in Physiology, Biochemistry and Pharmacology 156:1-21.

Cramer P, Cirrito J, Wesson D, Lee C, Karlo J, Zinn A, Casali B, Restivo J, Goebel W, James M, Brunden K, Wilson D, Landreth G (2012) ApoE-directed therapeutics rapidly clear β-amyloid and reverse deficits in AD mouse models. Science 335:1503-1506.

Cripps D, Thomas S, Jeng Y, Yang F, Davies P, Yang A (2006) Alzheimer disease-specific conformation of hyperphosphorylated paired helical filament-Tau is polyubiquitinated through Lys-48, Lys-11, and Lys-6 ubiquitin conjugation. Journal of Biological Chemistry 281:10825-10838.

Cruz J, Tseng H, Goldman J, Shih H, Tsai L (2003) Aberrant Cdk5 activation by p25 triggers pathological events leading to neurodegeneration and neurofibrillary tangles. Neuron 40:471-483.

Czarnecka A, Campanella C, Zummo G, Cappello F (2006) Heat shock protein 10 and signal transduction: a "capsula eburnea" of carcinogenesis? Cell Stress and Chaperones 11:287-294.

Daugaard M, Rohde M, Jaattela M (2007) The heat shock protein 70 family: Highly homologous proteins with overlapping and distinct functions. FEBS Letters 581:3702-3710.

Dayanandan R, Van Slegtenhorst M, Mack T, Ko L, Yen S, Leroy K, Brion J, Anderton B, Hutton M, Lovestone S (1999) Mutations in Tau reduce its microtubule binding properties in intact cells and affect its phosphorylation. FEBS Letters 446:228-232.

De Strooper B, Annaert W, Cupers P, Saftig P, Craessaerts K, Mumm J, Schroeter E, Schrijvers V, Wolfe M, Ray W, Goate A, Kopan R (1999) A presenilin-1

dependent γ-secretase-like protease mediate release of Notch intracellular domain. Nature 398:518-522.

De Strooper B, Iwatsubo T, Wolfe M (2012) Presenilins and γ-secretase: structure, function, and role in Alzheimer disease. Cold Spring Harbor Perspectives in Medicine 2:1-19.

De Strooper B, Saftig P, Craessaerts K, Vanderstichele H, Guhde G, Annaert W, Von Figura K, Van Leuven F (1998) Deficiency of presenilin-1 inhibits the normal cleavage of amyloid precursor proteins. Nature 391:387-390.

DeBoer C, Wnuk R, Peterson D (1970) Geldanamycin, a new antibiotic. Journal of Antibiotics 23:442-447.

Demand J, Alberti S, Patterson C, Hohfeld J (2001) Cooperation of a ubiquitin domain protein and an E3 ubiquitin ligase during chaperone/proteasome coupling. Current Biology 11:1569-1577.

Deocaris C, Kaul S, Wadhwa R (2006) On the brotherhood of the mitochondrial chaperones mortalin and heat shock protein 60. Cell Stress and Chaperones 11:116-128.

Dickey C, Dunmore J, Lu B, Wang J, Lee W, Kamal A, Burrows F, Eckman CB, Hutton M, Petrucelli L (2006) HSP induction mediates selective clearance of Tau phosphorylated at proline-directed Ser/Thr sites but not KXGS (MARK) sites. The FASEB Journal 20:753-755.

Dickey CA, Kamal A, Lundgren K, Klosak N, Bailey RM, Dunmore J, Ash P, Shoraka S, Zlatkovic J, Eckman CB, Patterson C, Dickson DW, Jr. NSN, Hutton M, Burrows F, Petrucelli L (2007) The high-affinity HSP90-CHIP complex recognizes and

selectively degrades phosphorylated Tau client proteins. The Journal of Clinical Investigation 117:648-658.

Dickson D, Crystal H, Mattiace L, Masur D, Blau A, Davies P, Yen S, Aronson M (1992) Identification of normal and pathological aging in prospectively studied nondemented elderly humans. Neurobiology of Aging 13:179-189.

Dickson D, Farlo J, Davies P, Crystal H, Fuld P, Yen S (1988) Alzheimer's disease. A double-labeling immunohistochemical study of senile plaques. American Journal of Pathology 132:86-101.

Dokmanovic M, Clarke C, Marks P (2007) Histone deacetylase inhibitors: overview and perspective. Molecular Cancer Research 5:981-989.

Dorval V, Fraser P (2006) Small ubiquitin-like modifier (SUMO) modification of natively unfolded proteins Tau and α-synuclein. Journal of Biological Chemistry 281:9919-9924.

Dorval V, Fraser P (2007) SUMO on the road to neurodegeneration. Biochimica et Biophysica Acta 1773:694-706.

Dou F, Netzer W, Tanemura K, Li F, Hartl U, Takashima A, Gouras G, Greengard P, Xu H (2003) Chaperones increase association of Tau protein with microtubules. Proceedings of the National Academy of Sciences 100:721-726.

Dubois B, Feldman H, Jacova C, Dekosky S, Barberger-Gateau P, Cummings J, Delacourte A, Galasko D, Gauthier S, Jicha G, Meguro K, O'Brien J, Pasquier F, Robert P, Rossor M, Salloway S, Stern Y, Visser P, Scheltens P (2007) Research criteria for the diagnosis of Alzheimer's disease: revising the NINCDS-ADRDA criteria. Lancet Neurology 6:734-746.

Elliott E, Tsvetkov P, Ginzburg I (2007) BAG-1 Associates with Hsc70Tau Complex and Regulates the Proteasomal Degradation of Tau Protein. The Journal of Biological Chemistry 282:37276-37284.

Erbse A, Mayer MP, Bakau B (2004) Mechanism of substrate recognition by the Hsp70 chaperones. Biochemical Society Transactions 32:617-621.

Ferrarini M, Heltai S, Zocchi M, Rugarli C (1992) Unusual expression and localization of heat-shock proteins in human tumor cells. International Journal of Cancer 51:613-619.

Gabriela-Fita I, Enciu A-M, Stanoiu B (2001) New insights on Alzheimer's disease diagnostic. Romanian Journal of Morphology and Embryology 52:975-979.

Galvan M, David J, Delacourte A, Luna J, Mena R (2001) Sequence of neurofibrillary changes in aging and Alzheimer's disease: a confocal study with phospho-Tau antibody, AD2. Journal of Alzheimer's Disease 3:417-425.

Gamerdinger M, Carra S, Behl C (2011) Emerging roles of molecular chaperones and co-chaperones in selective autophagy: focus on BAG proteins. Journal of Molecular Medicine 89:1175-1182.

Gao Q, Memmott J, Lafyatis F, Stamm S, Screaton G, Andreadis A (2000) Complex regulation of Tau exon 10, whose missplicing cause frontotemporal dementia. Journal of Neurochemistry 74:490-500.

Goedert M, Jakes R (2005) Mutations causing neurodegenerative Tauopathies. Biochimica et Biophysica Acta 1739:240-250.

Goedert M, Spillantini M, Jakes R, Rutherford D, Crowther R (1989a) Multiple isoforms of human microtubule-associated protein Tau: sequences and localization in neurofibrillary tangles of Alzheimer's disease. Neuron 3:519-526.

Goedert M, Spillantini M, Potier M, Ulrich J, Crowther R (1989b) Cloning and sequencing of the cDNA encoding an isoform of microtubule-associated protein Tau containing four tandem repeats: differential expression of Tau protein mRNAs in human brain. EMBO 8:393-399.

Goetz M, Toft D, Reid J, Ames M, Stensgard B, Safgren S, Adjei A, Sloan J, Atherton P, Vasile V, Salazaar S, Adjei A, Croghan G, Erlichman C (2005) Phase I trial of 17-allylamino-17-demethoxygeldanamycin in patients with advanced cancer. Journal of Clinical Oncology 23:1078-1087.

Gong C, Shaikh S, Wang J, Zaidi T, Grundke-Iqbal I, Iqbal K (1995) Phosphatase activity toward abnormally phosphorylated Tau: decrease in Alzheimer disease brain. Journal of Neurochemistry 65:732-738.

Gong C, Singh T, Grundke-Iqbal I, Iqbal K (1993) Phosphoprotein phosphatase activities in Alzheimer disease brain. Journal of Neurochemistry 61:921-927.

Gotz J, Chen F, van Dorpe J, Nitsch R (2001) Formation of neurofibrillary tangles in P301L Tau transgenic mice induced by Abeta 42 fibrils. Science 293:1491-1495.

Gotz R, Wiese S, Takayama S, Camarero G, Rossoll W, Schweizer U, Troppmair J, Jablonka S, Holtmann B, Reed JC, Rapp UR, Sendtner M (2005) Bag1 is essential for differentiation and survival of hematopoietic and neuronal cells. Nature Neuroscience 8:1169-1178.

Grelle G, Kostka S, Otto A, Kersten B, Genser K, Muller E, Walter S, Boddrich A, Stelzl U, Hanig C, Volker-Engert R, Landgraf C, Alberti S, Hohfeld J, Strodicke M, Wanker E (2006) Identification of VCP/p97, carboxyl terminus of Hsp70-interacting protein (CHIP), and amphiphysin II interaction partners using membrane-based human proteome arrays. Molecular and Cellular Proteomics 5:234-244.

Grem J, Morrison G, Guo X, Agnew E, Takimoto C, Thomas R, Szabo E, Grochow L, Grollman F, Hamilton J, Neckers L, Wilson R (2005) Phase I and pharmacologic study of 17-(allylamino)-17-demethoxygeldanamycin in adult patients with solid tumors. Journal of Clinical Oncology 23:1885-1893.

Groswasser Z, Reider-Groswasser I, Schwab K, Ommaya A, Pridgen A, Brown H, Cole R, Salazar A (2002) Quantitative imaging in late TBI. Part II: Cognition and work after closed and penetrating heat injury: A report of the Vietnam Head Injury Study. Brain Injury 16:681-690.

Grundke-Iqbal I, Iqbal K, Quinlan M, Tung Y, Zaidi M, Wisniewski H (1986a) Microtubule-associated protein Tau. A component of Alzheimer paired helical filaments. Journal of Biological Chemistry 261:6084-6089.

Grundke-Iqbal I, Iqbal K, Tung Y, Quinlan M, Wisniewski H, Binder L (1986b) Abnormal phosphorylation of the microtubule-associated protein Tau (Tau) in Alzheimer cytoskeletal pathology. Proceedings of the National Academy of Sciences 83:4913-4917.

Guskiewicz K (2005) Association between recurrent concussion and late-life cognitive impairment in retired professional football players. Neurosurgery 57:719-726.

Haass C, Hung A, Schlossmacher M, Teplow D, Selkoe D (1993) β-Amyloid peptide and a 3-kDa fragment are derived by distinct cellular mechanisms. Journal of Biological Chemistry 268:3021-3024.

Haass C, Schlossmacher M, Hung A, Vigo-Pelfrey C, Mellon A, Ostazewski B, Lieberburg I, Koo E, Schenk D, Teplow D, Selkoe D (1992) Amyloid β-peptide is produced by cultured cells during normal metabolism. Nature 359:322-325.

Hageman J, Kampinga H (2009) Computational analysis of the human HSPH/HSPA/DNAJ family and cloning of a human HSPH/HSPA/DNAJ expression library. Cell Stress and Chaperones 14:1-21.

Hall C, Lipton R, Sliwinski M, Katz M, Derby C, Verghese J (2009) Cognitive activites delay onset of memory decline in persons who develop dementia. Neurology 73:356-361.

Hanger D, Betts J, Loviny T, Blackstock W, Anderton B (1998) New phosphorylation sites identified in hyperphosphorylated Tau (paired helical filament-Tau) from Alzheimer's disease brain using nanoelectrospray mass spectrometry. Journal of Neurochemistry 71:2465-2476.

Hardy J, Higgins G (1992) Alzheimer's disease: the amyloid cascade hypothesis. Science 256:184-185.

Hardy J, Selkoe D (2002) The amyloid hypothesis of Alzheimer's disease: progress and problems on the road to therapeutics. Science 297:353-356.

Hartl F, Hayer-Hartl M (2002) Molecular chaperones in the cytosol; from nascent chain to folded protein. Science 295:1852-1858.

Hatakeyama S, Matsumoto M, Kamura T, Murayama M, Chui D-H, Planel E, Takahashi R, Nakayama KI, Takashima A (2004) U-box protein carboxyl terminus of Hsc70-interacting protein (CHIP) mediates poly-ubiquitination preferentially on four-repeat Tau and is involved in neurodegeneration of Tauopathy. Journal of Neurochemistry 91:299-307.

Havasi A, Li Z, Wang Z, Martin J, Botla V, Ruchalski K, Schwartz J, Borkan S (2008) Hsp27 inhibits Bax activation and apoptosis via a phosphatidylinositol 3-kinase dependent mechanism. Journal of Biological Chemistry 283:12305-12313.

Heath E, Gaskins M, Pitot H, Pili R, Tan W, Marschke R, Liu G, Hillman D, Sarkar F, Sheng S, Erlichman C, Ivy P (2005) A phase II clinical trial of 17-allylamino-17-demethoxygeldanamycin in patients with hormone-refractory metastatic prostate cancer. Clinical Prostate Cancer 4:138-141.

Hebert L, Scherr P, Bienias J, Bennett D, Evans D (2003) Alzheimer's disease in the U.S. population: Prevalence estimates using the 2000 Consensus. Archives of Neurology 60:1119-1122.

Hebert L, Scherr P, McCann J, Beckett L, Evans D (2001) Is the risk of developing Alzheimer's disease greater for women than for men? American Journal of Epidemiology 152:132-136.

Hendrie H, Albert M, Butters M, Gao S, Knopman D, Launer L, Yaffe K, Cuthbert B, Edwards E, Wagster M (2006) The NIH cognitive and emotional health project: report of the critical evaluation study committee. Alzheimer's and Dementia 2:12-32.

Himmler A (1989) Structure of the bovie Tau gene: alternatively spliced transcripts generate a protein family. Molecular and Cellular Biology 9:1389-1396.

Ho A, Shen J (2011) Presenilins in synaptic function and disease. Cell Press 17:617-624.

Hong M, Zhukareva V, Vogelsberg-Ragaglia V, Wszolek Z, Reed L, Miller B, Geschwind D, Bird T, McKeel D, Goate A, Morris J, Wilhelmsen K, Schellenberg G, Trojanowski J, Lee V (1998) Mutation-specific functional impairments in distinct Tau isoforms of hereditary FTDP-17. Science 282:1914-1917.

Hsia A, Masliah E, McConlogue L, Yu G, Tatsuno G, Hu K, Kholodenko D, Malenka R, Nicoll R, Mucke L (1999) Plaque-independent disruption of neural circuits in Alzheimer's disease mouse models. Proceedings of the National Academy of Sciences 96:3228-3233.

Hsiung G-Y, Sadovnick A (2007) Genetics and dementia: risk factors, diagnosis, and management. Alzheimer's and Dementia 3:418-427.

Hundley H, Walter W, Bairstow S, Craig E (2005) Human Mpp11 J protein: ribosome-tethered molecular chaperones are ubiquitous. Science 308:1032-1034.

Hunt C, Morimoto RI (1985) Conserved features of eukaryotic hsp70 genes revealed by comparison with the nucleotide sequence of human hsp70. PNAS 19:6455-6459.

Hutton M, Lendon C, Rizzu P, Baker M, Froelich S, Houlden H, Pickering-Brown S, Chakraverty S, Isaacs A, Grover A, Hackett J, Adamson J, Lincoln S, Dickson D, Davies P, Petersen R, Stevens M, de Graaff E, Wauters E, van Baren J, Hillebrand M, Joosse M, Kwon J, Nowotny P, Che L, Norton J, Morris J, Reed L, Trojanowski J, Basun H, Lannfelt L, Neystat M, Fahn S, Dark F, Tannenberg T,

Dodd P, Hayward N, Kwok J, Schofield P, Andreadis A, Snowden J, Craufurd D, Neary D, Owen F, Oostra B, Hardy J, Goate A, van Swieten J, Mann D, Lynch T, Heutink P (1998) Association of missense and 5'-splice-site mutations in Tau with the inherited dementia FTDP-17. Nature 393:702-705.

Institutes of Medicine (2008) Retooling for an aging American: Building the health care workforce. The National Acadamies Press.

Iqbal K, Alonso A, Chen S, Chohan M, El-Akkad E, Gong C, Khatoon S, Li B, Liu F, Rahman A, Tanimukai H, Grundke-Iqbal I (2005) Tau pathology in Alzheimer disease and other Tauopathies. Biochimica et Biophysica Acta 1739:198-210.

Iqbal K, Grundke-Iqbal I, Smith A, George L, Tung Y, Zaidi T (1989) Identification and localization of Tau peptide to paired helical filaments of Alzheimer disease. Proceedings of the National Academy of Sciences 86:5646-5650.

Iqbal K, Grundke-Iqbal I, Zaidi T, Merz P, Wen G, Shaikh S, Wisniewski H, Alafuzoff I, Winblad B (1986) Defective brain microtubule assembly in Alzheimer's disease. Lancet 2:421-426.

Iqbal K, Zaidi T, Bancher C, Grundke-Iqbal I (1994) Alzheimer paired helical filaments. Restoration of biological activity by dephosphorylation. FEBS Letters 349:104-108.

Jack CJ, Petersen R, Xu Y, O'Brien P, Smith G, Ivnik R, Boeve B, Tangalos E, Kokmen E (2000) Rates of hippocampal atrophy correlate with change in clinical status in aging and AD. Neurology 55:484-489.

Jarrett J, Berger E, Lansbury P (1993) The carboxy terminus of the beta amyloid protein is critical for seeding of amyloid formation: implications for the pathogenesis of Alzheimer's disease. Biochemistry 32:4693-4697.

Kampinga H, Craig E (2010) The HSP70 chaperone machinery: J proteins as drivers of functional specificity. Nature Reviews Molecular Cell Biology 11:579-592.

Katzman R, Terry R, DeTeresa R, Brown T, Davies P, Fuld P, Renbing X, Peck A (1988) Clinical, patholgocial, and neurochemical changes in dementia: a subgroup with preserved mental status and numerous neocortical plaques. Annals of Neurology 23:138-144.

Kaul Z, Yaguchi T, Kaul S, Wadhwa R (2006) Quantum dot-based protein imaging and functional significance of two mitochondrial chaperones in cellular senescence and carcinogenesis. Annual New York Academy of Sciences 1067:460-473.

Khalil A, Kabapy N, Deraz S, Smith C (2011) Heat shock proteins in oncology: Diagnost biomarker of therapeutic targets? Biochimica et Biophysica Acta 1816:89-104.

Khatoon S, Grundke-Iqbal I, Iqbal K (1992) Brain levels of microtubule-associated protein Tau are elevated in Alzheimer's disease: a radioimmno-slot-blot asssay for nanograms of protein. Journal of Neurochemistry 59:750-753.

Khatoon S, Grundke-Iqbal I, Iqbal K (1994) Levals of normal and abnormally phosphorylated Tau in different cellular and regounal compartments of Alzheimer's disease and control brains. FEBS Letters 351:80-84.

Khatoon S, Grundke-Iqbal I, Iqbal K (1995) Guanosine triphosphate binding to beta-subunit of tubulin in Alzheimer's disease brain: role of microtubule-associated protein Tau. Journal of Neurochemistry 64:777-787.

Kivipelto M, Ngandu T, Fratiglioni L, Viitanen M, Kareholt I, Winblad B, Helkala E, Tuomilehto J, Soininen H, Nissinen A (2005) Obesity and vascular risk factors at midlife and the risk of dementia and Alzheimer disease. Archives of Neurology 62:1556-1560.

Kopke E, Tung Y, Shaikh S, Alonso A, Iqbal K, Grundke-Iqbal I (1993) Microtubule-associated protein Tau. Abnormal phosphorylation of a non-paired helical filament pool in Alzheimer's disease. Journal of Biological Chemistry 268:24374-24384.

Krukenberg K, Street T, Lavery L, Agard D (2011) Conformational dynamics of molecular chaperone Hsp90. Quarterly Reveiws in Biophysics 44:229-255.

Kumar-Singh S, Dewachter I, Moechars D, Lübke U, De Jonghe C, Ceuterick C, Checler F, Naidu A, Cordell B, Cras P, Van Broeckhoven C, Van Leuven F (2000) Behavioral disturbances without amyloid deposits in mice overexpressing human amuloid precursor protein with Flemish (A692G) or Dutch (E693Q) mutation. Neurobiology of Disease 7:9-22.

Kuret J, Chirita C, Congdon E, Kannanayakal T, Li G, Necula M, Yin H, Zhong Q (2005a) Pathways of Tau fibrillization. Biochimica et Biophysica Acta 1739:167-178.

Kuret J, Congdon E, Li G, Yin H, Yu X, Zhong Q (2005b) Evaluating triggers and enhancers of Tau fibrillization. Microscopy Research and Technique 67:141-155.

Kushakawa G, Saito T, Onuki R, Ishiguro K, Kishimoto T, Hisanaga S (2000) Calpain-dependent proteolytic cleavage of the p35 cyclin-dependent kinase 5 activator to p25. Journal of Biological Chemistry 275:17166-17172.

Layfield R, Cavey JR, Lowe J (2003) Role of ubiquitin-mediated proteolysis in the pathogenesis of neurodegenerative disorders. 2003 2:343-356.

Lee G, Neve R, Kosik K (1989) The microtubule binding domain. Neuron 2:1615-1624.

Lee V, Balin B, Otvos LJ, Trojanowski J (1991) A68: a major subunit of paired helical filaments and derivatized forms of normal Tau. Science 251:675-678.

Levy E, Carman M, Fernandez-Madrid I, Power M, Lieberburg I, van Duinen S, Bots G, Luyendijk W, Franjione B (1990) Mutation of the Alzheimer's disease amyloid gene in hereditary cerebral hemorrhage, Dutch type. Science 248:1124-1126.

Lew J, Huang Q, Qi Z, Winkfein R, Aebersold R, Hunt T, Wang J (1994) A brain-specific activator of cyclin-dependent kinase-5. Nature 371:423-426.

Lewis J, McGowan E, Rockwood J, Melrose H, Nacharaju P, Van Slegtenhorst M, Gwinn-Hardy K, Murphy M, Baker M, Yu X, Duff K, Hardy J, Corral A, Lin W, Yen S, Dickson D, Davies P, Hutton M (2000) Neurofibrillary tangles, amyotrophy and progressive motor disturbance in mice expressing mutant (P301L) Tau protein. Nature Genetics 25:402-405.

Li G, Faibushevich A, Turunen B, Yoon S, Georg G, Michaelis ML, Dobrowsky R (2003) Stabilization of the cyclin-dependent kinase 5 activator, p35, by paclitaxel decreases beta-amyloid toxicity in cortical neurons. Journal of Neurochemistry 84:347-362.

Li X, Lu F, Wang J, Gong C (2006) Concurrent alterations of O-GlcNAcylation and phosphorylation of Tau in mouse brains during fasting. European Journal of Neuroscience 23:2078-2086.

Li Y, Xu M, Lai M, Huang Q, Castro J, DiMuzio-Mower J, Harrison T, Lellis C, Nadin A, Neduvelil J, Register R, Sardana M, Shearman M, Smith A, Shi X, Yin K, Shafer J, Gardell S (2000) Photoactivated γ-secretase inhibitors directed to the active site covalently label presenilin 1. Nature 405:689-694.

Liman J, Ganesan S, Dohm C, Krajewski S, Reed J, Bahr M, Wouters F, Kermer P (2005) Interaction of BAG1 and Hsp70 mediated neuroprotectivity and increases chaperone activity. Molecular and Cellular Biology 25:3715-3725.

Lindquist S (1986) The heat-shock response. Annual Review of Biochemistry 55:1151-1191.

Lindquist S, Craig EA (1988) The heat-shock proteins. Annual Review of Genetics 22.

Lindwall G, Cole R (1984) Phosphorylation affects the ability of Tau protein to promote microtubule assembly Journal of Biological Chemistry 259:5301-5305.

Liu F, Iqbal K, Grundke-Iqbal I, Hart G, Gong C (2004) O-GlcNAcylation regulates phosphorylation of Tau: a mechanism involved in Alzheimer's disease. Proceedings of the National Academy of Sciences 101:10804-10809.

Lu Y, Ansar S, Michaelis M, Blagg B (2008) Neuroprotective activity and evaluation of Hsp90 inhibitors in an immortalized neuronal cell line. Bioorganics and Medicinal Chemistry Letters 17:1709-1715.

Luders J, Demand J, Hohfeld J (2000) The Ubiquitin-related BAG-1 Provides a Link between the Molecular Chaperones Hsc70/Hsp70 and the Proteasome. The Journal of Biological Chemistry 275:4613-4617.

Lukiw WJ (2007) Micro-RNA speciation in fetal, adult and Alzheimer's disease hippocampus. Neuroreport 18:297-300.

Luo W, Dou F, Rodina A, Chip S, Joungnam K, Zhao Q, Moulick K, Aguirre J, Wu N, Greengard P, Chiosis G (2007) Roles of heat-shock protein 90 in maintaining and facilitating the neurodegenerative phenotype in Tauopathies. Proceedings of the National Academy of Sciences 104:9511-9516.

Luo W, Rodina A, Chiosis G (2008) Heat shock protein 90: translation from cancer to Alzheimer's disease treatment? BMC Neuroscience 9:S7.

Lye T, Shores E (2000) Traumatic brain injury as a risk factor for Alzheimer's disease: A review. Neuropsychology Review 10:115-129.

Maeda S, Sahara N, Saito Y, Murayama M, Ikai A, Takashima A (2006) Increased levels of granular Tau oligomers: an early sign of brain aging. Neuroscience Research 54:197-201.

Maeda S, Sahara N, Saito Y, Murayama M, Yoshiike Y, Kim H, Miyasaka T, Murayama S, Ikai A, Takashima A (2007) Granular Tau oligomers as intermediates of Tau filaments. Biochemistry 46:3856-3861.

Mailliot C, Trojanowski J, Lee V (2002) Impaired Tau protein function following nitration-induced oxidative stress *in vitro* and *in vivo*. Neurobiology of Aging 23:415.

Maloney A, Workman P (2002) HSP90 as a new therapeutic target for cancer therapy: the story unfolds. Expert Opin Biol Ther 2:3-24.

Marcu M, Chandli A, Bouhouche I, Catelli M, Neckers L (2000a) The heat shock protein 90 antagonist novobiocin interacts with a previously unrecognized ATP-binding domain in the carboxyl terminus of the chaperone. Journal of Biological Chemistry 275:37181-37186.

Marcu M, Schulte T, Neckers L (2000b) Novobiocin and related coumarins and depletion of heat shock protein 90-dependent signaling proteins. Journal of the National Cancer Institute 92:242-248.

Marlow L, Cain M, Pappolla M, Sambamurti K (2003) Beta-secretase processing of the Alzheimer's amyloid protein precursor (APP). Journal of Molecular Neuroscience 20:233-239.

Masters C, Simms G, Weinman N, Malthaup G, McDonald B, Beyreuther K (1985) Amyloid plaque core protein in Alzheimer disease and Down syndrome. Proceedings of the National Academy of Sciences 82:4245-4249.

Mathis C, Price J, Klunk W, Weissfield L, McNamee R, Wolk D, Cohen A, Lopresti B, Dekosky S (2008) Longitudinal PIB measures in control, MCI, and AD subjects. Journal of Nuclear Medicine 49:35P.

Mazanetz M, Fischer P (2007) Untangling Tau hyperphosphorylation in drug design for neurodegenerative diseases. Nature Review Drug Discovery 6:464-479.

Meyer A, Gillespie J, Walther D, Millet I, Doniach S, Frydman J (2003a) Closing the folding chamber of the eukaryotic chaperonin requires the transition state of ATP hydrolysis. Cell 113:369-381.

Meyer P, Prodromou C, Hu B, Vaughan C, Roe S, Panaretou B, Piper P, Pearl L (2003b) Structural and functional analysis of the middle segment of hsp90: implications for ATP hydroylsis and client protein and cochaperone interactions. Molecular Cell 11:647-658.

Miller D, Papayannopoulos I, Styles J, Bobin S, Lin Y, Biemann K, Iqbal K (1993) Peptide compositions of the cerebrovascular and senile plaque core amyloid

deposits of Alzheimer’s disease. Archives of Biochemistry and Biophysics 301:41-52.

Moechars D, Dewachter I, Lorent K, Reverse D, Baekelandt V, Naidu A, Tesseur I, Spittaels K, Haute C, Checler F, Godaux E, Cordell B, Van Leuven F (1999) Early phenotypic changes in transgenic mice that overexpress different mutants of amyloid precursor protein in brain. Journal of Biological Chemistry 274:6483-6492.

Morishima-Kawashima M, Hasegawa M, Takio K, Suzuki M, Yoshida H, Titani K, Ihara Y (1995) Proline-directed and non-proline-directed phosphorylation of PHF-Tau. Journal of Biological Chemistry 270:823-829.

Mosconi L, Pupi A, De Leon M (2008) Brain glucose hypometabolism and oxidative stress in preclinical Alzheimer's disease. Annal New York Academy of Sciences 1147:180-195.

Muchowski P (2002) Protein misfolding, amyloid formation, and neurodegeneration: a critical role for molecular chaperones? Neuron 35:9-12.

Muchowski P, Wacker J (2005) Modulation of neurodegeneration by molecular chaperones. Nature Reviews Neuroscience 6:11-22.

Münch G, Deuther-Conrad W, Gasic-Milenkovic J (2002) Glycoxidative stress creates a vicious cycle of neurodegeneration in Alzheimer's disease -- a target for neuroprotective treatment strategies? Journal of Neural Transmission 62:303-307.

Mymrikov E, Seut-Nebi A, Gusev N (2011) Large potentials of smal heat shock proteins. Physiology Reviews 91:1123-1159.

Nacharaju P, Lewis J, Easson C, Yen S, Hackett J, Hutton M, Yen S (1999) Accelerated filament formation from Tau proteins with specific FTDP-17 missense mutations. FEBS Letters 447:195-199.

National Institutes of Health (2009) Participating in alzheimer's disease clinical trials and studies fact sheet. National Institutes of Health.

National Institutes of Health (2010) Alzheimer's disease medication fact sheet. National Institutes of Health.

Naylor D, Hartl F (2001) Contribution of molecular chaperones to protein folding in the cytoplasm of prokaryotic and eukaryotic cells. Biochemical Society Symposia 68:45-68.

Noble W, Olm V, Takata K, Casey E, Mary O, Meyerson J, Gaynor K, LaFrancois J, Wang L, Kondo T, Davies P, Burns M, Veeranna N, Dickinson D, Matsuoka Y, Ahlijanian M, Lau L, Duff K (2003) Cdk5 is a key factor in Tau aggregation and tangle formation *in vivo*. Neuron 38:555-565.

Oddo S, Caccamo A, Kitazawa M, Tseng B, LaFerla F (2003a) Amyloid deposition precedes tangle formation in a triple transgenic model of Alzheimer's disease. Neurobiology of Aging 24:1063-1070.

Oddo S, Caccamo A, Shepard J, Murphy M, Golde TE, Kayed R, Metherate R, Mattson M, Akbari Y, LaFerla F (2003b) Triple-transgenic model of Alzheimer's disease with plaques and tangles: intracellular Abeta and synaptic dysfunction. Neuron 39:409-421.

Oddo S, Caccamo A, Tran L, Lambert M, Glabe C, Klein W, LaFerla F (2006) Temporal profile of amyloid-β (Aβ) oligomerization in an *in vivo* model of Alzheimer

disease: a link between Aβ and Tau pathology. Journal of Biological Chemistry 281:1599-1604.

Oliver C, Shenolikar S (1998) Physiologic importance of portein phosphatase inhibitors. Frontiers in Bioscience 3:D961-D972.

Orgogozo J, Gilman S, Dartigues J, Laurent B, Puel M, Kirby L, Jouanny P, Dubois B, Eisner L, Flitman S, Michel B, Boada M, Frank A, Hock C (2003) Subacute meningoencephalitis in a subset of patients with AD after Abeta42 immunization. Neurology 61:46-54.

Page J, Heath J, Fulton R, Yalkowsky E, Tabibi E, Tomaszewski J, Smith A, Rodman L (1997) Comparison of geldanamycin (NSC-122750) and 17-allylaminogeldanamycin (NSC-330507D) toxicity in rats. Proceedings of the American Association of Cancer Research 38:308.

Panaretou B, Siligardi G, Meyer P, Maloney A, Sullivan J, Singh S, Millson S, Clarke P, Naaby-Hansen S, Stein R, Cramer R, Mollapour M, Workman P, Piper P, Pearl L, Prodromou C (2002) Activation of ATPase activity of hsp90 by the stress-regulated cochaperone aha1. Molecular and Cellular Biology 10:1307-1318.

Pearl L, Prodromou C (2006) Structure and mechanism of the Hsp90 molecular chaperone machinery. Annual Review of Biochemistry 75:271-294.

Pei J, Braak E, Braak H, Grundke-Iqbal I, Iqbal K, Winblad B, Cowburn R (1999) Distribution of active glycogen synthase kinase 3beta (GSK-3beta) in brains staged for Alzheimer disease neurofibrillary changes. Journal of Neuropatholoy and Experimental Neurology 58:1010-1019.

Pei J, Gong C, An W, Winblad B, Cowburn R, Grundke-Iqbal I, Iqbal K (2003) Okadaic-acid-induced inhibition of protein phosphatase 2A produces activation of mitogen-activated protien kinases ERK1/2, MEK1/2, and p70 S6, similar to that in Alzheimer's disease. American Journal of Pathology 163:845-858.

Pei J, Grundke-Iqbal I, Iqbal K, Bogdanovic N, Winblad B, Cowburn R (1998) Accumulation of cyclin-dependent kinase 5 (cdk5) in neurons with early stages of Alzheimer's disease neurofibrillary degeneration. Brain Research 787:267-277.

Pendlebury S, Rothwell P (2009) Prevalence, incidence, and factors associated with pre-stroke and post-stroke dementia: A systematic review and meta analysis. Lancet Neurology 8:1006-1018.

Perez M, Hernandez F, Lim F, Diaz-Nido J, Avila J (2003) Chronic lithium treatment decreases mutant Tau protein aggregation in a transgenic mous model. Journal of Alzheimer's Disease 5:301-308.

Perez N, Sugar S, Charya S, Johnson G, Merril C, Bierer L, Perl D, Haroutunian V, Wallace W (1991) Increased synthesis and accumulation of heat shock 70 proteins in Alzheimer's disease. Brain Research Molecular Brain Research 1:249-254.

Petrucelli L, Dickson D, Kehoe K, Taylor J, Snyder H, Grover A, Lucia MD, McGowan E, Lewis J, Prihar G, Kim J, Dillmann WH, Browne SE, Hall A, Voellmy R, Tsuboi Y, Dawson TM, Wolozin B, Hardy J, Hutton M (2004) CHIP and Hsp70 regulate Tau ubiquitintation, degradation, and aggregation. Human Molecular Genetics 13:703-714.

Plassman B, Havlik R, Steffens D, Helms M, Newman T, Drosdick D, Phillips C, Gau B, Welsh-Bohmer K, Burke J, Guralnik J, Breitner J (2000) Documented head injury in early adulthood and risk of Alzheimer's disease and other dementias. Neurology 55:1158-1166.

Pockley A (2001) Heat shock proteins in health and disease: therapeutic targets or therapeutic agents? Expert Reviews of Molecular Medicine 3:1-21.

Polidori M, Pratico D, Mangialasche F, Mariani E, Aust O, Anlasik T, Mang N, Pientka L, Stahl W, Sies H, Mecocci P, Nelles G (2009) High fruit and vegetable intake is postively correlated with antioxidant status and cognitive performance in healthy subjects. Journal of Alzheimer's Disease 17:921-927.

Poorkaj P, Bird T, Wijsman E, Nemens E, Garruto R, Anderson L, Andreadis A, Wiederholt W, Raskind M, Schellenberg G (1998) Tau is a candidate gene for chromosome 17 frontotemporal dementia. Annals of Neurology 43:815-825.

Porter J, Fritz C, Depew K (2010) Discovery and development of HSP90 inhibitors: a promising pathway for cancer therapy. Current Opinions in Chemical Biology 14:1-9.

Raji C, Ho A, Neelroop N, Parikshak N, Becker J, Lopez O, Kuller L, Hua X, Leow A, Toga A, Thompson P (2010) Brain structure and obesity. Human Brain Mapping 31:353-364.

Ramanathan R, Trump D, Eiseman J, Belani C, Agarwala S, Zuhowski E, Lan J, Potter D, Ivy S, Ramalingam S, Brufsky A, Wong M, Tutchko S, Egorin M (2005) Phase I pharmacokinetic-pharmacodynamic study of 17-(allylamino)-17-demethoxygeldanamycin (17-AAG, NSC-330507), a novel inhibitor of heat shock

protein 90, in patients with refractory advanced cancers. Clinical Cancer Research 11:3385-3391.

Ranford J, Henderson B (2002) Chaperonins: in disease: mechanisms, models, and treatments. Molecular Pathology 55:209-213.

Rde CG, Gomes SL (2007) Comparative expression analysis of members of the Hsp70 family in the chytridiomycete Blastocladiella emersonii. Gene 386:24-34.

Reimenschneider M, Lautenschlager N, Wagenpfeil S, Diehl J, Drzezga A, Kurz A (2001) Cerebrospinal fluid Tau and beta-amyloid 42 proteins identify Alzheimer disease in subjects with mild cognitve impairment. Archives of Neurology 59:1729-1734.

Rinne J, Brooks D, Rosser M, Fox N, Bullock R, Klunk W, Mathis C, Blennow K, Barakos J, Okello A, Llano S, Liu E, Koller M, Gregg K, Schenk D, Black R, Grundman M (2010) 11-C-PiB PET assessment of change in fibrillar amyloid-β load in patients with Alzheimer's disease treated with bapineuzumab: a phase 2, double-blind, placebo-controlled, ascending-dose study. Lancet Neurology 9:363-372.

Roberts G, Allsop D, Bruton C (1990) The occult aftermath of boxing. Journal of Neurology, Neurosurgery & Psychiatry 53:373-378.

Ross C, Poirier M (2004) Protein aggregation and neurodegenerative disease. Nature Medicine 10:S10-S17.

Rusanen M, Kivipelto M, Quesenberry C, Zhou J, Whitmer R (2010) Heavy smoking in midlife and long-term risk of Alzheimer disease and vascular dementia. Archives of Internal Medicine 171:333-339.

Sahara N, Murayama M, Mizoroki T, Urushitani M, Imai Y, Takahashi R, Murata S, Tanaka K, Takashima A (2005) In vivo evidence of CHIP up-regulation attenuating Tau aggregation. Journal of Neurochemistry 94:1254-1263.

Schipper H (2011) Apolipoprotein E: Implications for AD neurobiology, epidemiology and risk assessment. Neurobiology of Aging 32:778-790.

Schulte T, Neckers L (1998) The benzoquinone ansamycin 17-allylamino-17-demethoxygeldanamycin binds to HSP90 and shares important biological activities with geldanamycin. Cancer Chemotherapeutics and Pharmacology 42:273-279.

Selkoe D (2001) Alzheimer's disease: genes, proteins and therapy. Journal of Physiological Reviews 81:741-766.

Seshandri S, Drachman D, Lippa C (1995) Apolipoprotein E epsilon 4 allele and the lifetime risk of Alzheimer's disease. What physicians know, and what they should know. Archives of Neurology 52:1074-1079.

Seshandri S, Wolf P, Beiser A, Au R, McNulty K, White R, D'Agostino R (1997) Lifetime risk of dementia and Alzheimer's disease. The impact of mortality on risk estimates in the Framingham Study. Neurology 49:1498-1504.

Seyb K, Ansar S, Li G, Bean J, Michaelis ML, Dobrowsky R (2007) p35/Cyclin-dependent kinase 5 is required for protection against beta-amyloid-induced cell death but not Tau phosphorylation by ceramide. Journal of Molecular Neuroscience 31:23-35.

Shioi J, Georgakopoulos A, Mehta P, Kouchi Z, Litterst C, Baki L, Robakis N (2007) FAD mutants unable to increase neurotoxic Abeta 42 suggest that mutation

effects on neurodegeneration may be independent of effect on Abeta. Journal of Neurochemistry 101:674-681.

Sinha S, Anderson J, Barbour R, Basi G, Caccavello R, Davis D, Doan M, Dovey H, Frigon N, Hong J, Jacobson-Croak K, Jewett N, Keim P, Knops J, Lieberburg I, Power M, Tan H, Tatsuno G, Tung J, Schenk D, Seubert P, Suomensaari S, Wang S, Walker D, Zhao J, McConlogue L, John V (1999) Purification and cloning of amyloid precursor protein beta-secretase from human brain. Nature 402:537-540.

Solomon A, Kivipelto M, Wolozin B, Zhou J, Whitmer R (2009) Midlife serum cholesterol and increased risk of Alzheimer's and vascular dementia three decades later. Dementia and Geriatric Disorders 28:75-80.

Sonderman H, Scheufler C, Schneider C, Hohfeld J, Hartl F, Moarefi I (2001) Stucture of Bag/Hsc70 complex: convergent functional evolution of Hsp70 nucleotide exchange factors. Science 291:1552-1557.

Spillantini M, Murrell J, Goedert M, Farlow M, Klug A, Ghetti B (1998) Mutation in the Tau gene in familial multiple system Tauopathy with presenile dementia. Proceedings of the National Academy of Sciences 95:7737-7741.

Sreedhar A, Kalma R, Csermely P, Shen Y (2004) Hsp90 isoforms: functions, expression, and clinical importance. FEBS Letters 562:11-15.

Supko J, Hickman R, Grever M, Malspeis L (1995) Preclinical pharmacological evaluation of geldanamycin as an antitumor agent. Cancer Chemotherapeutics and Pharmacology 36:305-315.

Takayama S, Bimston D, Matsuzawa S-i, Freeman B, Aime-Sempe C, Xie Z, Morimoto RI, Reed JC (1997) Bag-1 modulates the chaperone activity of Hsp70/Hsc70. The EMBO Journal 16:4887-4896.

Takayama S, Krajewski S, Krajewski M, Kitada S, Zapata J, Kochel K, Knee D, Scudiero D, Tudor G, Miller G, Miyashita T, Yamada M, Reed J (1998) Expression and location of Hsp70/Hsc-binding anti-apoptotic protein BAG-1 and its variants in normal tissues and tumor cell lines. Cancer Research 58:3116-3131.

Takayama S, Reed J (2001) Molecular chaperone targeting and regulation by BAG family proteins. Nature Cell Biology 3:E237-E241.

Takayama S, Xie Z, Reed JC (1999) An Evolutionarily Conserved Family of Hsp70/Hsc70 Molecular Chaperone Regulators. The Journal of Biological Chemistry 274:781-786.

Taldone T, Gozman A, Maharaj R, Chiosis G (2008) Targeting HSP90: small-molecule inhibitors and their clinical development. Current Opinions in Pharmacology 8:370-374.

Tatebayashi Y, Haque N, Tung Y, Iqbal K, Grundke-Iqbal I (2004) Role of Tau phosphorylation by goycogen synthase kinase-3beta in the regulation of organelle transport. Journal of Cellular Science 117:1653-1663.

Tavaria M, Gabriele T, Kola I, Anderson RL (1996) A hitchhiker's guide to the human Hsp70 family. Cell Stress and Chaperones 1:23-28.

Urban M, Li C, Yu C, Lu Y, Krise J, McIntosh M, Rajewski R, Blagg BS, Dobrowsky R (2010) Inhibiting heat-shock protien 90 reverses sensory hypoalgesia in diabetic mice. ASN Neuro 2:189-199.

von Bergen M, Barghorn S, Li L, Marx A, Biernat J, Mandelkow E, Mandelkow E (2001) Mutations of Tau protein in frontotemporal dementia promote aggregation of paired helical filaments by enhancing local β-structure. Journal of Biological Chemistry 276:48165-48174.

Wadhwa R, Takano S, Kaur K, Aida S, Yaguchi T, Kaul Z, Hirano T, Taira K, Kaul S (2005) Identification and characterization of molecular interactions between mortalin/mtHsp70 and Hsp60. Biochemical Journal 391:185-190.

Wandinger S, Richter K, Buchner J (2008) The Hsp90 chaperone machinery. The Journal of Biological Chemistry 283:18473-18477.

Wang J, Wu Q, Smith A, Grundke-Iqbal I, Iqbal K (1998) Tau is phosphorylated by GSK-3 at several sites found in Alzheimer disease and its biological activity markedly inhibitied only after it is prephosphorylated by A-kinase. FEBS Letters 436:28-34.

Wei M, Andreadis A (1998) Splicing of a regulated exon reveals additional complexity in the axonal microtubule-associated protein Tau. Journal of Neurochemistry 70:1346-1356.

Weingarten M, Lockwood A, Hwo S, Kirschner M (1975) A protein factor essential for microtubule assembly. Proceedings of the National Academy of Sciences 72:1865-1862.

Whitmer R, Gustafson D, Barrett-Conner E, Haan M, Gunderson E, Yaffe K (2008) Central obesity and increased risk of dementia more than three decades later. Neurology 71:1057-1064.

Wolfe M, Xia W, Ostazewski B, Diehl T, Kimberly W, Selkoe D (1999) Two transmembrane aspartates in presenilin-1 required for presenilin endoproteolysis and γ-secretase activity. Nature 398:513-517.

Woodgett J (1990) Molecular cloning and expression of glycogen synthase kinase-3/factor A. EMBO 9:2431-2438.

Wu W, Brickman A, Luchsinger J, Ferrazzano P, Pichiule P, Yoshita M, Brown T, DeCarli C, Barnes C, Mayeux R, Vannucci S, Small S (2008) The brain in the age of old: The hippocampal formation is targeted differentially by diseases of late life. Annals of Neurology 64:698-706.

Yaffe K (2007) Metabolic syndrome and cognitive decline. Current Alzheimer Research 4:123-126.

Yaffe K, Lindquist K, Schwartz A, Vitartas C, Vittinghoff E, Satterfield S, Simonsick E, Launer L, Rosano C, Cauley J, Harris T (2011) Advanced glycation end product level, diabetes, and accelerated cognitive aging. Neurology 77:1351-1356.

Yu C, Kim S, Ikeuchi T, Xu H, Gasparini L, Wang R, Sisodia S (2001) Characterization of a presenilin-mediated amyloid precursor protein carboxyl-terminal fragment gamma. Evidence for distinct mechanisms involved in gamma-secretase processing of the APP and Notch1 transmembrane domains. Journal of Biological Chemistry 276:43756-43760.

Zannis V, Kardassis D, Zanni E (1993) Genetic mutations affecting human lipoproteins, their receptors, and their enzymes. Advances in Human Genetics 21:145-319.

CHAPTER TWO: Novel C-Terminal Hsp90 Modulators are Neuroprotective in Cellular Models of Alzheimer's Disease

I. Introduction

Alzheimer's disease (AD), like most age-related neurodegenerative disorders, is associated with the deposition of two pathological proteins; senile plaques (SPs) composed of β-amyloid peptides, and neurofibrillary tangles (NFTs) comprised of hyper-phosphorylated Tau protein. These aggregates lead to synaptic dysfunction, and ultimately to cognitive decline (Muchowski, 2002). The manifestation of these misfolded aggregates in neurodegenerative disorders implies that the cellular machinery responsible for proper protein folding may become jeopardized as neurons age, therefore increasing the vulnerability of the brain to "proteotoxicity" (Spires et al., 2006, Peterson and Blagg, 2009).

Recent studies have demonstrated that stimulation of the cellular protein quality control system, particularly the molecular chaperone family of heat shock proteins (HSPs), helps to prevent or protect against these misfolded toxic aggregates (Muchowski and Wacker, 2005a, Wilhelmus et al., 2007, Salminen et al., 2011). This system consists of multiple protein complexes with Hsp90 as the major regulator (Peterson and Blagg, 2009). Inhibitors of Hsp90 were originally developed as cancer therapeutics, but some compounds increase levels of molecular chaperones involved in protein re-folding or clearance such as Hsp70 and its co-chaperone Hsp40 (Fan et al., 2003).

Previously identified compounds that inhibit the N-terminal ATPase of Hsp90, such as geldanamycin (GA), have been effective in providing protection against pathological aggregates in AD brain; however, these compounds have a small therapeutic window (Supko et al., 1995). Therefore, our studies have focused on Hsp90 inhibitors designed against the C-terminus of the protein, and are derivatives of the well-characterized C-terminal Hsp90 inhibitor, novobiocin (Marcu et al., 2000a).

A previous report from our lab identified a novel C-terminal Hsp90 inhibitor, A4, which demonstrated neuroprotective effects *in vitro*. This compound did not decrease neuronal survival even at concentrations up to 10 μM, whereas GA caused ~80% death (Ansar et al., 2007). Recently, we discovered a novel novobiocin analog, KU-32, that displayed greater potency in neuronal protection against Aβ toxicity (Figure 1.1). The purpose of our studies was to characterize the neuroprotective effects of various novobiocin analogs, namely KU-32.

II. Materials and Methods

Preparation of primary neuronal cultures

Primary cortical neurons were prepared from day 18 embryonic rat fetuses (Harlan Sprague Dawley) as described previously (Michaelis et al., 1994, Michaelis et al., 1998, Michaelis et al., 2005). All animal procedures were approved by the Institutional Animal Care and Use Committee (IACUC) in compliance with the regulations and standards of care and use of laboratory rodents as outlined by the National Institutes of Health. After the final dissociation step, cells were re-suspended in DMEM/F12 medium (Sigma-Aldrich, St. Louis, MO) supplemented with 10% fetal

bovine serum (Atlanta Biologicals, Lawrenceville, GA). Neurons were plated at a density of 250,000 cells per 35mm^2 glass-bottom dishes (Mat-Tek Co., Ashland, MA) coated with 10 µg/mL poly-D-lysine (PDL) and 5 µg/mL laminin. Twenty-four hours after initial plating, the serum-containing medium was removed and replaced with Neurobasal medium containing 2% B-27 supplements (Invitrogen, Carlsbad, CA). Cells were grown at 37°C in 5% CO_2 and 97% humidity.

Aβ peptide preparation and cell culture treatments

The Aβ peptides were purchased from Anaspec (Fremont, CA). The $Aβ_{1-42}$ and $Aβ_{25-35}$ peptides were dissolved in 50mM Tris-HCL pH 7.4 and aliquots stored at -80°C. Prior to adding these peptides to the tissue culture medium, they were incubated at 37°C for 24 hours to allow them to oligomerize.

Primary neurons were allowed to grow 7 days *in vitro* (DIV7) before any treatments. Cultures were pretreated for 2 hours with vehicle (5% Captisol®) or a novobiocin derivative (KU-32, KU426, KU-430, and KU-433) dissolved in 5% Captisol® followed by the addition of 10 or 25 µM Aβ peptides and incubated for 48 or 96 hours as indicated in the figures. In a separate experiment, following pre-treatment for 2 hours with the novobiocin derivatives, 200 nM thapsigargin (Tg), an inhibitor of the sarco-ER-calcium-ATPase (SERCA), was added for 20 or 24 hours as noted in the figure legend. Additional experiments were performed with KU-426, KU-430, and KU-433 in which each compound was incubated for 2 hours before the addition of 25 nM Okadaic Acid (OA), a protein phosphatase 2A inhibitor, for 24 hours.

Measurement of cell viability

After treatments, the Live-Dead assay was performed as previously described (Michaelis et al., 1998, Michaelis et al., 2005). Briefly, 20 μM propidium iodide and 150 nM calcein acetoxy-methylester (Invitrogen, Carlsbad, CA) were added to label the live neurons with green fluorescence and dead neurons with red. Images were captured from 8 fields per dish, and the number of dead and viable cells counted. The percent of live cells was calculated in each dish. All experiments were completed from 3 neuronal preparations, with ~1,000 cells assessed per treatment condition. Data were graphed as the percent viable cells calculated from the total number of neurons counted per treatment condition (SigmaPlot 11). Significant differences between treated and control cells were determined using Student's *t*-test. One-way ANOVA analysis with a Bonferroni post-hoc test was used to determine statistical significant between treated groups as demonstrated in the figure legend.

Transfection of neuroblastoma cells

The neuroblastoma SH-SY5Y cell line (ATCC, Monasses, VA) was used for studies with transfected mutant Tau. The cells were grown on 100 mm^2 dishes with 15 mL of DMEM/F12 medium (Sigma-Aldrich, St. Louis, MO) supplemented with 10% fetal bovine serum (Atlanta Biologicals, Lawrenceville, GA). When the SY5Y cells reached 90-95% confluency, wild type and mutant P301L Tau isoforms without exons 2 or 3, but with exon 10 (-2-3 P301L and -2-3 Tau4 DNA plasmids; gifts from Dr. Mike Hutton, Eli Lilly Co.), were prepared for transfecting the cells. Initially the cells were diluted in 1.5 mL of Opti-MEM I Reduced Serum medium (Invitrogen, Carlsbad, CA), termed Mixture

1. A second mixture, Mixture 2, of Lipofectamine 2000 diluted in the appropriate Opti-MEM I medium was prepared with a final ratio of 1:3 (DNA (µg): Lipofectamine 2000 (µL)), and the mixture was incubated ~25 minutes at room temperature. After the 25-minute incubation, Mixture 1 and Mixture 2 were combined and permitted to incubate for 20 minutes at room temperature. Finally, the DNA/Lipofectamine 2000 mixture complex was added to 100 mm^2 dishes of the SY5Y cells. These cells were placed in the incubator at 37°C in 5% CO_2 and 97% humidity for about 6 hours. The medium was replaced with 0.2 mg/mL of the selection compound G418 (Sigma-Aldrich, St. Louis, MO) in DMEM/F12 medium with 10% fetal bovine serum. The DNA transfection plasmids contain a neomycin resistant gene, allowing them to grow in the presence of G418; therefore the non-transfected cells die leaving only transfected cells growing. In order to produce a stably transfected cell line, twenty-four hours post-transfection, the concentration of G418 in the medium was increased to 0.5 mg/mL. The cells remained growing in this concentration of G418 to maintain the stable transfection.

Verification of successful transfection

PCR analysis

The SY5Y, wild type Tau and P301L Tau-transfected cells were genotyped using reverse transcription-PCR-amplification. Purified plasmids for the wild type Tau and P301L Tau transfectants were used a positive control. For the presence of the pcDNA3.1 vector, the following primers were used: forward primer, PCDNAF, 5'-CTAGAGAACCCACTGCTTACTG-3'; reverse primer, TauAmR, 5'-

CAGGGAGGCAGACACCTC-3'. A 1300 bp band indicated the presence of the vector, as well as a successful transfection.

Immunoblot analysis

The SY5Y, wild type Tau, and P301L Tau transfectants were washed twice in phosphate buffered saline (PBS), lysed in kinase lysis buffer (20 mM Tris-HCl pH 7.4, 140 mM NaCl, 1 mM PMSF, 1 mM sodium orthovanadate, 10 mM NaF, 0.1% Nonidet-40, 1 mM EDTA, 26 uM ALLN, protease inhibitors cocktail set III (Calbiochem), and phosphatase inhibitors cocktail III (Sigma)), and collected by scraping the dishes, recovering, and homogenizing all contents. The protein concentration was determined using the bicinchoninic acid assay (BCA) from Thermo Fisher Scientific. Reducing sample buffer (50mM Tris-HCl at pH 6.8, 6.7% glycerol, 2.7% SDS, 0.05% Bromophenol Blue, and 250 mM dithiothreitol) was added to 25 µg aliquots of each sample and resolved by SDS-PAGE. The proteins were transferred to polyvinylidene fluoride (PVDF) membrane as described previously (Zaidi and Michaelis, 1999). The membrane was probed with: PHF-1, an antibody that recognizes pS396/404 hyperphosphorylated Tau; Tau5, an antibody for total Tau; and Actin, which served as a loading control. Immunoreactive proteins were detected using chemiluminescence. All primary incubations were completed on the same membrane using One Minute Stripping Buffer (GM Biosciences) to remove the previous antibody reaction.

Lactate dehydrogenase assay for necrotic cell death

The SY5Y and transfected cells were plated at a density of 400,000 cells per well in a 48-well plate. Twenty-four hours after plating, the cells were differentiated by placing the cells in serum-free medium (Schubert et al., 1969, Seeds et al., 1970, Evangelopoulos et al., 2005). The cells were differentiated for 24 hours and were treated with 100 nM KU-32 or 5% Captisol®. Two, 4, 6, and 12 hours post-treatment the LDH assay was performed by measuring release of LDH into the medium as an indication of the loss of cell membrane integrity. The LDH activity was determined by removing the medium, and centrifuging it at 1,000 rpm for 30 seconds. Each sample was placed into 3 wells on a 96-well plate. Fresh medium was used as the blank, and medium from cells treated with 1% Triton-X 100, which releases all the LDH, was used as an indicator for maximal loss of membrane integrity. To measure LDH in the medium, the substrate/enzyme solution (1.2 mM INT, 104 mM L-Lactate, 20 mM NAD+ (all from Sigma-Aldrich, St. Louis, MO), Diaphorase (Worthington, Lakewood, NJ), and 0.2M Tris, (pH 8.6) was added to each well and the mixture incubated at room temperature in the dark for 30 minutes. The stop solution (6% acetic acid/0.5% Triton-X 100) was added, and the plate was read at 490 nm. Results were graphed as percent cell death (SigmaPlot 11). All treatments were performed in triplicate.

MTT assay for succinate dehydrogenase

The SY5Y cells, -2-3 Tau4, and -2-3 P301L-transfected cells were grown at a density of 500,000 cells per 35-mm^{2-}dish. Twenty-four hours after plating, the cells were differentiated in non-serum containing medium. Differentiation was allowed to proceed

for 24 hours (Schubert et al., 1969, Seeds et al., 1970, Evangelopoulos et al., 2005), and then the cells were treated with either 100 nM KU-32 or 5% Captisol for 2, 4, and 6 hours. After the indicated treatments, the medium was aspirated. The cells were washed once with warm non-phenol red-containing medium, and 1.5 mL of the assay solution (1 to 10 dilution of 5 mg/mL MTT in non-phenol red containing medium) was added. The cells were placed at 37°C for 1 to 3 hours to allow crystal formation. After crystals formed, the assay solution was aspirated and replaced with 1 mL solvent (0.4 M HCl in absolute isopropanol). The mixture was triturated to dissolve crystals completely, transferred to Eppendorf tubes, and centrifuged at 13,000 rpm for 2 minutes. The samples were read at 570 nm (and 650 nm for background subtraction). Results were normalized to no treatment and graphed as percent cell death. Each treatment condition was repeated 6 times, and the statistical significance between treatment groups was determined using Student's *t*-test.

III. Results

KU-32 protection against various toxic agents in primary neuronal culture

In AD brain, Aβ oligomers are believed to lead to synaptic loss and neuronal cell death. The death of the neuron is often due to calcium dysregulation as a result of various types of stress (Seyb et al., 2006, Zempel et al., 2010). In our study, we used two different ways to increase intraneuronal calcium levels: either $A\beta_{1-42}$, $A\beta_{25-35}$ peptides or Tg, an inhibitor of the sarco-ER calcium-ATPase (SERCA). Our goal was to determine if KU-32 protects against these toxic compounds in a fashion similar to the previously identified novobiocin derivative, A4 (Ansar et al., 2007). Primary cortical

neurons were treated with varying doses of KU-32 ranging from 1 nM to 100 nM dissolved in 5% Captisol®. Primary neurons were pre-treated for 2 hours before Aβ peptides or Tg was added. Live-Dead assays were performed to test cell viability. Figure 2.1 demonstrates that KU-32 is protective against $A\beta_{1-42}$, $A\beta_{25-35}$ and Tg in a dose dependent fashion with an estimated EC_{50} ~ 0.1nM.

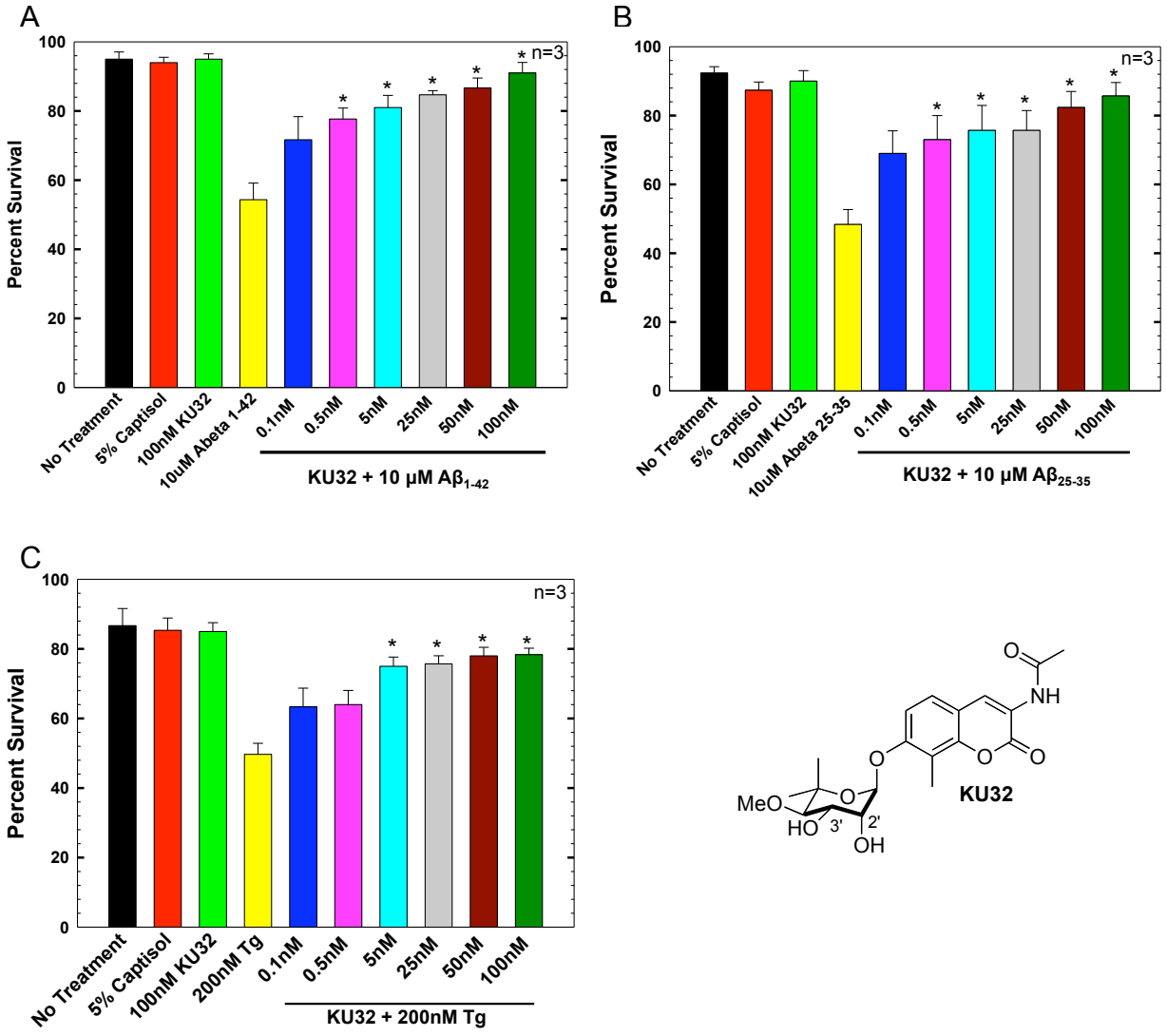

Figure 2.1: Dose dependent protection exhibited by KU-32 against Aβ peptides and Tg. Primary cortical neurons were pre-treated for 2 hours with the indicated doses of KU-32 dissolved in 5% Captisol® (vehicle) followed by incubation in (A) 10 μM $A\beta_{1-42}$, (B) 10 μM $A\beta_{25-35}$, or (C) 200nM Tg. The Aβ peptides were incubated with cells for 48 hours and Tg was present for 24 hours. The Live-Dead assay was used to determine

percent survival. All experiments were completed in triplicate. Statistical analyses were completed using a one-way ANOVA with Bonferroni. * p <0.05.

Analogs of KU-32 provide differential protection against various toxic agents

The synthesis for KU-32 is a lengthy, multi-step process. In an effort to decrease the synthesis time, analogs were produced that require fewer steps for production. We tested these analogs in the Live-Dead assay to see if any provided similar protection as KU-32. We used 100 nM concentrations and pre-treated primary cortical neurons for 2 hours prior to stimulation with the toxic Aβ peptides, Tg and the protein phosphatase 2A (PP2A) inhibitior, okadaic acid (OA). As shown in Figure 2.2, the analog KU-426 provided significant protection against Tg- and $A\beta_{1-42}$-induced cell death. However, unlike KU-32, KU-426 did not provide statistically significant protection against $A\beta_{25-35}$ toxicity (Figure 2.2). A second novobiocin derivative, KU-430 significantly protected neurons against the two Aβ peptides and Tg-induced toxicity (Figure 2.3), similarly to KU-32. A third novobiocin analog, KU-433, was significantly protective against Tg only (Figure 2.4). Surprisingly, KU-433 did not significantly protect against the Aβ peptides, and was less like KU-32 than the other test novobiocin derivatives. Interestingly, none of the compounds were able to protect against OA. Overall, these results reveal that the derivative KU-430 provided the best protection against the same toxic agents as KU-32.

It should be noted that the no treatment groups used in the novel drug treatment studies had lower survival than those in the dose response studies (Figures 2.2-2.5) completed with only KU-32 (Figure 2.1). In the KU-32 dose dependent protection studies, the no treatment group displayed about 90% to 95% survival while the novel

novobiocin derivative studies showed about 55% to 60% survival. These differences in survival can be attributed to poorly optimized culture conditions. Also, as a result of the lowered survivability of the cell preparations used for the novobiocin derivative studies, these cell populations were less susceptible to 10 μM $A\beta_{25-35}$ treatments. Therefore, we increased the concentration to 25 μM $A\beta_{25-35}$ in order to test for statistically significant toxicity in these neuronal cultures.

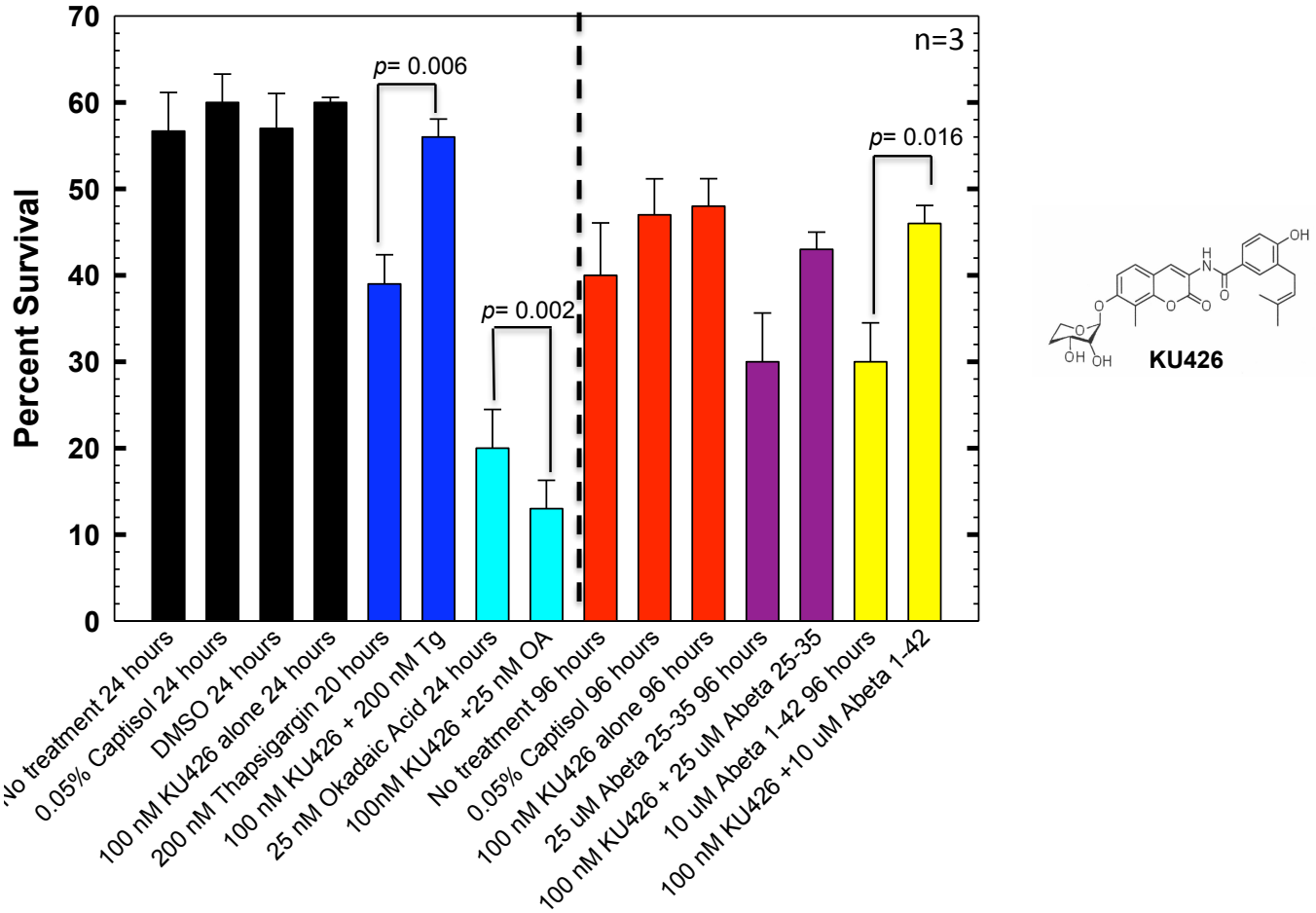

Figure 2.2: KU-426, a protective analog of KU-32. Primary cortical neurons were pre-treated with 100 nM of KU-426 dissolved in 5% Captisol® (vehicle) for 2 hours before incubation in 200 nM Tg for 20 hours, 25 nM OA for 24 hours, 25 μM $A\beta_{25-35}$ or 10 μM $A\beta_{1-42}$ for 96 hours. The Live-Dead assay was used to determine percent survival. Experiments were completed in triplicate. *p* values are indicated on graph.

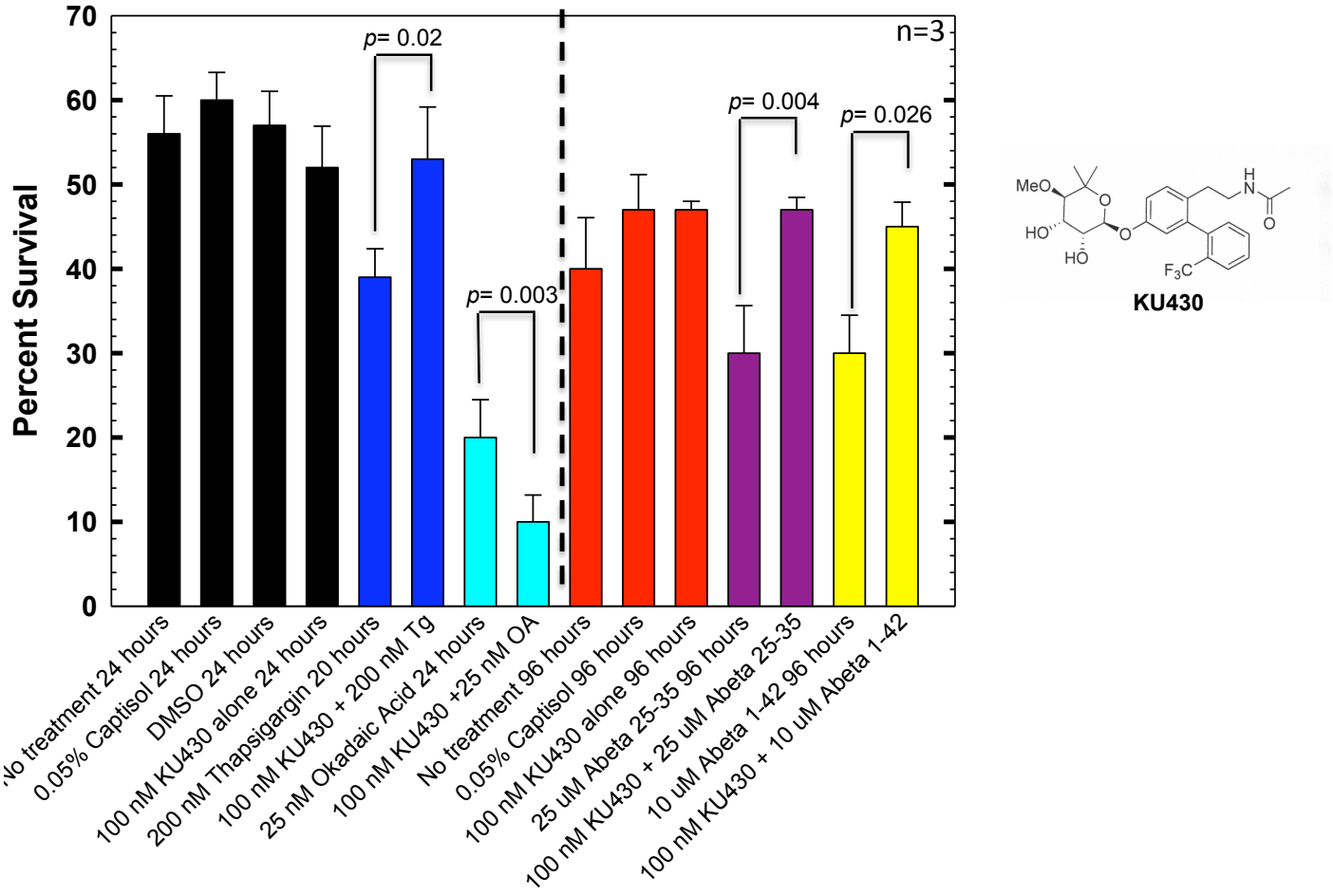

Figure 2.3: KU-430 a neuroprotective novobiocin derivative similar to KU-32. Primary cortical neurons were pre-treated with 100 nM of KU-430 dissolved in 5% Captisol® (vehicle) for 2 hours before incubation in 200 nM Tg for 20 hours, 25 nM OA for 24 hours, 25 μM $A\beta_{25\text{-}35}$ or 10 μM $A\beta_{1\text{-}42}$ for 96 hours. The Live-Dead assay was used to determine percent survival. Experiments were completed in triplicate. *p* values are indicated on graph.

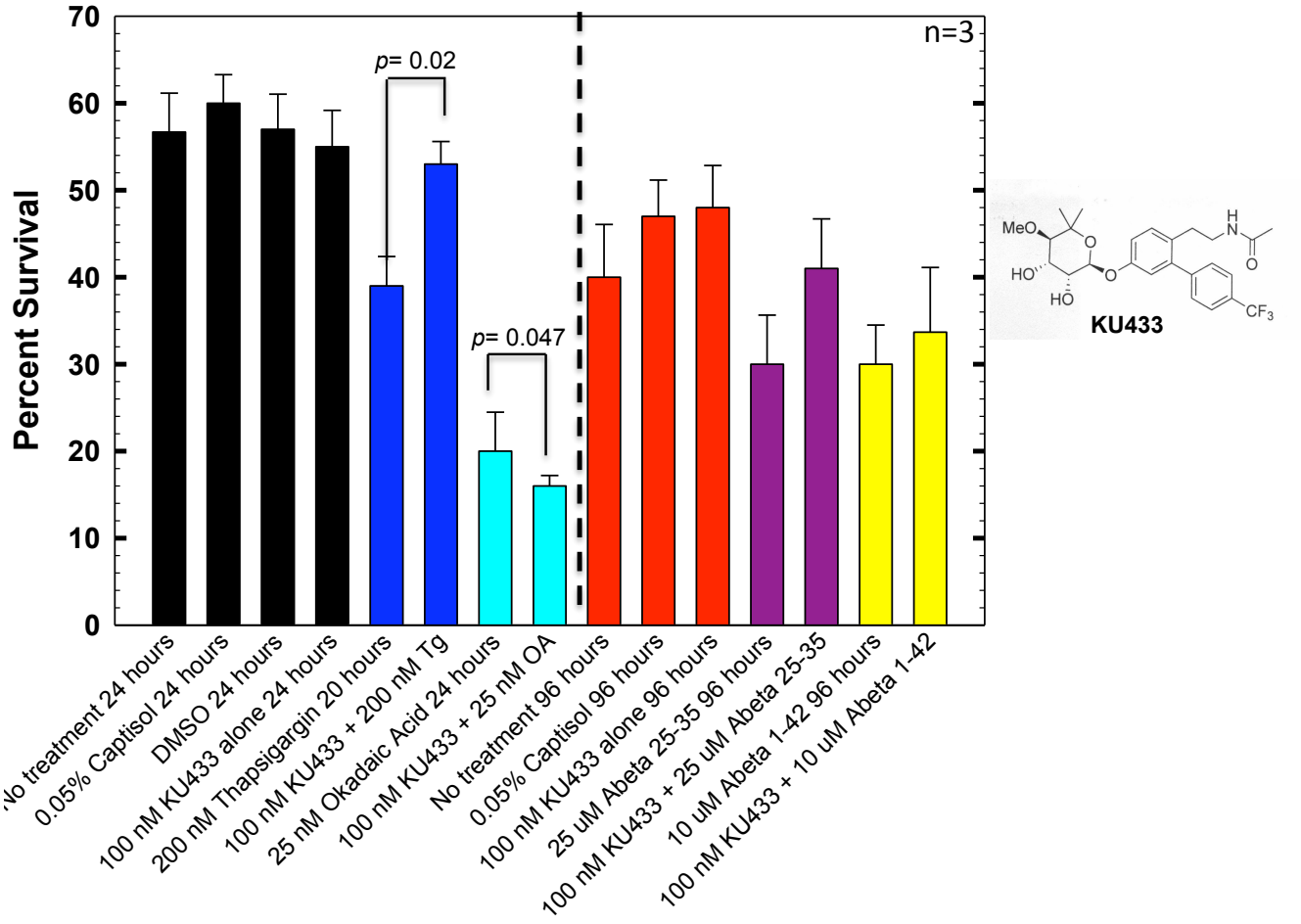

Figure 2.4: KU-433, an analog of KU-32. Primary cortical neurons were pre-treated with 100 nM of KU-433 dissolved in 5% Captisol® (vehicle) for 2 hours before incubation in 200 nM Tg for 20 hours, 25 nM OA for 24 hours, 25 μM $A\beta_{25\text{-}35}$ or 10 μM $A\beta_{1\text{-}42}$ for 96 hours. The Live-Dead assay was used to determine percent survival. Experiments were completed in triplicate. *p* values are indicated on graph.

KU-430 provides similar protection to KU-32 in primary cortical culture

Since the analog KU-430 (Figure 2.3) demonstrated the best protection against toxic species in the Live-Dead assay, we wanted to determine if KU-430 and KU-32 provide a similar level of protection. Using the Live-Dead assay, we pre-treated primary cortical neurons with 100 nM KU-32 or KU-430 then treated with 25 μM $A\beta_{25\text{-}35}$ or 10 μM $A\beta_{1\text{-}42}$ for 96 hours. The results indicate that 100 nM pre-treatment with KU-430 offered

similar protection against $A\beta_{25-35}$; however, KU-32 provided ~10% better protection against $A\beta_{1-42}$ at the same concentration although this difference is not statistically significant (p=0.112) (Figure 2.5). These data suggest that KU-430 is about as protective as KU-32 in shielding against amyloid-β toxicity.

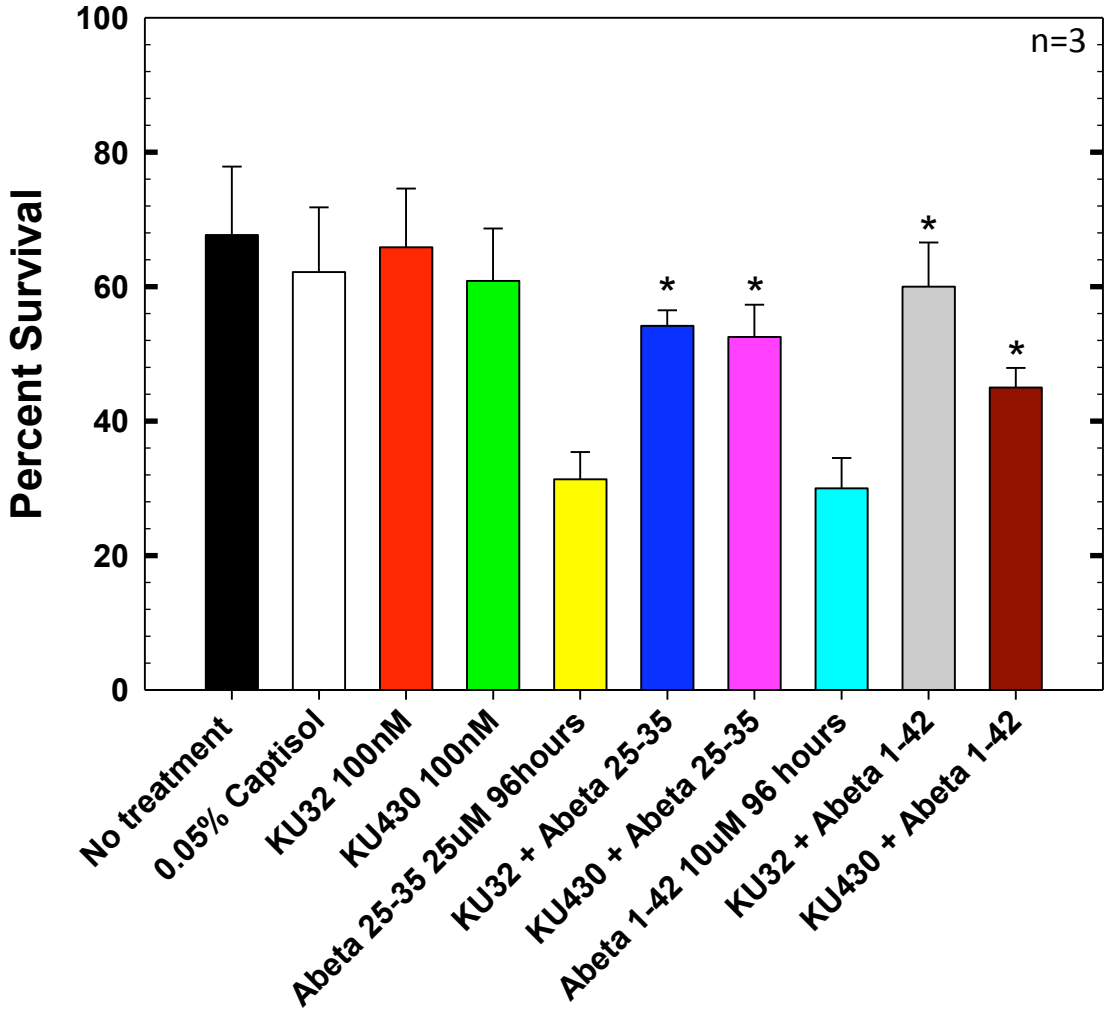

Figure 2.5: Neuronal protection of KU-32 and KU-430. Primary cortical neurons were pre-treated with 100 nM of KU-430 or KU-32 dissolved in 5% Captisol® (vehicle) for 2 hours before incubation in 25 μM $A\beta_{25-35}$ or 10 μM $A\beta_{1-42}$ for 96 hours. The Live-Dead assay was used to determine percent survival. Experiments were completed in triplicate. Statistical analysis was completed using a one-way ANOVA with Bonferroni. * p <0.05.

KU-32 treatment against toxicity of stable P301L Tau mutation in SY5Y cells

In order to determine if KU-32 could protect against an inherent genetic mutation leading to aggregated Tau protein formation, we transfected the immortalized human neuroblastoma cell line, SH-SY5Y, with mutant P301L Tau. This mutation leads to increases in hyper-phosphorylated Tau as observed in neurofibrillary tangles (NFTs) in AD brain. We used two different plasmids. One contained normal human Tau, which served as a control for Tau overexpression, and the other expressed mutated human Tau: -2-3 Tau4 and -2-3 P301L. The Tau protein is essential in maintaining the axonal integrity of neurons. In disease states, like AD, it becomes hyperphosphorylated and dissociates from the axons leading to axonal deterioration and NFT formation. Missense mutations within Tau, like P301L, V337M and R406W, hasten the formation of Tau fibrils (Nacharaju et al., 1999). Normal human Tau exists in six different isoforms as a result of alternative splicing. Tau contains 16 exons, of which 8 are alternatively spliced. These include exons 2, 3, 4A, 6, 8, 10, 13, and 14 (Goedert et al., 1989a, Goedert et al., 1989b, Himmler, 1989, Wei and Andreadis, 1998, Gao et al., 2000). The plasmids used in our studies did not contain exons 2 or 3, but they did contain exon 10, which resides within the microtubule-binding domain. The P301L mutation found in exon 10 accelerates fibril formation (Nacharaju et al., 1999), while the presence or absence of exons 2 and 3 have no effect on microtubule binding (Binder et al., 1985). The stable transfection was performed and confirmed by PCR and immunoblotting (Figure 2.6). The PCR results revealed a 1319 base pair long sequence that was not amplified in the non-transfected SY5Y cells. A successful transfection was also demonstrated by the immunoblots. The PHF-1 labeling, which recognizes paired helical

filament formation as a result of hyperphosphorylated Tau, demonstrated higher levels of immunoreactivity in the transfected cells. These results were expected as mutant P301L Tau leads to fibril formation, and it has also been demonstrated that overexpression of wild type human Tau can lead to increases in hyperphosphorylated Tau (Andorfer et al., 2003). The second immunoblot labeled with Tau5, which recognizes phosphorylated and non-phosphorylated forms of Tau, revealed that the transfectants had higher levels of total Tau in comparison to the SY5Y cells. These results were expected since wild type and mutant P301L Tau were added to these cells.

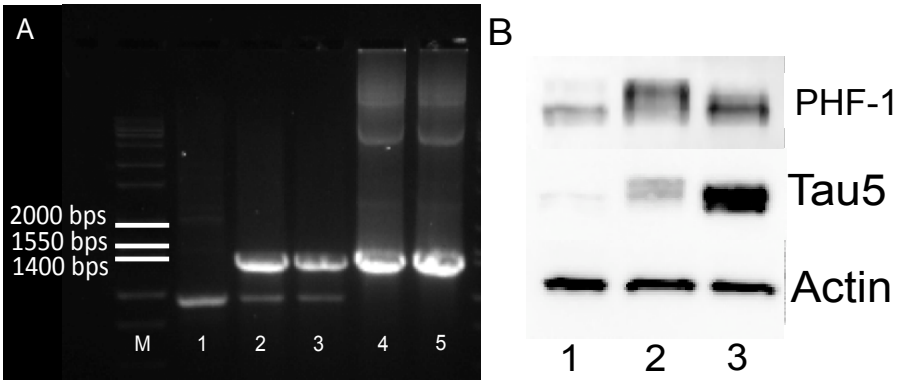

Figure 2.6: PCR and immunoblots of Tau transfection in SY5Y cells. (A) PCR was performed to amplify a 1319 bp fragment present only in transfected cells. M= marker, 1=SY5Y cells, 2=Tau4 transfected cells, 3=P301L transfected cells, 4=Tau4 plasmid, and 5=P301L plasmid. (B) Immunoblotting of transfected cells with antibodies recognizing Tau fibrils (PHF-1), total Tau (Tau5) and the loading control (Actin) 1=SY5Y, 2=Tau4 transfected cells, and 3=P301L transfected cells.

Before looking for KU-32 protection against mutant P301L-induced death in the SY5Y cells, we first had to see if the presence of the mutant Tau potentiated cell death. LDH release was assessed at 0, 12, 24, and 30 hours after non-serum containing medium was added for differentiation. The assay demonstrates that cells containing the P301L mutation exhibited about 12% more cell death starting at 12 hours post differentiation and sustained a greater level of cell death until 30 hours post

differentiation than the wild type Tau transfectants and SY5Y cells (Figure 2.7). The increase in cell death by the P301L mutation was relatively small; however, it was statistically significant.

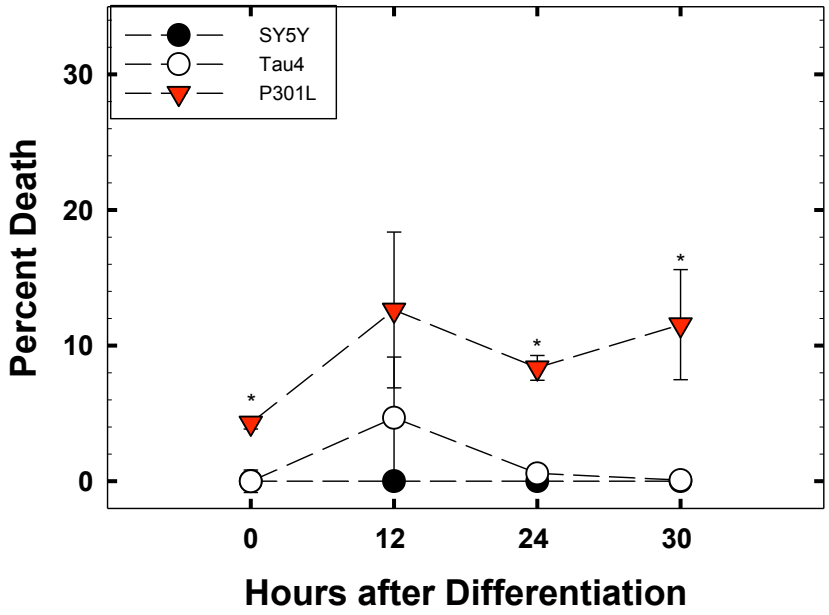

Figure 2.7: LDH measurement of cell death in transfected cells. Transfected and non-transfected SY5Y cells were grown in the presence of serum-free medium for the indicated times. LDH assays were performed in triplicate to determine percent death. *p<0.001 for SY5Y vs. P301L cells.

After confirming an increase in necrosis with the presence of the P301L mutation, we tested if KU-32 could protect the cells against this genetic mutation that increased cell death. Twenty-four hours post differentiation, the transfected cells were treated with 100nM KU-32 or 5% Captisol® for 2, 4, 6, and 12 hours. The LDH results revealed that KU-32 did not protect cells against necrotic death (Figure 2.8). Surprisingly, KU-32 enhanced cell death in the P301L transfected cells.

Since the LDH assay is a measure of necrosis and KU-32 did not show protection of the mutant cells, we hypothesized that the P301L mutation was possibly

inducing another route of cell death like apoptosis. The MTT assay measures apoptotic as well as necrotic cell death; so we used this assay to assess protection with KU-32 in the stable transfectants. The results in Figure 2.9 demonstrated that KU-32 did not protect against apoptotic cell death in these cells (Figure 2.9). Similarly, the MTT results indicated that KU-32 significantly increased cell death in both the P301L and wild-type Tau4 transfected cells.

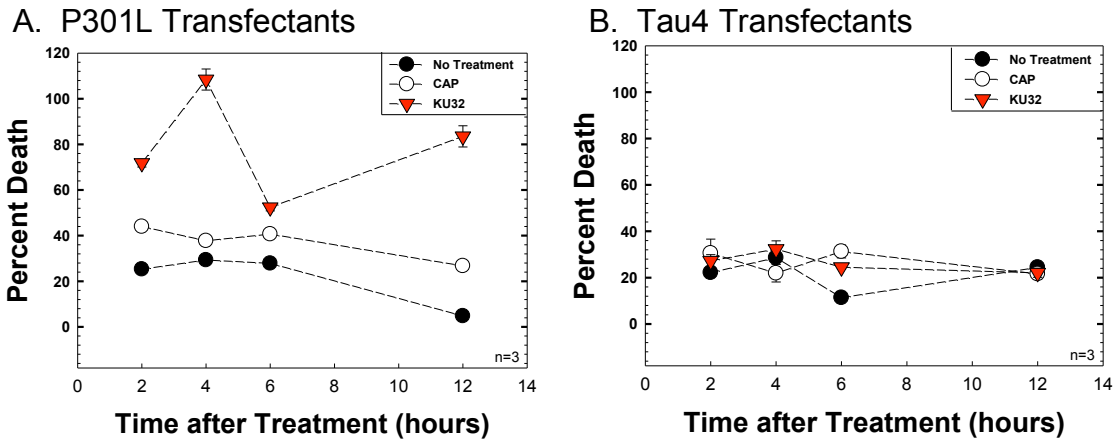

Figure 2.8: Effect of KU-32 treatment in transfected cells as monitored by LDH release. Transfected cells were grown in 48-well plate for 24 hours and then differentiated in non-serum containing medium for 24 hours. 100 nM KU-32 or 5% Captisol® was applied to the cell culture medium and LDH assays were performed at the indicated times after treatment. Percent cell death in (A) P301L transfected cells and (B) wild-type Tau4 transfected cells was graphed.

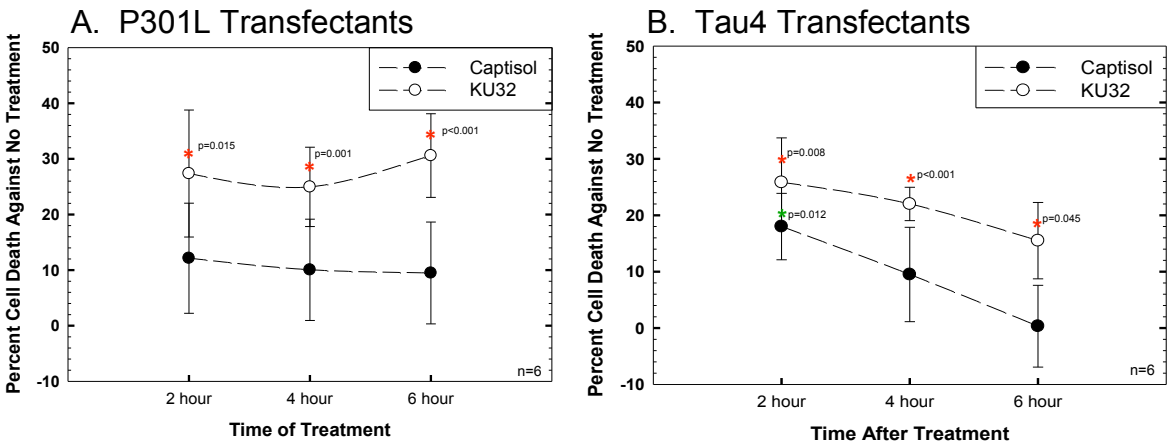

Figure 2.9: Effect of KU-32 in transfected cells as determined by MTT assay. Transfected cells were grown in 35 mm^2 dishes for 24 hours and then differentiated in non-serum containing medium for 24 hours. 100 nM KU-32 or 5% Captisol® was given to the cell culture medium and MTT assays were performed at the indicated times after treatment. The data from (A) P301L transfected cells and (B) wild-type Tau4 transfected cells were graphed as percent cell death against no treatment.

IV. Discussion

Previous studies in the Michaelis lab have demonstrated that the novobiocin derivative, A4, protects against Aβ-induced cell death (Ansar et al., 2007). Our observations with the A4 analog, KU-32, are consistent with the previously published results, indicating that KU-32 protects against Aβ-induced cell death as well as Tg toxicity in primary rat neurons (Figure 2.1). The other novobiocin derivatives: KU-426, KU-430, and KU-433 (Figures 2.2-2.4), further substantiate the neuroprotective qualities of these novel C-terminal Hsp90 modulator analogs. However, these analogs led to differential protection, and KU-430 was the only analog that provided protection similar to that seen with KU-32 (Figure 2.5). Other studies involving KU-32, KU-430, and KU-433 have demonstrated protection against *in vitro* glucose toxicity (Kusuma et al., 2012). KU-32 has also revealed protection against neuregulin-induced demyelination in primary rat sensory neurons (Urban et al., 2010). Previous reports also demonstrate

that KU-32 protects against Aβ-induced toxicity in differentiated and non-differentiated neuroblastoma cells (Lu et al., 2008).

Previous studies with other Hsp90 inhibitors further demonstrate protective properties of these compounds in models of AD. Greengard's group demonstrated that GA provided protection in AD models by decreasing phosphorylated Tau in COS-1 cells (Dou et al., 2003), and his group later revealed that a novel N-terminal Hsp90 inhibitor developed in their lab was protective by apparently decreasing phosphorylated Tau in both COS-7 cells and the JNPL3 AD mouse model (Luo et al., 2007). Greengard's studies suggest that the N-terminal Hsp90 inhibitors are initiating proper folding of the phospho-Tau aggregates. Dickey and colleagues developed a novel Hsp90 inhibitor that demonstrated neuroprotection through decreases in phosphorylated Tau in HeLa cells that overexpress Tau, as well as lowered levels of phosphorylated Tau, in a mouse model of Tauopathy by targeting clearance of p-Tau through the proteasome (Dickey et al., 2007). The inhibitors Dickey and Greengard's groups developed were directed to the N-terminal portion of Hsp90 while KU-32 acts at the C-terminal end of Hsp90 (Matts et al., 2011).

Our *in vitro* cell model expressing the mutant P301L Tau did not demonstrate decreases in necrotic (Figure 2.8) or apoptotic death (Figure 2.9) with KU-32 treatment. Our transfection produced the appropriate phenotype as shown in Figure 2.6. The SY5Y cells transfected with wild-type Tau, which was used as a control for Tau overexpression, and mutant P301L Tau both demonstrated increases in PHF-1, an early marker of Tau fibrillization and hyperphosphorylation (Reed et al., 1997, Reed et al., 1998). Both of the transfectants also showed increases in total Tau levels, as

should be expected in comparison to SY5Y cells. It is possible that we did not observe protection in the P301L transfected cells because of low Hsp70 levels. The SY5Y cell line, with or without the presence of the transfectants, has low levels of Hsp70 protein (Myung et al., 2004). Previous reports demonstrated that Hsp70 is required for KU-32 neuroprotection (Urban et al., 2010). Thus, it is possible KU-32 did not prevent cell death in the mutant transfectants because they lack sufficient induction of Hsp70 by KU-32 that would theoretically lead to the refolding of the Tau fibrils.

As AD treatment efforts progress, the focus of treatment development has shifted from disease pathology to neuroprotection. As many clinical trials have failed in their development of drugs targeting the pathology of AD, it has been hypothesized that previously developed therapeutic treatments have been directed at the wrong problem (Golde et al., 2011). Instead of trying to ameliorate the pathological problems associated with the disease markers such as senile plaques and Tau tangles, we should focus our efforts in providing neuroprotection. Improvements in cognitive function have been demonstrated even in the presence of Tau aggregates, as revealed in a study by SantaCruz and colleagues. Using the tet-off rTg4510 mouse model, where the presence of doxycycline prevents the development of mutant P301L Tau aggregates, the group administered doxycycline to 2.5-month old mice that had developed NFT pathology. At 4.5 months, the group performed behavioral analysis using the Morris water maze to demonstrate that the mice were able to improve cognition in the presence of hyperphosphorylated Tau aggregates when the development of new Tau aggregates was prevented (SantaCruz et al., 2005).

Consequently, this study reveals that clearing Tau pathology may not be necessary for functional improvements.

As AD develops in humans, not every cell has the abnormal aggregates. However, even though neurons are post-mitotic, Liu and colleagues have demonstrated that pathological Tau is transferred to nearby or susceptible neurons through synaptic transmission (Liu et al., 2012). Therefore, it is important to capitalize on the properties of a given cell to clear faulty proteins quickly and prevent the passage of aggregates to new cells. This suggests that we should center our efforts on enhancing cellular functions in the presence of the pathological entities as opposed to trying to remove them. Therefore, our discovery of a neuroprotective novel compound to promote the protein folding machinery is in line with the current shift in AD research, where the focus is now centered on neuroprotective agents that may indeed be disease-modifying agents.

V. References

Andorfer C, Kress Y, Espinoza M, de Silva R, Tucker K, Barde Y, Duff K, Davies P (2003) Hyperphosphorylation and aggregation of Tau in mice expressing normal human Tau isoforms. Journal of Neurochemistry 86:582-590.

Ansar S, Burlison JA, Hadden MK, Yu XM, Desino KE, Bean J, Neckers L, Audus KL, Michaelis ML, Blagg BS (2007) A non-toxic Hsp90 inhibitor protects neurons from Abeta-induced toxicity. Bioorganic and Medicinal Chemistry Letters 17:1984-1990.

Binder L, Frankfurter A, Rebhun L (1985) The distribution of Tau in the mammalian central nervous system. Journal of Cellular Biology 101:1371-1378.

Dickey CA, Kamal A, Lundgren K, Klosak N, Bailey RM, Dunmore J, Ash P, Shoraka S, Zlatkovic J, Eckman CB, Patterson C, Dickson DW, Jr. NSN, Hutton M, Burrows F, Petrucelli L (2007) The high-affinity HSP90-CHIP complex recognizes and selectively degrades phosphorylated Tau client proteins. The Journal of Clinical Investigation 117:648-658.

Dou F, Netzer W, Tanemura K, Li F, Hartl U, Takashima A, Gouras G, Greengard P, Xu H (2003) Chaperones increase association of Tau protein with microtubules. Proceedings of the National Academy of Sciences 100:721-726.

Evangelopoulos M, Weis J, Kruttgen A (2005) Signalling pathways leading to neuroblastoma differentiation after serum withdrawal: HDL blocks neuroblastoma differentiation by inhibtion of EGFR. Oncogene 24:3309-3318.

Fan C, Lee S, Cyr D (2003) Mechanisms for regulation of Hsp70 function by Hsp40. Cell Stress and Chaperones 8:309-316.

Gao Q, Memmott J, Lafyatis F, Stamm S, Screaton G, Andreadis A (2000) Complex regulation of Tau exon 10, whose missplicing cause frontotemporal dementia. Journal of Neurochemistry 74:490-500.

Goedert M, Spillantini M, Jakes R, Rutherford D, Crowther R (1989a) Multiple isoforms of human microtubule-associated protein Tau: sequences and localization in neurofibrillary tangles of Alzheimer's disease. Neuron 3:519-526.

Goedert M, Spillantini M, Potier M, Ulrich J, Crowther R (1989b) Cloning and sequencing of the cDNA encoding an isoform of microtubule-associated protein

Tau containing four tandem repeats: differential expression of Tau protein mRNAs in human brain. EMBO 8:393-399.

Golde TE, Schneider LS, Koo EH (2011) Anti-Aβ therapeutics in Alzheimer's disease: the need for a paradigm shift. Neuron 69:203-213.

Himmler A (1989) Structure of the bovie Tau gene: alternatively spliced transcripts generate a protein family. Molecular and Cellular Biology 9:1389-1396.

Kusuma B, Zhang L, Sundstrom T, Peterson L, Dobrowsky R, Blagg B (2012) Synthesis and evaluation of novologues as C-terminal Hsp90 inhibitors with cytoprotective activity against sensory neuron glucotoxicity. Journal of Medicinal Chemistry Epub ahead of print.

Liu L, Drouet V, Wu J, Witter M, Small S, Clelland C, Duff K. (2012) Trans-synaptic spread of Tau pathology *in vivo*. PLOS One. 7:1-9.

Lu Y, Ansar S, Michaelis M, Blagg B (2008) Neuroprotective activity and evaluation of Hsp90 inhibitors in an immortalized neuronal cell line. Bioorganic and Medicinal Chemistry Letters 17:1709-1715.

Luo W, Dou F, Rodina A, Chip S, Joungnam K, Zhao Q, Moulick K, Aguirre J, Wu N, Greengard P, Chiosis G (2007) Roles of heat-shock protein 90 in maintaining and facilitating the neurodegenerative phenotype in Tauopathies. Proceedings of the National Academy of Sciences 104:9511-9516.

Marcu M, Chandli A, Bouhouche I, Catelli M, Neckers L (2000) The heat shock protein 90 antagonist novobiocin interacts with a previously unrecognized ATP-binding domain in the carboxyl terminus of the chaperone. Journal of Biological Chemistry 275:37181-37186.

Matts RL, Dixit A, Peterson LB, Sun L, Voruganti S, Kalyanaraman P, Hartson S, Verkhivker GM, Blagg BSJ (2011) Elucidation of the Hsp90 C-terminal inhibitor binding site. ACS Chemical Biology 6:800-807.

Michaelis M, Ansar S, Chen Y, Reiff E, Seyb K, Himes R, Audus K, Georg G (2005) Beta-Amyloid-induced neurodegeneration and protection by structurally diverse microtuble-stabilizing agents. Journal of Pharmacology and Experimental Therapeutics 312:659-668.

Michaelis M, Ranciat N, Chen Y, Bechtel M, Ragan R, Hepperle M, Liu Y, Georg G (1998) Protection against beta-amyloid toxicity in primary neurons by paclitaxel (Taxol). Journal of Neurochemistry 70:1623-1627.

Michaelis M, Walsh J, Pal R, Hurlbert M, Hoel G, Bland K, Foye J, Kwong W (1994) Immunologic localization and kinetic characterization of a Na+/Ca2+ exchanger in neuronal and non-neuronal cells. Brain Research 661:104-116.

Muchowski P (2002) Protein misfolding, amyloid formation, and neurodegeneration: a critical role for molecular chaperones? Neuron 35:9-12.

Muchowski P, Wacker J (2005) Modulation of neurodegeneration by molecular chaperones. Nature Reviews Neuroscience 6:11-22.

Myung J, Afjehi-Sadat L, Felizardo-Cabatic M, Slavc I, Lubec G (2004) Expressional patterns of chaperone in ten human tumour cell lines. BMC Proteomic Science 2:8.

Nacharaju P, Lewis J, Easson C, Yen S, Hackett J, Hutton M, Yen S (1999) Accelerated filament formation from Tau proteins with specific FTDP-17 missense mutations. FEBS Letters 447:195-199.

Peterson LB, Blagg BS (2009) To fold of not to fold; modulation and consequences of Hsp90 inhibition. Future Medicinal Chemistry 1:267-283.

Reed L, Grabowski T, Schmidt M, Morris J, Goate A, Solodkin A, Hoesen GV, Schelper R, Talbot C, Wragg M, Trojanowski J (1997) Autosomal dominant dementia with widespread neurofibrillary tangles. Annals of Neurology 42:564-572.

Reed L, Schmidt M, Wszolek Z, Balin B, Soontornniyomkij V, Lee V, Trojanowski J, Schelper R (1998) The neuropathology of a chromosome 17-linked autosomal dominant parkisonism and dementia ("pallido-ponto-nigral degeneration"). Journal of Neuropatholoy and Experimental Neurology 57:588-601.

Salminen A, Ojala J, Kaarniranta K, Hiltunen M, Soininen H (2011) Hsp90 regulates Tau pathology through co-chaperone complexes in Alzheimer's disease. Progress in Neurobiology 93:99-110.

SantaCruz K, Lewis J, Spires T, Paulson J, Kotilinek L, Ingelsson M, Guimaraes A, DeTure M, Ramsden M, McGowan E, Forster C, Yue M, Orne J, Janus C, Mariash A, Kuskowski M, Hyman B, Hutton M, Ashe K (2005) Tau suppression in a neurodegenerative mouse model improves memory function. Science 309:476-481.

Schubert D, Humphreys S, Baroni C, Cohn M (1969) In vitro differentiation of a mouse neuroblastoma. Proceedings of the National Academy of Sciences 64:316-323.

Seeds N, Gilman A, Amano T, Nirenberg M (1970) Regulation of axon formation by clonal lines of of a neural tumor. Proceedings of the National Academy of Sciences 66:160-167.

Seyb K, Ansar S, Bean J, Michaelis ML (2006) Beta-amyloid and endoplasmic reticulum stress responses in primary neurons. Journal of Molecular Neuroscience 28:111-124.

Spires T, Orne J, SantaCruz K, Pitstick R, Carlson G, Ashe K, Hyman B (2006) Region-specific dissociation of neuronal loss and neurofibrillary pathology in a mouse model of Tauopathy. The American Journal of Pathology 168:1598-1607.

Supko J, Hickman R, Grever M, Malspeis L (1995) Preclinical pharmacological evaluation of geldanamycin as an antitumor agent. Cancer Chemotherapeutics and Pharmacology 36:305-315.

Urban M, Li C, Yu C, Lu Y, Krise J, McIntosh M, Rajewski R, Blagg BS, Dobrowsky R (2010) Inhibiting heat-shock protien 90 reverses sensory hypoalgesia in diabetic mice. ASN Neuro 2:189-199.

Wei M, Andreadis A (1998) Splicing of a regulated exon reveals additional complexity in the axonal microtubule-associated protein Tau. Journal of Neurochemistry 70:1346-1356.

Wilhelmus M, de Waal R, Verbeek M (2007) Heat shock proteins and amateur chaperones in amyloid-beta accumulation and clearance in Alzheimer's disease. Molecular Neurobiology 35:203-216.

Zaidi A, Michaelis ML (1999) Effects of reactive oxygen species on brain synaptic plasma membrane Ca(2+)-ATPase. Free Radical Biology & Medicine 27:810-821.

Zempel H, Thies E, Mandelkow E, Mandelkow E (2010) Abeta oligomers cause localized calcium elevation, missorting of endogenous Tau into dendrites, Tau

phosphorylation, and destruction of microtubules and spines. Journal of Neuroscience 30:11938-11950.

CHAPTER THREE: KU-32 is Neuroprotective in Mouse Models of AD

I. Introduction

Typically Tau is associated with microtubules, and functions in the support of axonal structure and neuronal development (Weingarten et al., 1975). Tau dissociates from the microtubules when it is hyperphosphorylated and this leads to pathological Tau aggregates called neurofibrillary tangles (NFTs) (Grundke-Iqbal et al., 1986, Kosik et al., 1986). Diseases characterized by aggregated Tau include Alzheimer's disease (AD), frontotemporal dementia with parkinsonism linked to chromosome 17 (FTDP-17), and Pick's disease (Dickson, 1997). Of the 'Tauopathies,' AD is associated with two protein aggregates: amyloid-β and Tau; however, it is Tau aggregation that most closely correlates with loss of neurons (Gomez-Isla et al., 1997) and dementia (Ihara et al., 1986, Crystal et al., 1988). Several studies have demonstrated that mutations in the Tau gene lead to various diseases known as 'Tauopathies,' the most common of which is FTDP- 17. These studies were the first to prove that abnormalities in Tau alone directly lead to neurodegeneration (Hutton et al., 1998, Spillantini et al., 1998). Nevertheless, the signaling events that lead to sporadic NFT formation, as seen in AD brain, are still widely debated.

In order to investigate the different signaling events that lead to NFT formation in AD, studies require that mouse models express mutated Tau in order for them to develop the characteristic protein aggregates associated with the disease. Some models only generate aggregates of Aβ peptides, which contain mutations in the amyloid precursor protein (APP) and/or the Presenilins (Chapman et al., 1999,

Gureviciene et al., 2004). Other models are designed to develop the neurofibrillary pathology associated with AD through the use of mutated Tau gene. Most of these mouse models overexpress the P301L mutation found within the microtubule-binding motif of Tau. The Tau becomes hyperphosphorylated, eventually leading to formation of Tau aggregates within mouse brains (Lewis et al., 2000). There is also one model that contains both Aβ plaques and neurofibrillary pathology, and is called the 3xTg mouse model. This model has three mutations: one in APP; one in presenilin; and one in Tau (Oddo et al., 2003).

In this chapter, two different mouse models that express mutant Tau tangles were used to investigate the effect of the novel C-terminal inhibitor, KU-32 on Tau fibrils and their consequences. The first mouse model was provided by Dr. Jada Lewis and called JNPL3. This model contains the human P301L transgene under the control of the mouse prion promoter (MoPrP). The mouse develops Tau pathology predominately in the spinal cord and cortical region of the brain, with limited NFT formation in the hippocampus. Unfortunately, JNPL3 mice develop motor defects, which are correlated with degeneration of motor neurons, and thus become impaired in walking. There is little brain neurodegeneration in the JNPL3 mouse model, as opposed to human AD, which is associated with significant neurodegeneration (Lewis et al., 2000).

The second mutant Tau mouse model we used was the rTg4510. These mice contain the human P301L transgene, but unlike the JNPL3 mice, P301L expression is driven by the CamKII promoter containing a tet-off cassette. CamKII drives production of high expression of the P301L mutant Tau in the cortical and hippocampal regions of the brain, which is similar to human AD (Spires et al., 2006). In comparison to the

JNPL3 mice, the rTg4510 mice have 17-fold higher expression of P301L Tau in the absence of doxycycline, and, importantly, the rTg4510 mice develop classic neurodegeneration much like that observed in human AD (Berger et al., 2007).

In Chapter Two of this dissertation, we demonstrated significant protection with a novel C-terminal Hsp90 modulator, KU-32, in primary neuronal cultures subjected to various cellular toxins i.e. Aβ peptides and Thapsigargin (Tg). The purpose of the studies in this chapter was to determine if KU-32 could lead to neuroprotective effects *in vivo*. Previous studies using blood brain barrier (BBB) permeable N-terminal Hsp90 inhibitors showed decreases in hyperphosphorylated Tau in mouse models of Tauopathy using immunohistochemical and Western blotting analysis (Dou et al., 2003, Dickey et al., 2007, Luo et al., 2007). Our novel compound, KU-32, demonstrates BBB permeability, and does not exhibit toxic effects at concentrations required to test properties of the drug (unpublished results). We hypothesized that our novel C-terminal Hsp90 modulator, KU-32, would act similarly to the N-terminal Hsp90 inhibitors and significantly decrease hyperphosphorylated Tau in the two P301L transgenic mouse models, as well as restore and/or protect against neuronal damage.

II. Materials and Methods

Mutant Tau mouse models and exposure to KU-32

JNPL3 mice

A Tau mutant mouse model was developed as described in *Nature Genetics* by Lewis et al. (Lewis et al., 2000), and heterozygous breeder mice were given to the Michaelis lab by Dr. Jada Lewis.

In order to examine the effect of KU-32 treatments, two to four month old JNPL3 or C57BL/6 (wild type control) mice were treated intraperitoneally with 20 mg/kg of KU-32 or vehicle (12.5% Captisol®), five times a week, for six months. Seven JNPL3 mice were treated with 20 mg/kg, and ten JNPL3 mice were treated with the vehicle. Four wild type mice were used, two of which were treated with 20 mg/kg of KU-32 and two treated with vehicle.

rTg4510 mice

Heterozygous inducible Tau responder mice containing a tetracycline-operon-responsive (TRE) system upstream from the P301L transgene and heterozygous CamKIIa activator mice with a tet-off open reading frame downstream of the promoter, where activation of P301L gene expression occurs upon removal of doxycycline, were received from the Neuroscience Department, Mayo Clinic, Jacksonville, FL (Ramsden et al., 2005, SantaCruz et al., 2005). To create the colony, four lines of mouse were required. The Tau responders were bred and maintained onto an FVB/N mouse background, while the CamKIIa activator mice were bred and maintained onto the SVJ129S6 model. All progeny from each litter were genotyped. Only mice containing the responder sequences were bred with mice expressing the activator sequences to obtain the F1 hybrid rTg4510 mice that were used in these studies. FVB mice were used as wild-type controls.

To test the effects of KU-32 on Tau phosphorylation and neurodegeneration, 2.5-month old mice were put on a treatment regimen with

intraperintoneal (i.p.) injections of vehicle (5% Captisol®) or KU-32. Eight rTg4510 mice were injected 2 times per week with 60 mg/kg of KU-32 for a period of 10 weeks. Eight rTg4510 mice received only the 5% Captisol® vehicle on the same schedule. Four non-transgenic littermates served as the controls, 2 treated with KU-32 and 2 treated with 5% Captisol®.

Analysis of brain sections of treated mice

Immunohistochemical labeling of Tau in JNPL3 mutant mice

After 6 months of KU-32 treatment, brains were recovered from 8 to 10 month old mice. Hemibrains were fixed in 4% paraformaldehyde, submerged in 30% sucrose for 7 days, flash frozen in 4-methyl-butane in liquid N_2, and cut on a cryostat. Free-floating sections were cut at 20 µm and stored at 4°C in 1xPBS. Sections were placed in 12-well plates, and permeabilized with 0.1% Triton-X 100 for 30 minutes, rinsed 2 times in 1xPBS and incubated for 30 minutes in 1% hydrogen peroxide in 50% methanol with 0.1% sodium azide to block endogenous peroxidase activity. The slides were rinsed 2 times with 1xPBS and then incubated in 2% gelatin for 1 hour at 37°C to further block endogenous antibody binding. Primary antibodies directed against phospho-specific Tau epitopes, CP13, which recognizes pS202 (a gift from Dr. Peter Davies) and AT8, which recognizes pS202/T205 (Pierce Endogen, Rockford, IL) were incubated overnight at 4°C. A Vectastain kit, standard streptavidin-peroxidase labeling against mouse antibodies was used to visualize antibody labeled proteins with DAB as the chromagen (Vector, Burlingame, CA). Sections were viewed with the

Nikon Eclipse 80i microscope and images were captured at 40x magnification with a Photometrics CoolSnap camera. Positive labeling was quantified using Metamorph. Data were analyzed for statistical significance using Student's *t* test (SigmaPlot 11).

Immunofluorescent labeling of brain sections in rTg4510 Tau mutant mice

Following 10 weeks of KU-32 administration, the mice were sacrificed, the brains excised, and the cerebella removed. The brains were fixed in 4% paraformaldehyde. Hemibrains were submerged in 30% sucrose for 7 days, flash frozen in 4-methyl butane in liquid N_2, and cut on a cryostat. Free-floating sections were cut at 20 μm and stored at 4°C in 1xPhosphate-buffered saline (PBS). Sections were transferred to 12-well plates and incubated in 2% gelatin for 1 hour at 37°C to block endogenous fluorescence, rinsed 3 times with 1x PBS, and incubated for 15 min with 1 mg/mL sodium borohydride to further reduce background fluorescence. Sections were rinsed 3 times in 1xPBS and incubated for 15 minutes with 0.01% Triton-X 100 at room temperature, and rinsed 3 times in 1xPBS. The following primary antibodies were used to label the sections: microtubule-associated protein 2 (MAP2) (1:250), Synaptophysin (1:500), and neuronal nuclei (NeuN) (1:500), all from Millipore (Bellerica, MA) as well as CP13 (1:100) antibodies against phosphorylated S202 of Tau. The sections were incubated with the specific primary antibodies at 4°C overnight.

The next day, sections were rinsed 3 times with 1xPBS and incubated with goat anti-mouse AlexaFluor 488 (1:1000) and/or goat anti rabbit AlexaFluor 568

(1:1000), both from Invitrogen (Carlsbad, CA), for 2 hours at 37°C. The antibody-labeled sections were transferred to microscope slides, viewed with an Olympus/3I spinning disk confocal/epifluorescence/TIRF inverted microscope, and images were captured at 40x magnification with SlideBook version 5. Positive labeling was quantified using ImageJ. Data were analyzed for statistical significance using Student's *t*-test (SigmaPlot 11).

III. Results

The effect of KU-32 treatment on abnormal Tau in the JNPL3 transgenic mice

We first tested to see if KU-32 could protect the brain against consequences of the P301L mutation in the JNPL3 mouse model of Tau pathology. We determined if KU-32 decreased levels of hyperphosphorylated Tau following six months of treatment in the JNPL3 mice. For these studies, we used two different phospho-Tau antibodies, AT8 and CP13. AT8 recognizes phosphorylated S202 and T205, while CP13 recognizes phosphorylated S202. Phosphorylation at these sites has been used in order to determine the stages of AD progression (Braak et al., 2006). Also, these areas of Tau phosphorylation are considered essential sites that switch Tau function to the pathological phenotype observed in AD brain (Biernat et al., 1992). Phospho-Tau labeling was performed on coronal sections from JNPL3 mice chronically treated with 20 mg/kg of KU-32 and 12.5% Captisol®. These mice expressed the human P301L Tau mutation under the mouse prion promoter that drove expression primarily in the frontal cortex and spinal cord. Immunohistochemical labeling revealed that KU-32 significantly decreased the amount of Tau phosphorylated at S202 as observed in the

CP13-labeled Tau (Figure 3.1). These significant decreases in the KU-32-treated mice were observed in the premotor cortical region of JNPL3 mice.

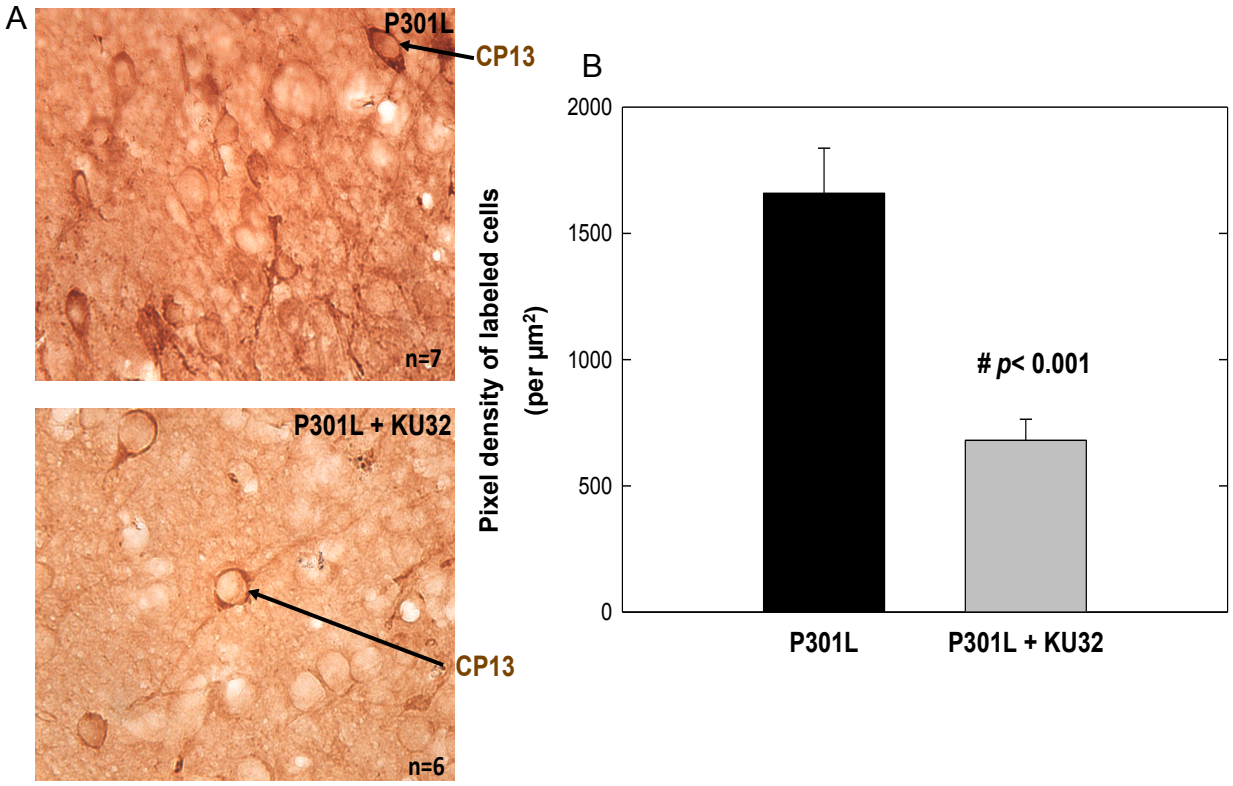

Figure 3.1: CP13-labeled phospho-Tau in the premotor cortex of KU-32 treated JNPL3 mice. (A) Representative examples of brain sections labeled with CP13 antibodies. Black arrows indicate positive CP13 labeling. (B) Quantitative data from the densitometric analysis was determined using the number of pixels labeled per square micron. (n=7 P301L mice and n=6 P301L + KU-32 mice). Statistical evaluation of significance of differences was carried out using Student's *t* test.

A similar decrease in labeling by the AT8 antibodies that react with phosphorylated Tau at S202/T205 was observed in the premotor cortex of KU-32-treated JNPL3 mice (Figure 3.2).

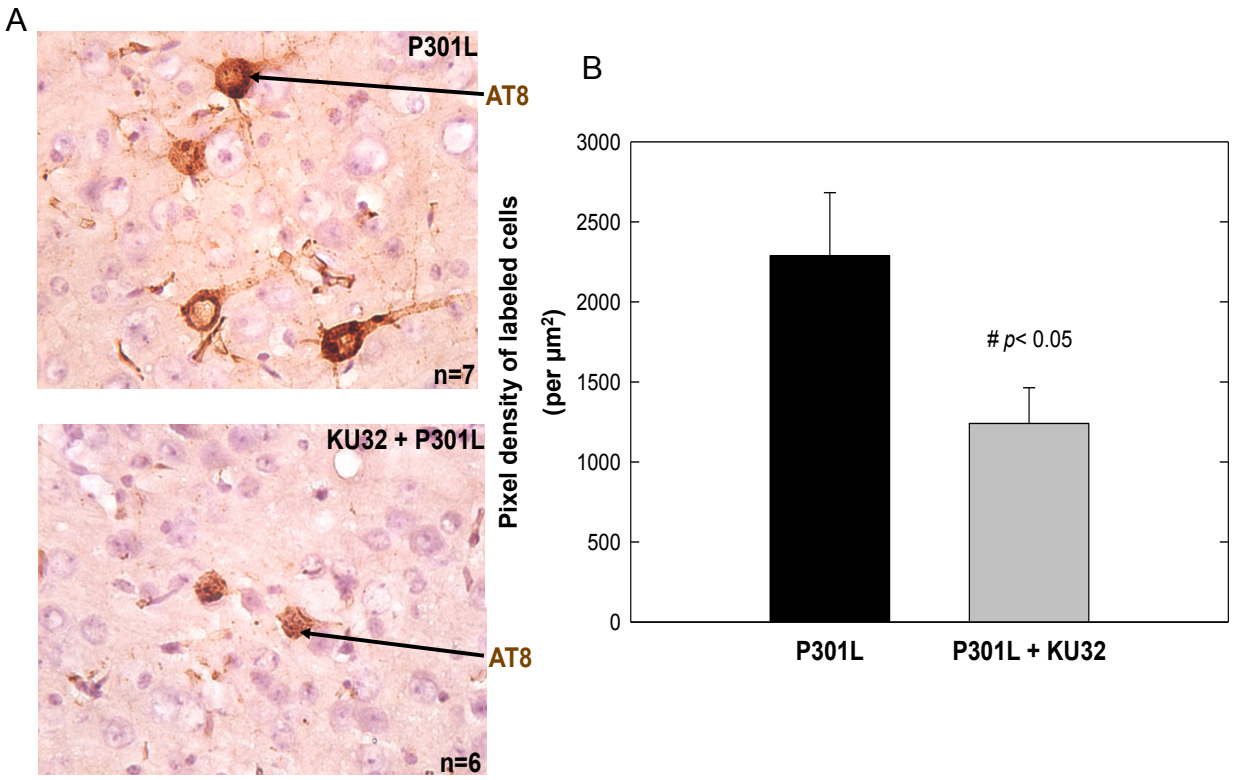

Figure 3.2: AT8-labeled phospho-Tau in the premotor cortex of KU-32 treated JNPL3 mice. (A) Representative examples of brain sections labeled with AT8 antibodies. Black arrows indicate positive AT8 labeling. (B) Quantitative data from the densitometric analysis was determined using the number of pixels labeled per square micron. (n=7 P301L mice and n=6 P301L + KU-32 mice). Statistical evaluation of significance of differences was carried out using Student's *t* test.

The effect of KU-32 on CP13-labeled Tau rTg4510 mice

Since we observed significant decreases in hyperphosphorylated Tau in JNPL3 mice, we assessed whether KU-32 could decrease phospho-Tau levels in a more robust mouse model of P301L Tau pathology that also exhibits neurodegeneration, the rTg4510 mice. These mice expressed mutant Tau at a level 17 times higher than that in wild type mice. This genetic mutation was under the CamKIIa promoter that was driving expression in the frontal cortex and the hippocampus (SantaCruz et al., 2005). Immunofluorescent labeling of brain sections was performed using CP13 antibodies that recognize phosphorylated S202 on Tau. Images from KU-32 and vehicle-treated

rTg4510 mice showed a significant decrease in CP13-labeled Tau in the premotor portion of the frontal cortex (Figure 3.3).

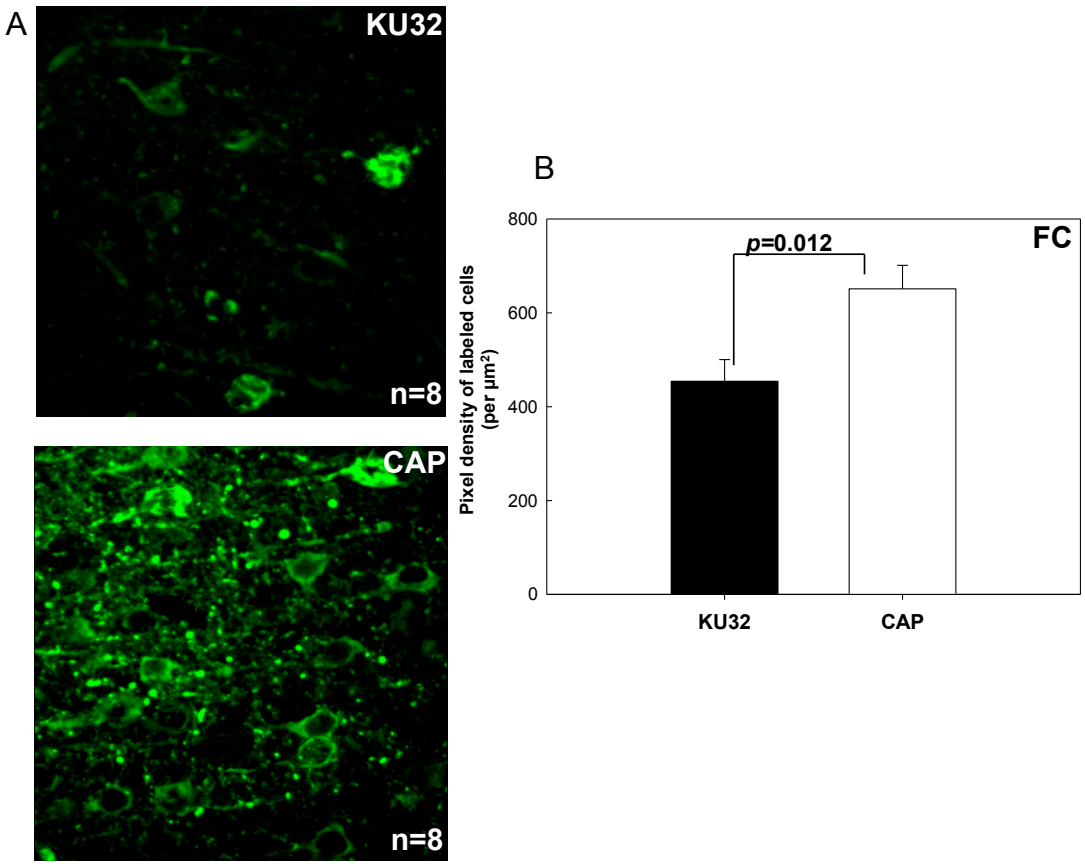

Figure 3.3: Chronic administration of KU-32 on CP13-labeled Tau in rTg4510 mice. (A) Representative examples of brain sections labeled with CP13 antibodies. (B) Quantitative data from densitometric analysis was based on the number of pixels labeled per square micron. (n=8 KU-32-treated mice and n=8 CAP-treated mice). Statistical evaluation of significance of differences was carried out using Student's *t* test.

The effect of KU-32 on neuroprotection in rTg4510 mice

The rTg4510 mice show severe neurodegeneration and synaptic pathology beginning at about 2.5 months of age (Spires et al., 2006). Therefore, we evaluated several indicators of neuronal and synaptic integrity and viability in the rTg4510 mice treated with KU-32 or Captisol® only as described in Methods. First, we performed immunofluorescent labeling to determine if KU-32 provides protection against

development of dystrophic neurites typically associated with mutant Tau overexpression. Sections from the wild type, KU-32, and 5% Captisol®-treated transgenic mouse brains were labeled with the dendritic marker MAP2. Images were captured from the premotor cortex (Figure 3.4A) and the CA1 of the hippocampus (Figure 3.4B) demonstrated that in transgenic mice treated with KU-32 there was improved dendritic morphology when compared with the dendritic field in 5% Captisol®-treated rTg4510 mice. Morphometric analyses of dendritic labeling from the hippocampal CA1 and the premotor cortex indicated that KU-32-treatment significantly increased positive labeling and the integrity of dendrites in comparison to when similar sections were analyzed in the Captisol®-treated mice (Figure 3.5). Dendritic labeling in the premotor cortex of the KU-32-treated mouse brains was not significantly different from the wild type indicating that KU-32 preserved dendritic structures and resulted in nearly normal fields in the treated mouse (Figure 3.5). In the hippocampal CA1 region, the dendritic labeling in the KU-32-treated brains was statistically higher than the Captisol®-treated mice. The MAP2 labeling in the treated mice did not reach the levels of that in the wild type mice. Given that the wild type mice have no lesions due to mutant Tau expression, one would expect that there is a basic difference between the treated-transgenic mice and the wild-type mice.

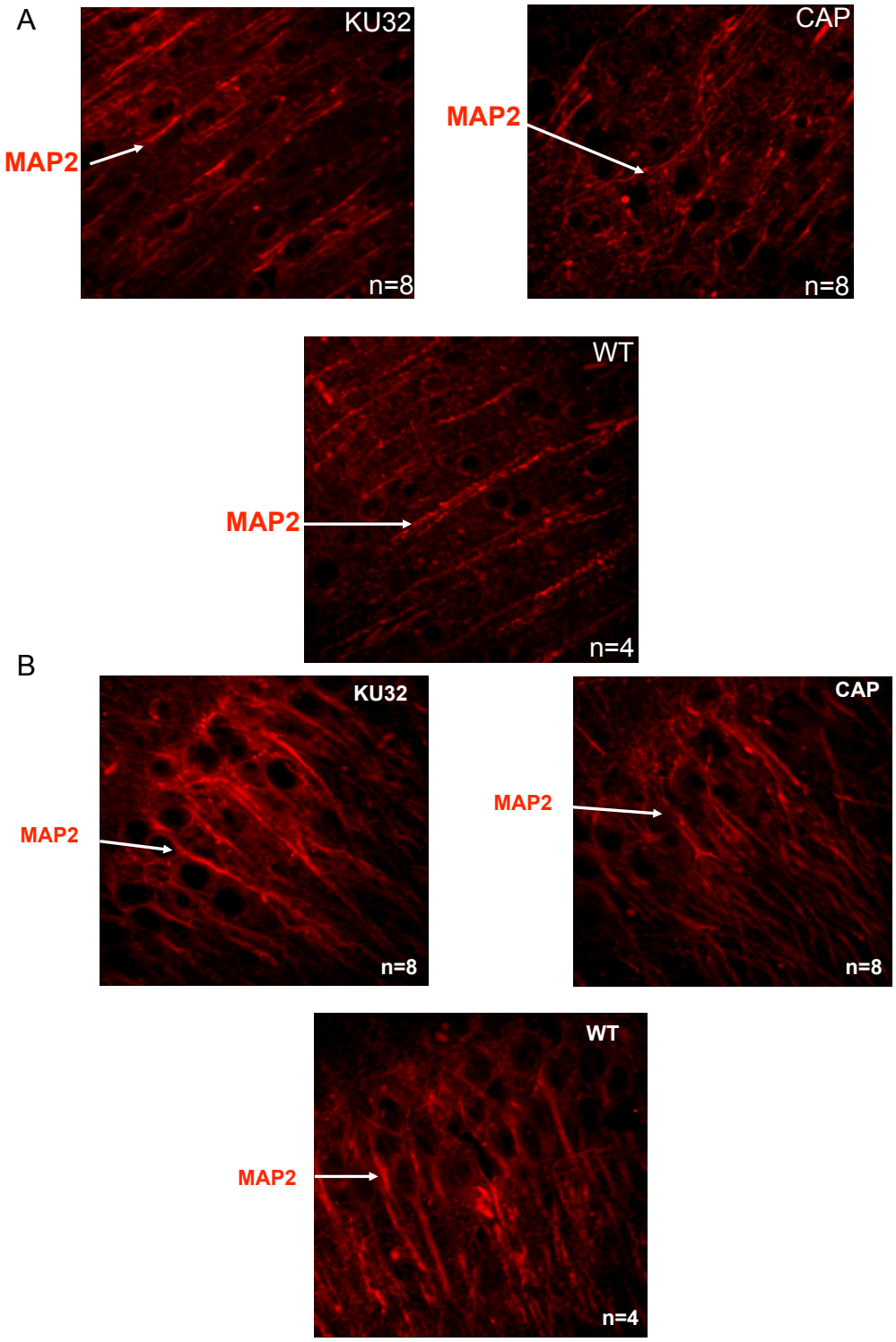

Figure 3.4: MAP2 labeling in the premotor cortex and CA1 of rTg4510 mice. (A) Representative examples of brain sections from the premotor cortex were labeled with MAP2 antibodies. (B) Representative images of brain sections from the CA1 of the hippocampus labeled with MAP2 antibodies. White arrows indicate positive MAP2 labeling. (n=8 KU-32-treated, n=8 CAP-treated, and n=4 WT mice)

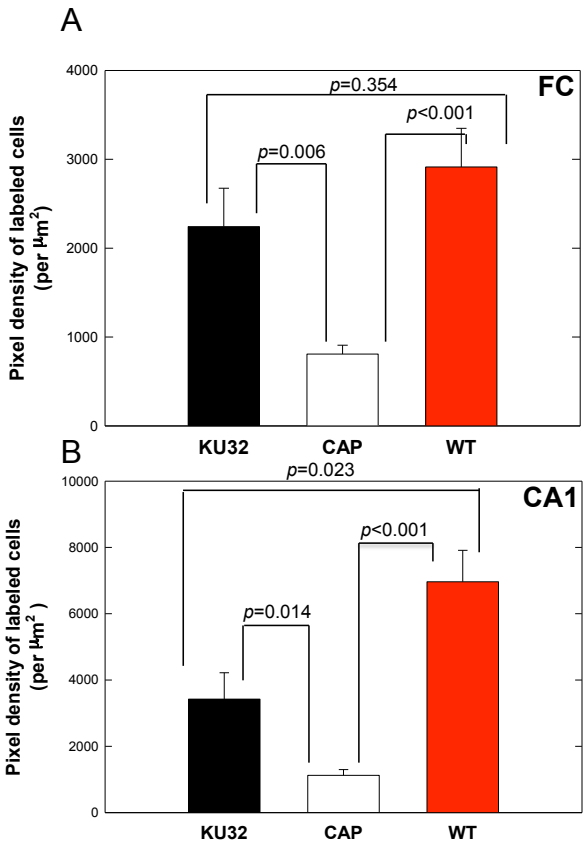

Figure 3.5: Densitometric analysis of MAP2 labeling in rTg4510 mice. Quantitative data from the (A) premotor cortex and (B) CA1 of the hippocampus were determined using the number of pixels labeled per square micron. (n=8 for KU-32-treated, n=8 for CAP-treated, and n=4 for WT mice). Statistical evaluation of significance of differences was carried out using Student's *t* test.

Another marker we evaluated for *in vivo* neuroprotection with KU-32 in the rTg4510 mice was synaptic density. Synaptophysin, which labels synaptic vesicles present in nerve terminals, showed statistically significant protection against damage in the KU-32-treated rTg4510 mice in comparison to the vehicle-treated rTg4510 mice (Figure 3.7). This protection was observed in both the premotor cortex (Figure 3.6A) and the CA1 of the hippocampus (Figure 3.6B). Significant differences were not observed when we compared labeling between the KU-32-treated and the wild-type mice in either the premotor cortex or the hippocampal regions implying that KU-32 was

able to preserve synaptic density to near normal levels in both brain regions. Although there appears to be a difference between the KU-32-treated and wild type mice (Figure 3.7), the variability in the wild-type mice is quite high which may have contributed to the lack of statistical significance.

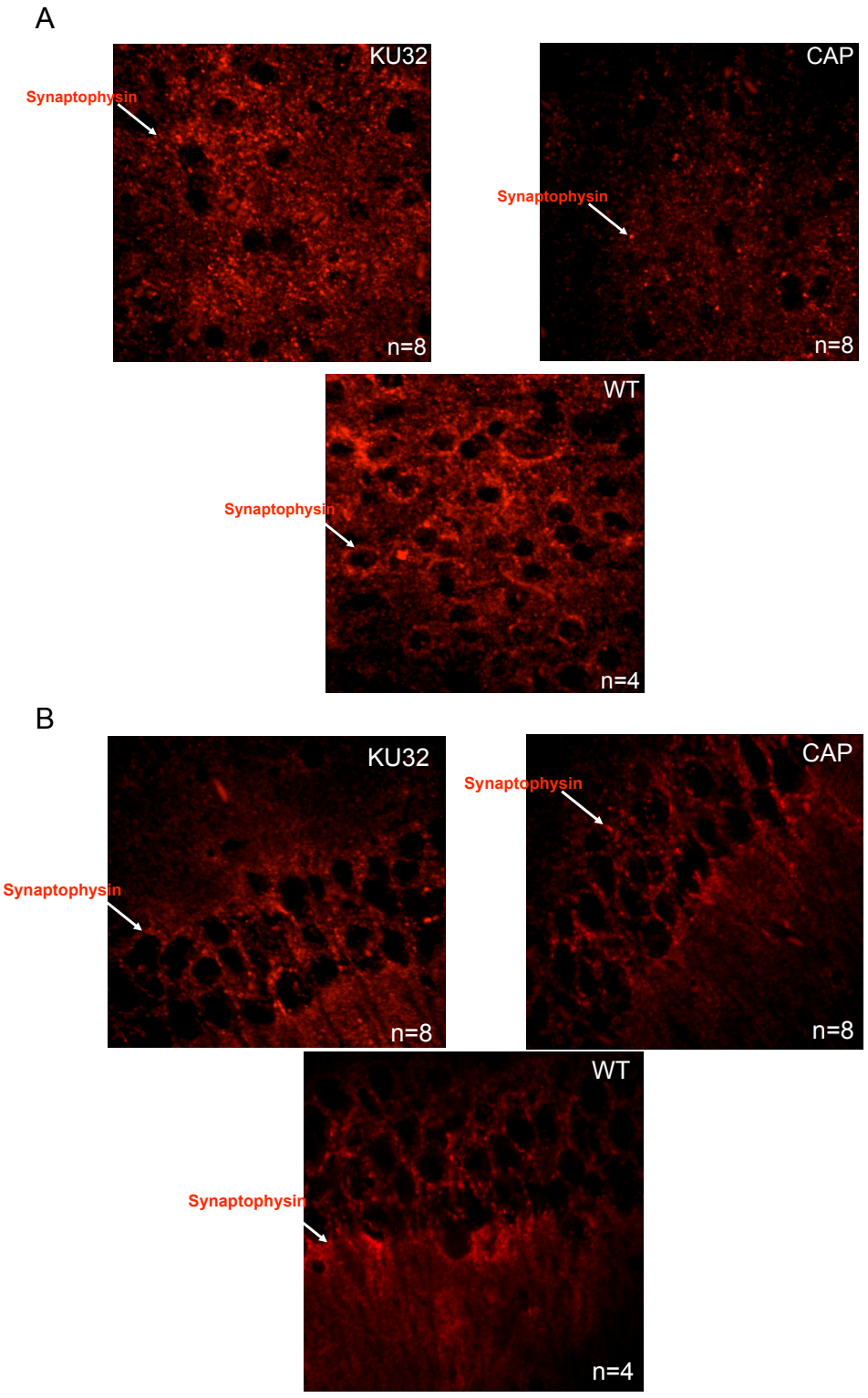

Figure 3.6: Synaptophysin labeling in the premotor cortex and CA1 regions of rTg4510 mice. Representative images labeled with synaptophysin from the (A) premotor cortex and (B) CA1 of the hippocampus. White arrows indicate positive synaptophysin labeling. (n=8 KU-32-treated, n=8 CAP-treated, n=4 WT mice).

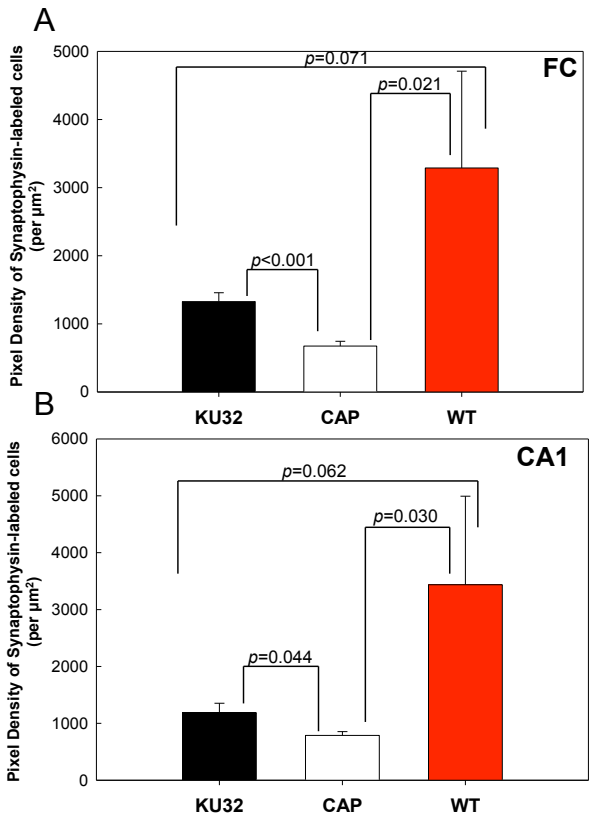

Figure 3.7: Densitometric analysis of synaptophysin labeling in rTg4510 mice. Quantitative data from the (A) premotor cortex and (B) CA1 of the hippocampus were determined using the number of pixels labeled per square micron. (n=8 KU-32-treated, n=8 CAP-treated, and n=4 WT mice). Statistical evaluation of significance of differences was carried out using Student's *t* test.

A third aspect we assessed for neuroprotection was the neuronal marker, NeuN. The NeuN antibodies label cell bodies of living neurons and are used as a measure of neurodegeneration, i.e., neuronal cell death. Our results showed that KU-32-treatment significantly protected neurons against degeneration in comparison to vehicle treatment in the premotor cortex (Figure 3.8A) and the hippocampal CA1 (Figure 3.8B) of rTg4510 mice. Morphometric analyses of these images indicate that the protection with KU-32 was significant in both the premotor cortex and the CA1 of the hippocampus (Figure 3.9). NeuN labeling in the frontal cortex of the KU-32-treated mice differed significantly

between wild type and KU-32-treated mice, but the labeling between these two sets of mice in the hippocampus was not significant, suggesting marked prevention of neuronal death with the treatment.

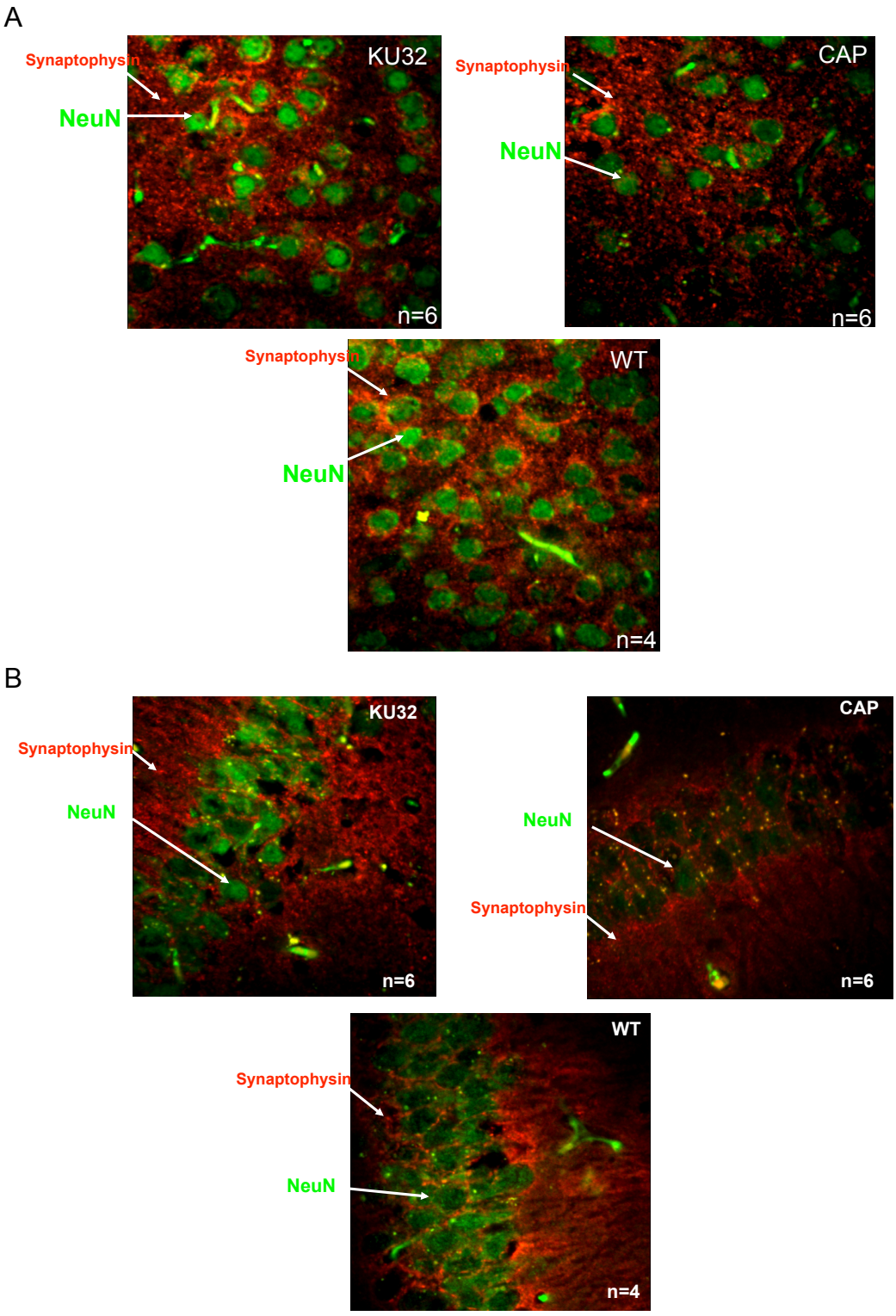

Figure 3.8: NeuN labeling in the premotor cortex and CA1 regions of rTg4510 mice. Representative images labeled with NeuN from the (A) premotor cortex and (B) CA1 of the hippocampus. White arrows indicate positive NeuN labeling. (n=6 KU-32=treated, n=6 CAP-treated, and n=4 WT mice).

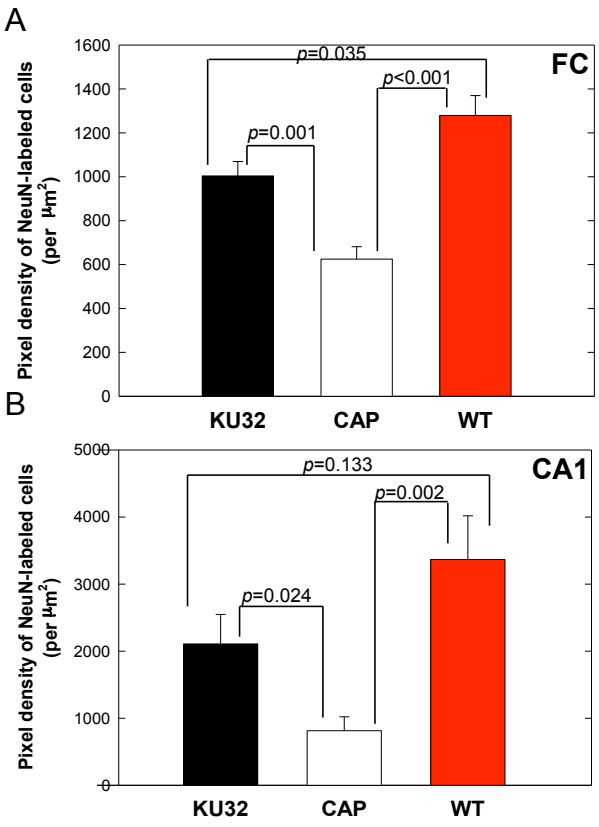

Figure 3.9: Densitometric analysis of NeuN labeling in rTg4510 mice. Quantitative data from the (A) premotor cortex and (B) CA1 of the hippocampus were determined using the number of pixels labeled per square micron. (n=6 KU-32-treated, n=6 CAP-treated, and n=4 WT mice). Statistical evaluation of significance of differences was carried out using Student's *t* test.

IV. Discussion

As shown in previous studies, analogs of novobiocin, a C-terminal Hsp90 inhibitor protect against Aβ-induced cell death in cellular models (Ansar et al., 2007, Lu et al., 2008). In the present study, we used *in vivo* models of AD to evaluate the neuroprotective efficacy of KU-32. We showed significant decreases in Tau pathology in two mutant Tau mouse models as well as neuroprotection against dendritic damage, preservation of synaptic density, and decreased cell death. Our *in vivo* neuroprotective results are similar to previously published results with KU-32 demonstrating motor

neuron protection in a mouse model of diabetic peripheral neuropathy (Urban et al., 2010).

First we investigated the effect of KU-32 on hyperphosphorylated Tau in two mouse models expressing human P301L Tau. The less robust Tau pathology model, JNPL3, demonstrated significant decreases in both CP13 (Figure 3.1) and AT8 (Figure 3.2)-labeled Tau in the premotor cortex of KU-32 treated mouse brains. The more robust Tau pathology model, rTg4510, exhibited statistically significant decreases in CP13 (Figure 3.3) labeled-Tau in the premotor cortex. Thus, the KU-32 treatment decreaseed Tau pathology in mouse models expressing low and high levels of abnormal Tau.

Prior publications support our observations of decreases in hyperphosphorylated Tau through treatment with inhibitors of Hsp90. Greengard's group used the JNPL3 mouse model to show lowered levels of abnormally phosphorylated Tau with administration of a the N-terminal Hsp90 inhibitor, GA (Dou et al., 2003). Dickey and colleagues also demonstrated decreases in hyperphosphorylated Tau in the JNPL3 mouse model using a novel N-terminal Hsp90 inhibitor, EC-102 (Dickey et al., 2006). As a whole, our results regarding KU-32 mediated *in vivo* decreases in abnormal Tau support previously reported findings.

Our results with the rTg4510 mouse model have shown that the presence of mutant P301L Tau in mouse brain leads to neurodegeneration (Figure 3.8), synaptic loss (Figure 3.6), and neuritic dystrophy (Figure 3.4). The literature contains many accounts of synaptic loss associated with AD (Scheff et al., 2006, Knight and Verkhratsky, 2010), and our results suggest that chronic treatment with KU-32 has the

potential to help preserve normal synaptic density in the premotor cortex and hippocampal CA1 (Figure 3.5). There are also previous reports linking AD with dendritic damage (Grace et al., 2002, Jin et al., 2011). We show significant dendritic damage in the premotor cortex and CA1 of the hippocampus in vehicle-treated mice that was significantly reduced with chronic KU-32 treatment (Figure 3.7). Neurodegeneration has also been described as a major morphological characteristic in the brain of the rTg4510 mouse model of AD (SantaCruz et al., 2005, Spires et al., 2006). Using NeuN as an index of neuronal cell survival, we observed much higher neuronal cell survival levels in the premotor cortex and hippocampal CA1 regions of the rTg4510 mice following KU-32 treatment (Figure 3.9). It should be noted that the images from NeuN labeling in the CA1 of the hippocampus (Figure 3.8B) was more diffuse than what was documented in the NeuN images from the premotor cortex (Figure 3.8A). This difference can be attributed to the fact that the NeuN antibody recognizes a specific nuclear protein called Fox-3 as well as a non-nuclear protein called synapsin I (Kim et al., 2009). The synapsin I protein is highly concentrated in areas of the hippocampus, while lower levels of the protein are found in the premotor cortex (Melloni et al., 1993). Therefore, the more diffuse anti-NeuN labeling of the hippocampus may be due to the recognition of the more hippocampal specific protein, synapsin I, found in the cell body of neurons.

Overall, the results from these experiments strongly support the *in vivo* efficacy of KU-32. These data warrant further investigations into the activity of KU-32 as a potential treatment of AD.

V. References

Ansar S, Burlison JA, Hadden MK, Yu XM, Desino KE, Bean J, Neckers L, Audus KL, Michaelis ML, Blagg BS (2007) A non-toxic Hsp90 inhibitor protects neurons from Abeta-induced toxicity. Bioorganic and Medicinal Chemistry Letters 17:1984-1990.

Berger Z, Roder H, Hanna A, Carlson A, Rangachari C, Yue M, Wszolek Z, Ashe K, Knight J, Dickson D, Andorfer C, Rosenberry T, Lewis J, Hutton M, Janus C (2007) Accumulation of pathological Tau species and memory loss in a conditional model of Tauopathy. Neurobiology of Disease 27:3650-3662.

Biernat J, Mandelkow EM, Schroter C, Lichtenberg-Kraag B, Steiner B, Berling B, Meyer J, Mercken M, Vandermeeren A, Goedert M (1992) The switch of Tau protein to an Alzheimer-like state includes the phosphorylation of Tau serine-proline motifs upstream of the microtubule binding region. EMBO J 11: 1593-1597

Braak H, Alafuzoff I, Arzberger T, Kretzschmar H, Del Tredici K (2006) Staging Alzheimer disease-associated neurofibrillary pathology using paraffin sections and immunocytochemistry. Acta Neuropathology 112: 389-404.

Chapman P, White G, Jones M, Cooper-Blacketer D, Marshall V, Irizarry M, Younkin L, Good M, Bliss T, Hyman B, Younkin S, Hsiao K (1999) Impaired synaptic plasticity and learning in aged amyloid precursor protein transgenic mice. Nature Neuroscience 2:271-276.

Crystal H, Dickson D, Fuld P, Masur D, Scott R, Mehler M, Masdeu J, Kawas C, Aronson M, Wolfson L (1988) Clinico-pathologic studies in dementia:

nondemented subjects with pathologically confirmed Alzheimer's disease. Neurology 38:1682-1687.

Dickey C, Dunmore J, Lu B, Wang J, Lee W, Kamal A, Burrows F, Eckman CB, Hutton M, Petrucelli L (2006) HSP induction mediates selective clearance of Tau phosphorylated at proline-directed Ser/Thr sites but not KXGS (MARK) sites. The FASEB Journal 20:753-755.

Dickey CA, Kamal A, Lundgren K, Klosak N, Bailey RM, Dunmore J, Ash P, Shoraka S, Zlatkovic J, Eckman CB, Patterson C, Dickson DW, Jr. NSN, Hutton M, Burrows F, Petrucelli L (2007) The high-affinity HSP90-CHIP complex recognizes and selectively degrades phosphorylated Tau client proteins. The Journal of Clinical Investigation 117:648-658.

Dickson DW (1997) Neurodegenerative diseases with cytoskeletal pathology: a biochemical classification. Annals of Neurology 42:541-544.

Dou F, Netzer W, Tanemura K, Li F, Hartl U, Takashima A, Gouras G, Greengard P, Xu H (2003) Chaperones increase association of Tau protein with microtubules. Proceedings of the National Academy of Sciences 100:721-726.

Gomez-Isla T, Hollister R, West H, Mui S, Growden JH, Petersen RC, Parisi JE, Hyman BT (1997) Neuronal loss correlates with but exceeds neurofibrillary tangles in Alzheimer's disease. Annals of Neurology 41:17-24.

Grace E, Rabiner C, Busciglio J (2002) Characterization of neuronal dystrophy induced by fibrillar amyloid beta: implications for Alzheimer's disease. Neuroscience 114:265-273.

Grundke-Iqbal I, Iqbal K, Tung YC, Quinlan M, Wisniewski HM, Binder L (1986) Abnormal phosphorylation of the microtubule-associated protein Tau in Alzheimer cytoskeletal pathology. PNAS 83:4913-4917.

Gureviciene I, Ikonen S, Gurevicius K, Sarkaki A, van Groen T, Pussinen R, Ylinen A, Tanila H (2004) Normal induction but accelerated decay of LTP in APP + PS1 transgenic mice. Neurobiology of Disease 15:188-195.

Hutton M, Lendon C, Rizzu P, Baker M, Froelich S, Houlden H, Pickering-Brown S, Chakraverty S, Isaacs A, Grover A, Hackett J, Adamson J, Lincoln S, Dickson D, Davies P, Petersen RC, Stevens M, de Graaff E, Wauters E, van Buren J, Hillebrand M, Joosse M, Kwon JM, Nowotny P, Che LK, Norton J, Morris JC, Reed LA, Trojanowski J, Basun H, Lannfelt L, Neystat M, Fahn S, Dark F, Tannenberg T, Dodd PR, Hayward N, Kwok JB, Schofield PR, Andreadis A, Snowden J, Craufurd D, Neary D, Owen F, Oostra BA, Hardy J, Goate A, van Swieten J, Mann D, Lynch T, Heutink P (1998) Association of missense and 5'-splice-site mutations in Tau with the inherited FTDP-17. Nature 393:702-705.

Ihara YI, Nukina N, Miura R, Ogawara M (1986) Phosphorylated Tau protein is integrated into paired helical filaments in Alzheimer's disease. Journal of Biochemistry 99:1807-1810.

Jin M, Shepardson N, Yang T, Chen G, Walsh D, Selkoe D (2011) Soluble amyloid beta-protein dimers isolated from Alzheimer cortex directly induce Tau hyperphosphorylation and neuritic degeneration. Proceedings of the National Academy of Sciences 108:5819-5824.

Kim K, Adelstein R, Kawamoto S (2009) Identification of neuronal nuclei (NeuN) as Fox-3, a new member of the Fox-1 gene family of splicing factors. Journal of Biological Chemistry 284:31052-31061.

Knight R, Verkhratsky A (2010) Neurodegenerative diseases: failures in brain connectivity? Cell Death and Differentiation 17:1069-1070.

Kosik K, Joachim CL, Selkoe D (1986) Microtubule-associated protein Tau (Tau) is a major antigenic component of paired helical filaments in Alzheimer's disease. PNAS 83:4044-4048.

Lewis J, McGowan E, Rockwood J, Melrose H, Nacharaju P, Van Slegtenhorst M, Gwinn-Hardy K, Murphy M, Baker M, Yu X, Duff K, Hardy J, Corral A, Lin W, Yen S, Dickson D, Davies P, Hutton M (2000) Neurofibrillary tangles, amyotrophy and progressive motor disturbance in mice expressing mutant (P301L) Tau protein. Nature Genetics 25:402-405.

Lu Y, Ansar S, Michaelis M, Blagg B (2008) Neuroprotective activity and evaluation of Hsp90 inhibitors in an immortalized neuronal cell line. Bioorganic and Medicinal Chemistry Letters 17:1709-1715.

Luo W, Dou F, Rodina A, Chip S, Joungnam K, Zhao Q, Moulick K, Aguirre J, Wu N, Greengard P, Chiosis G (2007) Roles of heat-shock protein 90 in maintaining and facilitating the neurodegenerative phenotype in Tauopathies. Proceedings of the National Academy of Sciences 104:9511-9516.

Melloni R Jr., Hemmendinger L, Hamos J, Degennaro L (1993) Synapsin I gene expression in the adult rat brain with comparitive analysis of mRNA and protein in the hippocampus. The Journal of Comparative Neurology 327:507-520.

Oddo S, Caccamo A, Shepard J, Murphy M, Golde TE, Kayed R, Metherate R, Mattson M, Akbari Y, LaFerla F (2003) Triple-transgenic model of Alzheimer's disease with plaques and tangles: intracellular Abeta and synaptic dysfunction. Neuron 39:409-421.

Ramsden M, Kotilinek L, Forster C, Paulson J, McGowan E, SantaCruz K, Guimaraes A, Yue M, Lewis J, Carlson G, Hutton M, Ashe K (2005) Age-dependent neurofibrillary tangle formation, neuron loss, and memory impairment in a mouse model of human Tauopathy (P301L). Journal of Neuroscience 25:10637-10647.

SantaCruz K, Lewis J, Spires T, Paulson J, Kotilinek L, Ingelsson M, Guimaraes A, DeTure M, Ramsden M, McGowan E, Forster C, Yue M, Orne J, Janus C, Mariash A, Kuskowski M, Hyman B, Hutton M, Ashe K (2005) Tau suppression in a neurodegenerative mouse model improves memory function. Science 309:476-481.

Scheff S, Price D, Schmitt F, Mufson E (2006) Hippocampal synaptic loss in early Alzheimer’s disease and mild cognitive impairment. Neurobiology of Aging 27:1372-1384.

Spillantini MG, Bird TD, Ghetti B (1998) Frontotemporal dementia and Parkinsonism linked to chromosome 17: a new group of Tauopathies. Brain Patholody 8:387-402.

Spires T, Orne J, SantaCruz K, Pitstick R, Carlson G, Ashe K, Hyman B (2006) Region-specific dissociation of neuronal loss and neurofibrillary pathology in a mouse model of Tauopathy. The American Journal of Pathology 168:1598-1607.

Urban M, Li C, Yu C, Lu Y, Krise J, McIntosh M, Rajewski R, Blagg BS, Dobrowsky R (2010) Inhibiting heat-shock protien 90 reverses sensory hypoalgesia in diabetic mice. ASN Neuro 2:189-199.

Weingarten M, Lockwood A, Hwo S, Kirschner M (1975) A protein factor essential for microtubule assembly. Proceedings of the National Academy of Sciences 72:1865-1862.

CHAPTER FOUR: Exploration of Potential Mechanisms Underlying the Actions of KU-32 *In Vitro* and *In Vivo*

I. Introduction

Most neurodegenerative disorders are characterized by the presence of protein aggregates. The most common neurodegenerative disease, Alzheimer's disease (AD) has two hallmark protein aggregates. One of the characteristic protein aggregates is the senile plaques, which are made-up of oligomers of the β-amyloid peptide, and the second is the neurofibrillary tangles (NFTs) comprised of hyperphosphorylated and fibrillar Tau protein. Designing therapeutics to remove these aggregated proteins seems quite likely to be helpful in AD, as there are no disease-modifying agents currently available to stop progression of the pathological process.

The development of the characteristic aggregates leading to AD is multi-faceted; however, the deposition of protein aggregates in the cell leads to an overall decrease in cellular function. Therefore, it seems reasonable to expect that designing therapeutics that enhance the protein quality control machinery of the cell would help to improve cellular function. One way to influence the cellular machinery that controls protein quality is through the modulation of the Hsp90 protein, a major regulator of the heat shock response (Muchowski, 2002, Muchowski and Wacker, 2005, Luo et al., 2008).

Previous reports regarding the testing of Hsp90 inhibitors designed to block the N-terminal ATPase activity of the protein have shown promising decreases in the Tau pathology associated with AD. Greengard and colleagues demonstrated that the N-terminal ATPase inhibitor, GA, decreased insoluble Tau in an *in vitro* model of AD, and

GA also decreased the levels of hyperphosphorylated Tau induced by okadaic acid (OA), a protein phosphatase 2A inhibitor (Dou et al., 2003). Later, this group of scientists performed *in vivo* studies using GA to demonstrate decreases in hyperphosphorylated Tau in cellular and animal models expressing mutant P301L Tau (Luo et al., 2007). Other researchers also demonstrated decreases in hyperphosphorylated Tau using novel derivatives of N-terminal ATPase Hsp90 inhibitors such as EC102 (Dickey et al., 2006, Dickey et al., 2007). Modulators of the C-terminal portion of Hsp90 also led to decreases in hyperphosphorylated Tau *in vivo* in mouse models expressing P301L mutant Tau (Chapter 3; unpublished results). Since these C-terminal modulators demonstrate promising therapeutic potential, it is important to try to understand the mechanism underlying their beneficial effects.

One potential mechanism for decreases in hyperphosphorylated Tau could be due to effects of the compound on the activity of kinases involved in Tau fibrillization that are also client proteins of Hsp90. One well-known kinase that has been associated with aberrant phosphorylation of Tau in AD is cyclin-dependent kinase-5 (cdk5) (Iqbal et al., 2005). The activity of cdk5 is dependent upon a small membrane-bound fragment called p35 (Takahashi et al., 2005). Previous reports by Greengard and colleagues demonstrated that a novel N-terminal Hsp90 ATPase inhibitor, PU24FCl, led to dose-dependent decreases in p35 with simultaneous decreases in cdk5 activity. These results suggest that N-terminal Hsp90 inhibition allows for p35 degradation by the proteasome (Dou et al., 2003). Since we have previously shown *in vivo* decreases of hyperphosphorylated Tau with KU-32 administration (Chapter 3), it is possible that KU-

32 could decrease p35 levels and cdk5 activity similarly to the N-terminal Hsp90 inhibitor used in Greengard's studies.

A second potential mechanism elicited upon KU-32 administration is heat shock protein stimulation. Groups using the N-terminal ATPase inhibitors, such as GA, suggest that the heat shock response is stimulated upon administration of these inhibitors (Sittler et al., 2001). The proposed mechanism is that inhibition of Hsp90 releases the transcription factor, HSF-1, that is normally bound to Hsp90 in a multi-component complex of proteins in the cytosol. Once HSF-1 is released, it becomes phosphorylated, trimerizes, and translocates to the nucleus where it binds to the heat shock element present in DNA encoding other chaperones. HSF-1 binding to these heat shock elements leads to up-regulation in transcription of several other heat shock proteins such as Hsp70, Hsp40 and Hsp27 (Bagatell et al., 2000). Research groups using N-terminal ATPase Hsp90 inhibitors demonstrated increases in Hsp70, Hsp40, and Hsp27, which suggests that these compounds do indeed stimulate the heat shock response (Dou et al., 2003, Dickey et al., 2006, Dickey et al., 2007, Luo et al., 2007).

Stimulation of the heat shock response also leads to increases in proteins that help regulate the function of HSPs that are regarded as co-chaperones, including the Bcl-2 associated athanogene (BAG) family. This family consists of 6 different members, 4 of which have been shown to associate with Hsp70 (Takayama and Reed, 2001). BAG proteins can induce the release of a bound substrate from Hsp70 by mediating nucleotide exchange allowing for more substrate-Hsp70 interactions (Sonderman et al., 2001).

One BAG family member, BAG1, interacts with Hsp70 and Tau (Luders et al., 2000). BAG1 contains an ubiquitin-like domain, and is correlated with ubiquitin-dependent degradation of Tau (Demand et al., 2001). BAG1 and the ubiquitin-ligase, carboxy terminus of Hsc70-binding protein (CHIP), simultaneously bind to Hsp70 to ubiquitinate client proteins and target them for degradation (Hartl and Hayer-Hartl, 2002, Gamerdinger et al., 2011).

Another member of the BAG family, BAG2, has been reported to play a critical role in mediating a highly efficient mode of Tau degradation through ubiquitin-independent mechanisms. It has been demonstrated that the BAG2/Hsp70 complex can tether hyperphosphorylated Tau to the proteasome for degradation without the ubiquitination of Tau (Carrettiero et al., 2009). Lukiw and colleagues have shown that expression of BAG2 is inhibited by miR-128, a microRNA that is up-regulated in Alzheimer's disease (Lukiw, 2007), thereby preventing BAG2-associated removal of aggregated Tau.

We have tested analogs of novobiocin, an inhibitor or modulator of the C-terminal portion of Hsp90, in order to assess their potential as a therapeutic for neurodegenerative diseases. As these are novel compounds, it was important to investigate the mechanism(s) through which these compounds produce neuroprotective effects. Our hypothesis was that C-terminal Hsp90 modulators essentially act through the same mechanism as N-terminal inhibitors. Therefore, using previous reports of the N-terminal Hsp90 inhibitors, we examined the effects of the C-terminal modulators on the same protein pathways involved in the established heat shock response.

Our studies focused on determining if the inhibition of the C-terminal nucleotide-binding site in Hsp90 transcriptionally regulated other molecular chaperones and co-chaperones, and if C-terminal inhibition of Hsp90 activated the same signaling pathway as the N-terminal ATPase inhibitors. We examined two potential mechanisms. First, we looked to see if KU-32 decreased p35 levels and cdk5 activity, which could be responsible for the decreases of hyperphosphorylated Tau observed *in vivo* (Chapter 3). Second, we looked at the effects of KU-32 on the heat shock response by investigating levels of: Hsp70; BAG1 and BAG2, co-chaperones of Hsp70; and HSF-1. We hypothesized that KU-32 would decrease kinase activity associated with AD while also stimulating the heat shock response thereby enhancing the refolding or ubiquitination and proteasomal degradation of misfolded Tau.

II. Materials and Methods

Preparation of primary neuronal cultures

Primary cortical neurons were prepared from day 18 embryonic rat fetuses (Harlan Sprague Dawley) as described previously in Chapter 2 of this dissertation (Michaelis et al., 1994, Michaelis et al., 1998, Michaelis et al., 2005). All animal procedures were approved by IACUC.

Aβ peptide preparation and cell culture treatments

The $A\beta_{25-35}$ peptide was purchased from Anaspec (Fremont, CA) and prepared as previously described in Chapter 2 of this dissertation.

Primary neurons were allowed to grow for 7 days *in vitro* (DIV7) before any treatments. In order to assess Hsp70 and p35 levels, the cells were treated with 0.01% DMSO (vehicle), 5 nM, 50 nM, 100 nM, and 10 μM concentrations of KU-32 for 24 hours. The N-terminal inhibitor, geldanamycin (GA), served as a positive control and was administered at 50, 200, and 400 nM concentrations for 24 hours. In a separate experiment to examine cdk5 activity, primary cortical neurons were treated with 5% Captisol® (vehicle) or 100 nM KU-32. Two hours later, 25 μM $A\beta_{25-35}$ or 30 μM Roscovitine, a cdk5 inhibitor, were added for 48 hours. The activity of cdk5 was measured by using chemiluminescence.

Chemiluminescence method to determine in vitro kinase activity

Forty-eight hours after initiation of exposure to $A\beta_{25-35}$, the cells were lysed using kinase lysis buffer containing 20 mM Tris-HCl pH, 7.4, 140 mM NaCl, 1 mM PMSF, 1 mM sodium orthovanadate, 10 mM NaF, 0.1% Nonidet-40, 1 mM EDTA, 26 μM N-[N-(N-Acetyl-L-leucyl)-L-leucyl]-L-norleucine (ALLN, a Calpain inhibitor), protease inhibitors cocktail set III (Calbiochem), and phosphatase inhibitors cocktail III (Sigma). Following homogenization, cellular debris was removed by centrifuging the samples at 10,000 g for 10 minutes at 4°C, and the protein concentrations of the supernatant were determined using the BCA assay. Two hundred micrograms of protein were mixed with 2 μg of cdk5 antibodies (SantaCruz, Santa Cruz, CA) and the samples incubated overnight at 4°C with continuous mixing. After 24 hours, Protein-A Sepharose beads (40 μL in a 50% slurry; Sigma) were added to samples, and immune complexes were permitted to form for 2 hours with continuous mixing at 4°C. The beads were collected

using centrifugation at 5,000g for 30 seconds and washed 3 times with kinase lysis buffer and 3 times with kinase activity buffer (50 mM Tris-HCl pH 7.4, 80 mM β-glycerphosphate, 20 mM EGTA, 15 mM $MgCl_2$ and 1 mM dithiothreitol), and finally re-suspended in 40 µL of kinase activity buffer. Twenty µL of beads were incubated with 2.5 µM ATP and 1 µg of the substrate Histone (H1) for 30 minutes at 24°C. The luminescent kinase reagent mixture (30 µL) from the KinaseGlo Assay Kit (Promega) was added to the samples and allowed to incubate for 10 minutes. This reagent reacts with any remaining ATP in the reaction mixture and emits 1 photon/mol ATP. A luminometer was used to measure luminescence, and ATP consumption was calculated by subtracting the luminescence of the sample from that of the ATP in a blank sample lacking protein. The ATP consumed was determined using a standard ATP curve concentration from 0 to 10 µM. cdk5 activity was graphed as pmol ATP consumed per µg of protein per minute. Statistical analysis of data was performed using Student's *t* test.

Immunoblotting for Hsp70 and p35 levels

KU-32 and DMSO-treated primary cortical neurons were rinsed twice in phosphate buffered saline (PBS), lysed in kinase lysis buffer containing 20 mM Tris-HCl (pH 7.4) 140 mM NaCl, 1 mM PMSF, 1 mM sodium orthovanadate, 10 mM NaF, 0.1% Nonidet-40, 1 mM EDTA, 26 µM N-[N-(N-Acetyl-L-leucyl)-L-leucyl]-L-norleucine (ALLN, a Calpain inhibitor), protease inhibitors cocktail set III (Calbiochem), and phosphatase inhibitor cocktail III (Sigma), and collected by scraping the dishes and recovering all the contents. Following homogenization, the protein concentration was determined using

the bicinchoninic acid assay (BCA) from Thermo Fisher Scientific. Reducing sample buffer (50mM Tris-HCl at pH 6.8, 6.7% glycerol, 2.7% SDS, 0.05% Bromophenol Blue, and 250 mM dithiothreitol) was added to 25 ug aliquots of each tissue sample and the proteins were resolved by SDS-PAGE. The proteins were transferred to polyvinylidene fluoride (PVDF) membranes as described previously (Zaidi and Michaelis, 1999). The membrane was probed with Hsp70 antibodies against the inducible isoform, Hsp70.1 (1:500; Assay Designs, Farmingdale, NY) or p35 antibodies (1:200; SantaCruz Biotechnology, Santa Cruz, CA). Actin (1:1000; SantaCruz Biotechnology, Santa Cruz, CA) served as a loading control. Immunoreactive proteins were detected using the chemiluminescence substrate kit (KPL, Gaithersburg, MD). All primary incubations were completed on the same membrane. One Minute Stripping Buffer (GM Biosciences, Rockville, MD) was used to remove the previously bound antibodies. Densitometry was performed on the p35-labeled immunoblots. Experiments were repeated as indicated in the figures for verification.

Mouse treatments to assess molecular chaperone levels

For immunohistochemistry studies, 129S6xFVB mice were treated one time with an intra-peritoneal injection of 20 mg/kg of KU-32 or 5% Captisol® (vehicle). Mice were sacrificed with CO_2 inhalation at 6 hours, 1 day, 2 days, 3 days, 4 days, 5 days, and 7 days post injection. The vehicle-treated mice were sacrificed on day 7 only. Three mice were used per treatment. Immunohistochemical analysis was performed on the mouse brains essentially as described in Chapter 3.

In order to assess levels of molecular chaperones with Western blotting and qPCR, three-month old FVB mice were treated with 20 mg/kg of KU-32 or 5% Captisol® one time. Three mice per group were sacrificed 96 hours after treatment and prepared for protein assessment by immunoblot.

For analysis of potential trimerization of HSF-1 in response to KU-32 treatment, three month old FVB mice were treated with 20 mg/kg of KU-32 or 5% Captisol® one time. The treated and non-treated mice were sacrificed at 6, 12, 24, and 48 hours post-injection. For each of the different time points, one mouse each was used for the no treatment and Captisol controls, and two mice were sacrificed per KU-32 treatment. We did not find previously published experimental protocols for *in* vivo analysis of HSF-1 multimer formation. Therefore, in order to test for multimer formation, we needed a positive control model. We used primary cortical neurons treated with GA as a positive control, while non-treated primary cortical neurons served as a negative control. The GA treated cells lead to HSF-1 trimer formation, while the non-treated cells only have the monomeric HSF-1.

Immunohistochemical analysis of 129S6xFVB mice injected with KU-32

Once the mice were sacrificed, the brains were extracted, cerebella removed, and the brains hemisected. Hemibrains were fixed in 4% paraformaldehyde, submerged in 30% sucrose for 7 days, flash frozen in 4-methyl-butane in liquid N_2, and cut on the cryostat. Free-floating sections were cut at 20 µm and stored at 4°C in 1xPBS. We placed sections in 12-well plates. The sections were permeabilized with 0.1% triton-X for 30 minutes, rinsed 2 times in 1xPBS and incubated 30 minutes in 1%

hydrogen peroxide in 50% methanol with 0.1% sodium azide to block endogenous peroxidase activity. Slides were rinsed 2 times in 1xPBS and incubated in 2% gelatin for 1 hour at 37°C to further block endogenous binding. Using a Vectastain kit, standard streptavidin-peroxidase labeling was used with the DAB chromagen (Vector, Burlingame, CA). Primary antibody, Hsp70 (Assay Designs, Farmingdale, NY; 1:500), BAG1 (Abcam; 1:500) or BAG2 (Abcam; 1:500) was incubated with the sections overnight at 4°C. Sections were viewed with the Nikon Eclipse 80i microscope and images were captured at 40x magnification with the Photometrics CoolSnap camera. Positive labeling was quantified using Metamorph. Experiments were performed in triplicate. Data were analyzed for statistical significance of differences using Student's *t* test (SigmaPlot 11).

Immunoblotting of brain tissue 96 hours after KU-32 injection in FVB mice

Mouse brains were extracted, cerebella removed, brains hemisected, and the hippocampus was dissected from each half of the remaining brain portions. One half of the remaining brain portion and hippocampal regions were homogenized in a buffer containing 0.32 M Sucrose, 0.5 mM $MgSO_4$, 10 mM ACA, 0.1 mM EGTA, 10 mM HEPES, 0.1 mM Benzamide, and 0.1 mM Benzamidine (pH 7.4) using a hand-held electric homogenizer. The homogenates were centrifuged at 5,000 rpm for 10 minutes to obtain crude nuclear and cytosolic fractions.

After centrifugation, the protein levels of each fraction were determined using the bicinchoninic acid assay (BCA) from Thermo Fisher Scientific. Reducing sample buffer (50mM Tris-HCl at pH 6.8, 6.7% glycerol, 2.7% SDS, 0.05% Bromophenol Blue, and

250 mM dithiothreitol) was added to 25 µg protein aliquots of each tissue sample and the proteins resolved by SDS-PAGE. The proteins were transferred to polyvinylidene fluoride (PVDF) membranes as described previously (Zaidi and Michaelis, 1999). The membrane was probed with Hsp70 (1:500; Assay Designs, Farmingdale, NY), HSF-1 (1:1000; Assay Designs, Farmingdale, NY) and actin antibodies (1:1000; SantaCruz, Santa Cruz, CA). Actin served as a loading control. Immunoreactive proteins were detected using a chemiluminescence substrate kit (KPL, Gaithersburg, MD). All primary incubations were completed on the same membrane using One Minute Stripping Buffer (GM Biosciences, Rockville, MD) to remove the previously reactive antibodies. Experiments were completed in triplicate and densitometry was performed.

Quantitative PCR to examine Hsp70 expression

Mouse brains were extracted, cerebella removed, brains hemisected, and the hippocampus was dissected from each half of the remaining brain portions. One half of the remaining brain portion and hippocampal regions were flash frozen in liquid N_2, and stored at -80°C. RNA was extracted using the RNeasy mini kit from Qiagen (Valencia, CA). The High Capacity Reverse Transcriptase kit (Applied Biosystems) was used to generate cDNA from the tissue extracted RNA. Nucleic acid concentration was estimated with the NanoDrop instrument. One-hundred nanograms of cDNA from each sample was used to measure the amount of Hsp70 and Enolase2 RNA by quantitative PCR (qPCR). The values for Enolase2 were used to standardize the RNA measurements for the determination of Hsp70 gene copy number in all samples. To measure Hsp70 expression, the TaqMan Gene Expression Assay kit was used from

Applied Biosystems, Mm01159846_s1 Hspa1a (Applied Biosystems, Carlsbad, CA). The Enolase2 gene assay kit, Mm00469062_n1 Enolase2, was used to determine expression levels of Enolase2 (Applied Biosystems, Carlsbad, CA). Gene copy numbers were calculated based on Hsp70 ratios of KU-32-treated to 5% Captisol-treated cycle threshold (Ct) values.

Blue native gel electrophoresis of brain samples from KU-32 treated FVB mice

Blue Native gels are used to assess changes in protein complexes and multimer formation (Nijtmans et al., 2002). Brain were prepared as above and sub fractionated by centrifugation into three separate fractions: P1, P2, and cytosolic. Centrifugation was performed using a three-spin procedure. First, the homogenates were spun for 5 minutes at 3,500 rpm. The supernatant from this spin was removed, and the pellet was re-suspended in homogenization buffer and, spun again for 5 minutes at 3,500 rpm. The supernatant was removed, and the pellet from this spin was labeled P1. The supernatants from the first and second spins were combined and centrifuged at 13,000 rpm for 10 minutes. The pellet from this spin was P2 and the supernatant was the cytosolic fraction.

Following centrifugation, 2% n-dodecyl β-D-maltoside (DDM) was added to each of the P1 and cytosolic fraction samples and each was homogenized using the hand-held homogenizer. Samples were centrifuged at 15,500 rpm for 60 minutes. After centrifugation with DDM, the protein levels of each fraction were determined using the bicinchoninic acid assay (BCA) from Thermo Fisher Scientific. NativePage Gel Loading Buffer (Invitrogen, Carlsbad, CA) was added to 6 µg protein aliquots of each sample

and the proteins were resolved on a NativePage gel (Invitrogen, Carlsbad, CA). The gels were run on ice at 150V for 1 hour using pre-chilled dark blue cathode buffer and 1X Running anode buffer (both provided by Invitrogen, Carlsbad, CA). After 1 hour, the dark blue cathode buffer was replaced with pre-chilled light blue cathode buffer (Invitrogen, Carlsbad, CA) and run at 250V for 3 hours. After the protein separation, the proteins were transferred to polyvinylidene fluoride (PVDF) membranes as described previously (Zaidi and Michaelis, 1999). The membrane was washed in 1% acetic acid in 1xPBS solution for 5 minutes before 60 minutes of blocking in 5% non-fat dry milk. The membrane was probed with HSF-1 antibodies (1:1000; Assay Designs, Farmingdale, NY). Immunoreactive proteins were detected using the chemiluminescence substrate kit (KPL, Gaithersburg, MD).

III. Results

KU-32 did not significantly alter p35 levels

Since we have observed decreases in hyperphosphorylated Tau in the brains KU-32-treated mouse models expressing mutant Tau (Chapter 3), it was of interest to determine if KU-32 treatment might decrease levels of p35. Given that p35 is required for cdk5 activity (Kushakawa et al., 2000), and since we observed decreases of the phospho-Tau labeling at sites that cdk5 is believed to phosphorylate, we assessed p35 levels to see if there is a change in p35 levels with KU-32 administration. Previously, Greengard and colleagues demonstrated that N-terminal Hsp90 inhibitors led to a dose-dependent decrease in p35 levels, which correlated with decreases in cdk5 activity (Luo

et al., 2007). We anticipated that KU-32 would lead to results similar to those published by Greengard, and show a dose dependent decrease in p35 levels in primary neurons.

Primary cortical neurons were treated with KU-32 concentrations ranging from 5 nM to 10 μM, and DMSO served as the vehicle control. After 24 hours, the cells were lysed and the p35 levels were assessed using Western blots. We performed these experiments 6 times, and determined that there were no changes in p35 levels with KU-32 treatment (Figure 4.1). Our positive control, GA, did show dose dependent decreases in p35 levels, although those data were not analyzed for densitometric values (Figure 4.1). Overall, these studies indicate that KU-32, unlike N-terminal Hsp90 inhibitors, did not decrease p35 levels.

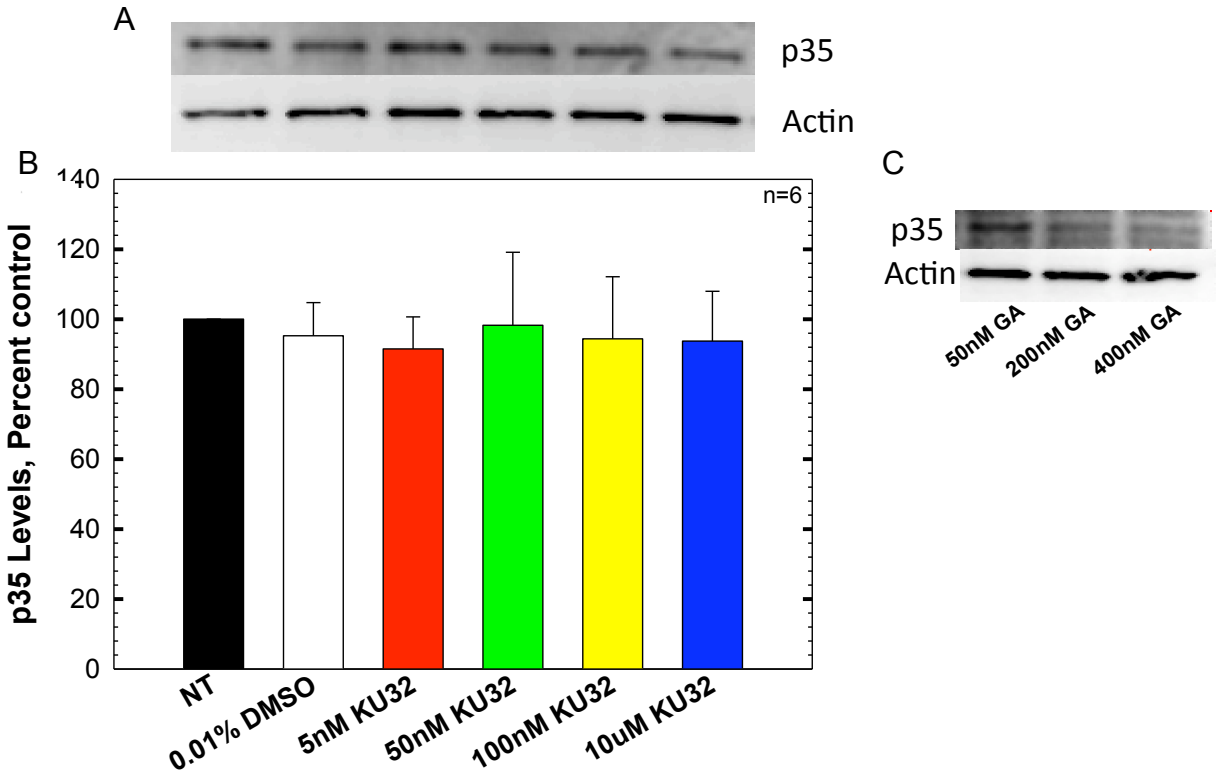

Figure 4.1: Effect of KU-32 on p35 levels in primary cortical neurons. Primary cortical neurons were treated with the vehicle (0.01% DMSO) or indicated doses of KU-32 and GA. Twenty-four hours after treatment, cells were lysed, and 25 μg aliquots of protein were separated on SDS-PAGE gels. (A) Representative immunoblot of KU-32

treatments on p35 protein levels. (B) Densitometric analysis of p35 levels using actin as the control. Experiments were repeated 6 times. (C) Representative immunoblot of GA treatment on p35 protein levels.

The activity of cdk5 was not changed with KU-32 treatment

Although we did not observe changes in p35 levels, it was possible that KU-32 could affect cdk5 activity without interfering with the interaction between cdk5 and p35. Therefore, we pre-treated primary cortical neurons with 100 nM KU-32 for 2 hours, and then incubated the cells with 25 μM $A\beta_{25-35}$ or 30 μM Roscovitine, a cdk5 inhibitor, for 48 hours. After the incubation, the cells were lysed, and cdk5 activity was evaluated. Our results showed no effect of KU-32 on the activity of cdk5. However, this assay presented problems that we could not explain. First, the well-known cdk5 activator, Aβ, (Lee et al., 2000) did not significantly increase cdk5 activity in comparison to the non-treated controls. Secondly, the potent cdk5 inhibitor, Roscovitine, also did not decrease cdk5 activity below control levels in our cultures. Thus, our failure to demonstrate activity under normal control conditions rendered our testing of KU-32 effects of cdk5 activity inconclusive (Figure 4.2).

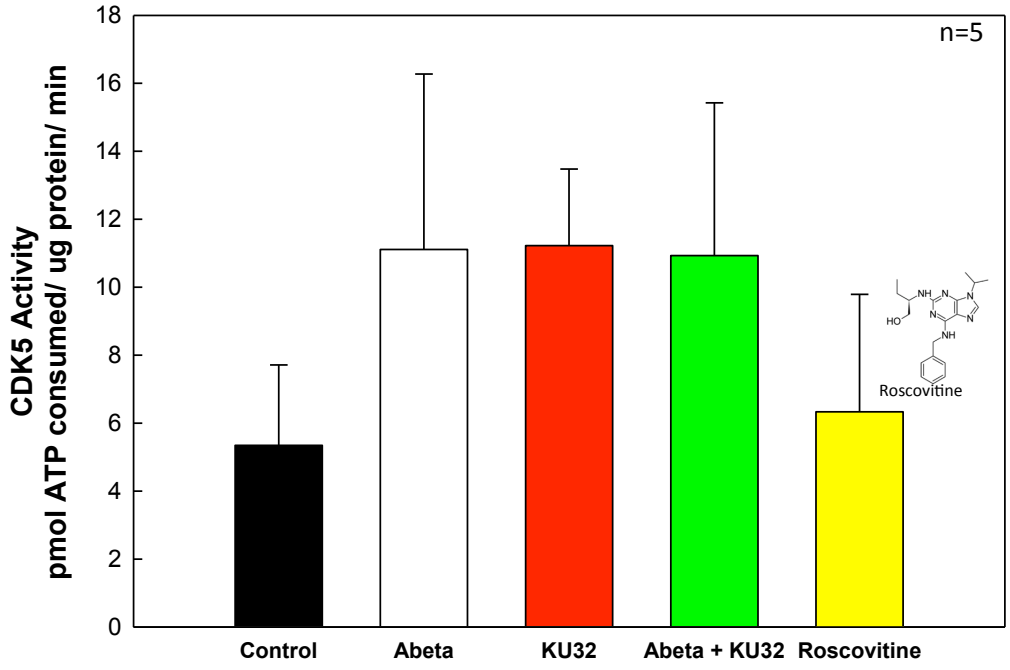

Figure 4.2: The effect of KU-32 on cdk5 activity in primary cortical neurons. Primary cortical neurons were pre-treated with the vehicle (5% Captisol®) or 100 nM KU-32 for 2 hours and then treated with 25 μM $A\beta_{25-35}$ or 30 μM Roscovitine. Forty-eight hours after treatment, cells were lysed, and cdk5 activity was examined. Experiments were repeated 5 times.

Hsp70 levels in primary cortical neurons treated with KU-32

A second potential mechanism for the *in vivo* effects of KU-32 is the stimulation of the heat shock response as is observed with N-terminal ATPase inhibitors. In order to determine if KU-32 treatment activates the heat shock response, we first investigated whether there were increased levels of molecular chaperones following exposure to KU-32. One molecular chaperone that has been clearly demonstrated to increase upon Hsp90 inhibition is Hsp70 (Dou et al., 2003, Dickey et al., 2007, Luo et al., 2007). We treated primary cortical neurons with 5 nM, 50 nM, 100 nM, and 10 μM KU-32 dissolved in DMSO as well as 50 nM, 200 nM, and 400 nM of the well-known inducer of the heat

shock response, the N-terminal Hsp90 ATPase inhibitor, geldanamycin (GA). The cells were lysed 24 hours post-treatment, and the proteins were separated using SDS-PAGE. The Hsp70 labeled immunoblot revealed that protein levels did not increase with KU-32 administration, even at micromolar concentrations. As expected, the positive control, GA, robustly increased Hsp70 levels at nanomolar concentrations (Figure 4.3). These data suggest that KU-32 does not increase Hsp70 levels upon administration, providing evidence that KU-32 does not stimulate the classical heat shock response.

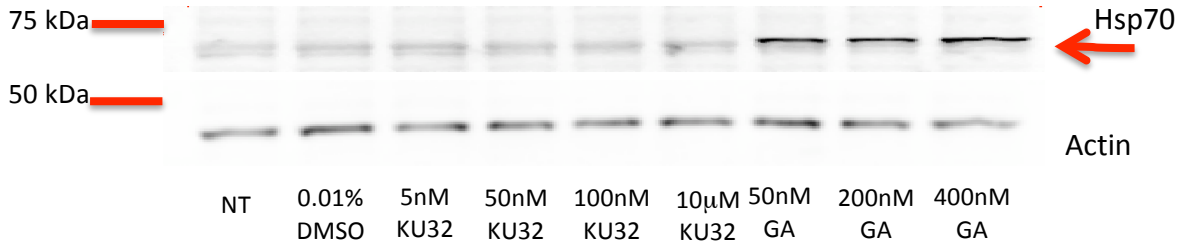

Figure 4.3: Hsp70 levels are not changed upon KU-32 administration. No treatment, vehicle (0.01% DMSO), KU-32 (concentration as indicated on the blot), and GA (concentration as indicated on the blot)-treated primary cortical lysates were separated by SDS-PAGE and analyzed for Hsp70 levels. Actin labeling was also performed and served as a loading control. GA-treated cells were used as the positive control. This is a representative blot from 2 separate experiments.

Expression of Hsp70 mRNA and protein after in vivo treatment with KU-32

Since we did not observe changes in Hsp70 protein levels in the primary cortical neurons treated with KU-32, but observed marked protection in a mouse model overexpressing mutant P301L Tau protein, we decided to determine if KU-32 treatment increased expression of Hsp70 protein levels *in vivo*. In order to assess potential transcriptional and translational up-regulation of Hsp70, we treated FVB mice with 20 mg/kg of KU-32 or 5% Captisol®, and sacrificed the mice 96 hours later. Once mice

were sacrificed, the cerebella were removed, and the brains were cut in half. One half of the brain was used for mRNA analysis, and the other half was used for protein analysis. The hippocampus was also removed from each brain hemisphere and treated separately, in order to assess region-specific changes. Once the mRNA was isolated, qPCR was performed to see if KU-32 administration increased transcriptional levels of Hsp70. The results indicated that KU-32 did not increase expression of Hsp70 in the hippocampus or the remaining brain tissues 96 hours post KU-32 treatment in comparison to vehicle treated tissue (Figure 4.4).

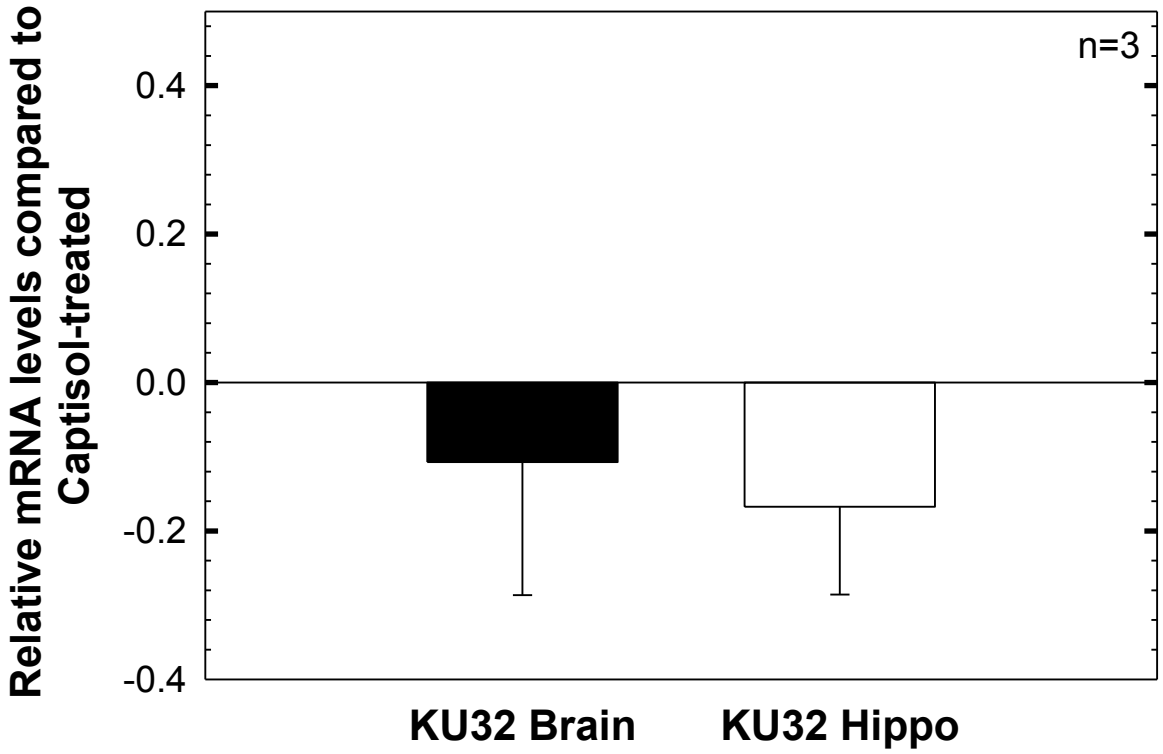

Figure 4.4: Hsp70 mRNA levels do not change with KU-32 treatment. Mice were treated one time with 20 mg/kg KU-32 and 5% Captisol®. Ninety-six hours post-treatment RNA from treated mouse brains and hippocampi were analyzed for Hsp70 expression. RNA levels were normalized to Enolase2 and graphed as relative mRNA expression compared to 5% Captisol®. Three mice were used per treatment group.

Student's *t* test demonstrated no statistically significant changes between KU-32 and 5% Captisol treated tissues.

As we did not detect changes in the mRNA levels of Hsp70, we determined if Hsp70 protein levels might be increased as the mRNA levels may have rapidly decreased, but the protein might be elevated for a longer time. Homogenates of the hippocampus and remaining brain were centrifuged to separate the cytosolic and nuclear fractions. These fractions were evaluated for levels of Hsp70 protein using Western blotting. Actin was used as a loading control. As shown in Figure 4.5, the Hsp70 levels did not change either in the cytosolic or nuclear fractions from the hippocampus or brain homogenates of KU-32-treated mice. Overall, these results indicate that KU-32 does not change expression or protein levels of Hsp70, and that KU-32 does not stimulate the heat shock response at 96 hours post treatment.

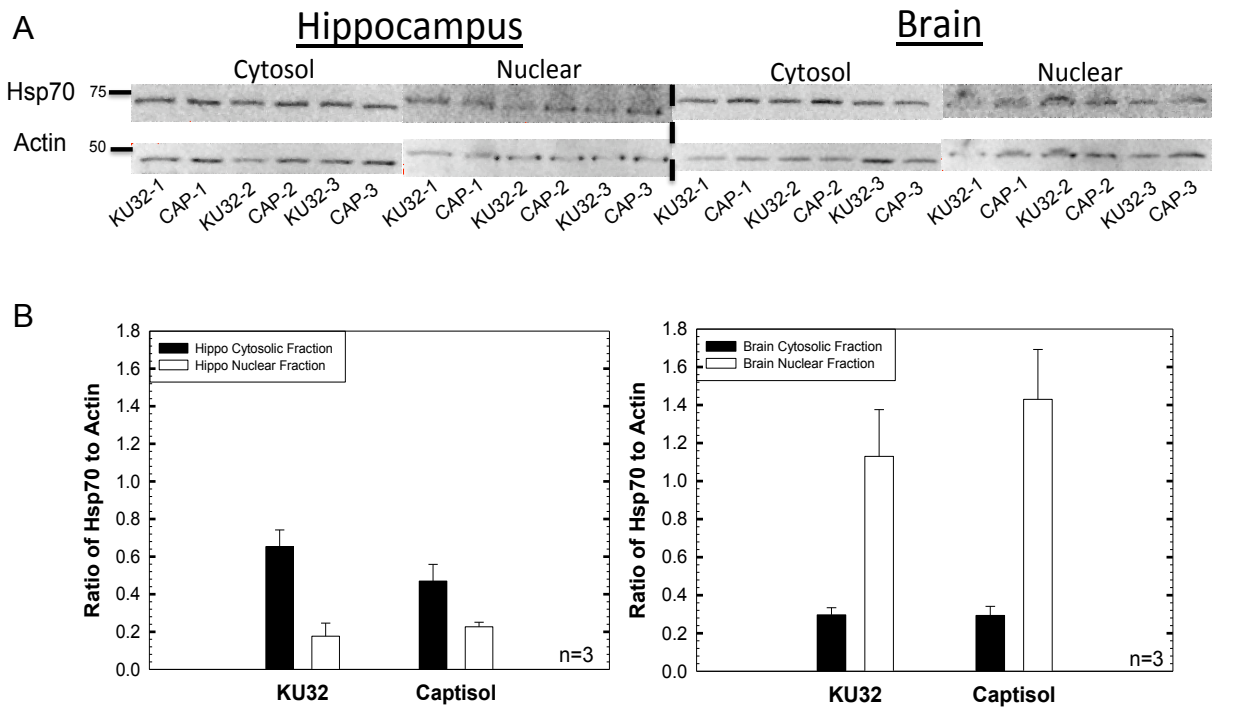

Figure 4.5: Hsp70 protein levels after 96 hours of KU-32 treatment. Three mice per group were treated with 20 mg/kg of KU-32 or 5% Captisol. (A) Cytosolic and nuclear fractions were separated from brain and hippocampal tissue and analyzed by Western blotting. Representative immunoblots of Hsp70 and Actin (the loading control) labeling from cytosolic and nuclear fractions of hippocampus and brain tissue. (B) Densitometric analyses of the immunoblots were completed using Actin as the loading control, and were graphed as ratio of Hsp70 to Actin labeling. The black bars represent the cytosolic fraction, and the white bars represent the nuclear fraction. The graph on the left is data from hippocampal tissue, and the graph on the right shows results from brain tissue. Student's *t* tests were performed and demonstrated no statistically significant changes in Hsp70 levels.

KU-32 increased Hsp70 labeling in the somatosensory region of the cortex

Although there were no changes in Hsp70 levels observed at 96 hours post-KU-32 treatment, we were interested in determining if the changes in protein levels were occurring earlier or later than 96 hours. Therefore, we treated 129S6 mice with an *i.p.* injection of 20 mg/kg KU-32 or 5% Captisol one time, and sacrificed mice at 6 hours, 2 days, 3 days, 4 days, and 7 days post injection. Since we did not detect differences in protein levels with immunoblotting and qPCR, we examined Hsp70 levels using

immunohistochemical techniques. This experimental procedure would allow us to observe changes in Hsp70 protein levels in all areas of the brain. Quite unexpectedly, we observed that KU-32 significantly increased Hsp70 labeling in the somatosensory region of the frontal cortex (Figure 4.6A). Peak Hsp70 levels were achieved by day 2, and Hsp70 returned to basal levels by day 3, as demonstrated by the quantitative analysis in figure 4.6B. These results indicate that KU-32 can increase Hsp70 levels *in vivo*, and that these increases appear to be region specific.

A

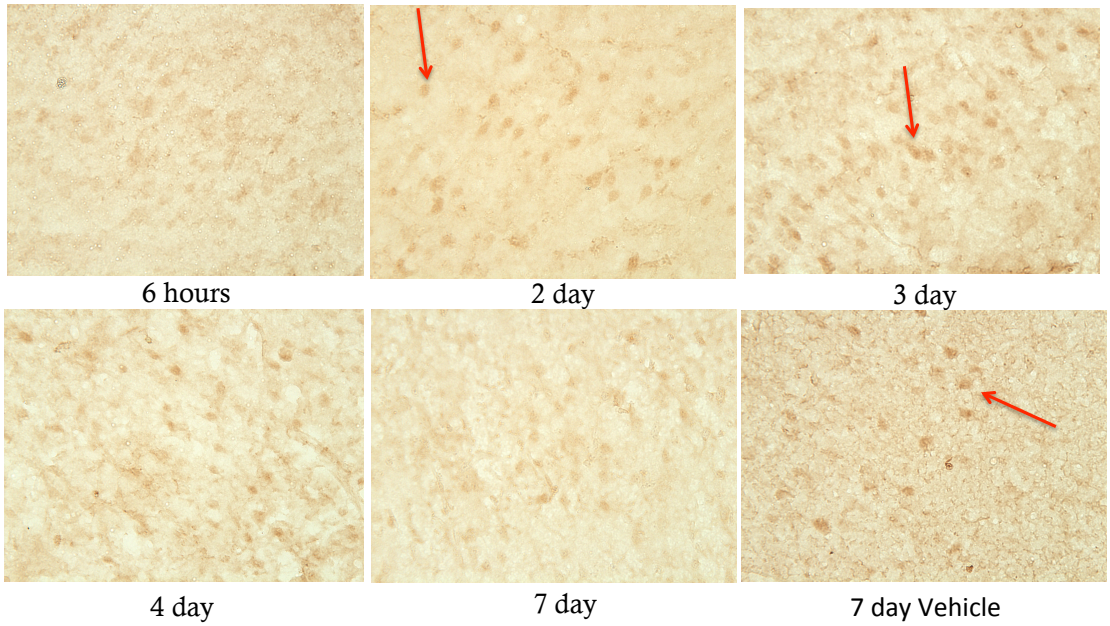

B

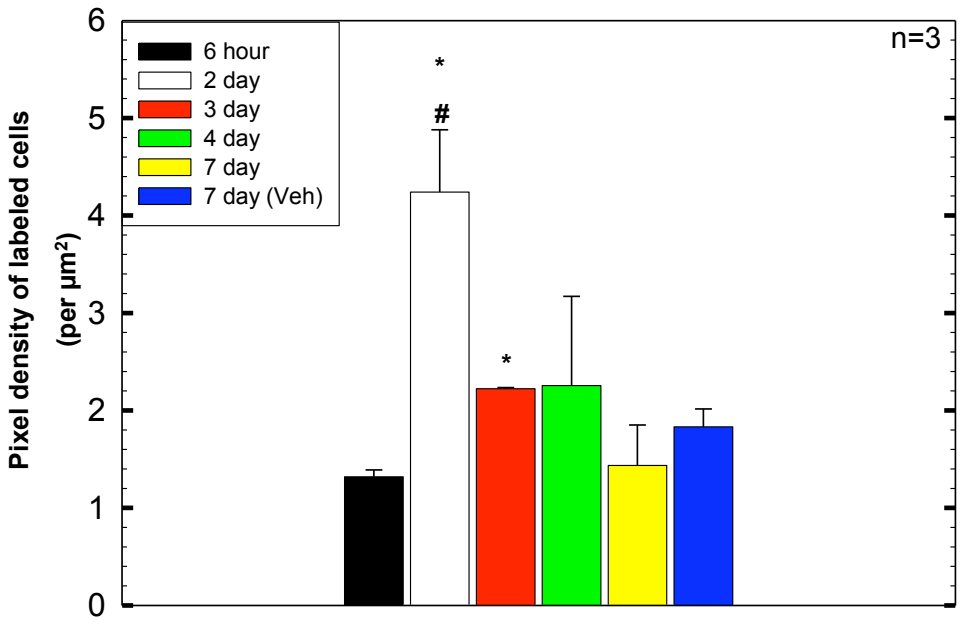

Figure 4.6: Effect of KU-32 treatment on Hsp70 levels in the somatosensory cortex. (A) Representative images from the somatosensory region of Hsp70 labeled mouse brains treated intraperitoneally with 20 mg/kg of KU-32 or 5% Captisol® starting at 6 hours for up to 7 days. The red arrow indicates positive Hsp70 labeling. (B) Quantification of three different mice per treatment day were analyzed and graphed. Statistical analysis was determined using Student's *t* test to compare each of the time points to each other. Statistical significance is indicated on the graph. * $p<0.05$ vs. 6 hour treatment, and # $p=0.04$ vs. 7 day vehicle.

Protein levels of co-chaperones, BAG1 and BAG2, after KU-32 administration

Co-chaperone interaction with Hsp70 is important, as this interaction directs the outcome of the client protein bound to Hsp70. The fate of the client protein will depend on which co-chaperone is bound to Hsp70 (Kampinga and Craig, 2010). Since region and time specific increases were described with Hsp70 upon KU-32 administration, we set out to determine if two well-described Hsp70 co-chaperones, BAG1 or BAG2, were changed with KU-32 administration at the same time and in the same region. 129S6 mice were treated once with an *i.p.* injection of 20 mg/kg of KU32 or 5% Captisol®. The mice were sacrificed 6 hours, 2 days, 3 days, 4 day, and 7 days post treatment, and the brains were prepared for immunohistochemical labeling. Antibodies against the co-chaperones, BAG1 and BAG2, were used to determine if KU-32 administration changed the protein levels of these Hsp70 binding partners. The results from the BAG1 labeling indicate that KU-32 treated mice trended toward an increase in the protein levels in the somatosensory cortex by day 2, and that this was sustained until day 7 (Figure 4.7). It is important to note that these differences were not statistically significant. BAG2 labeling results demonstrated increases in the protein by day 2 that was maintained until day 4 (Figure 4.8). These results suggest that as levels of Hsp70 increase, so do levels of these co-chaperones, indicating a potential mechanism for neuroprotection.

A

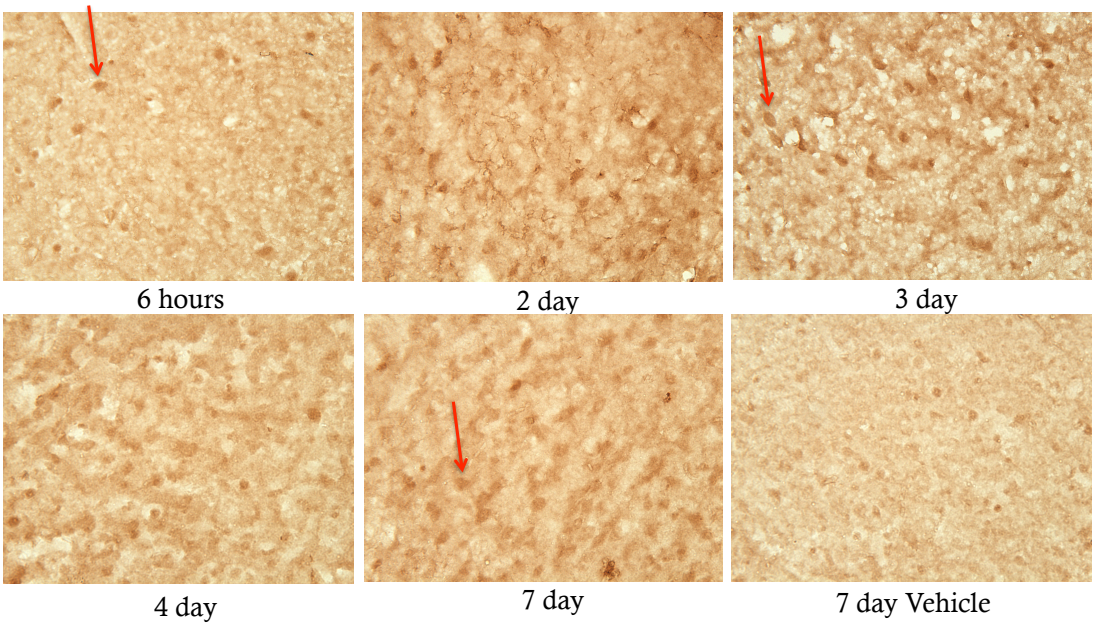

B

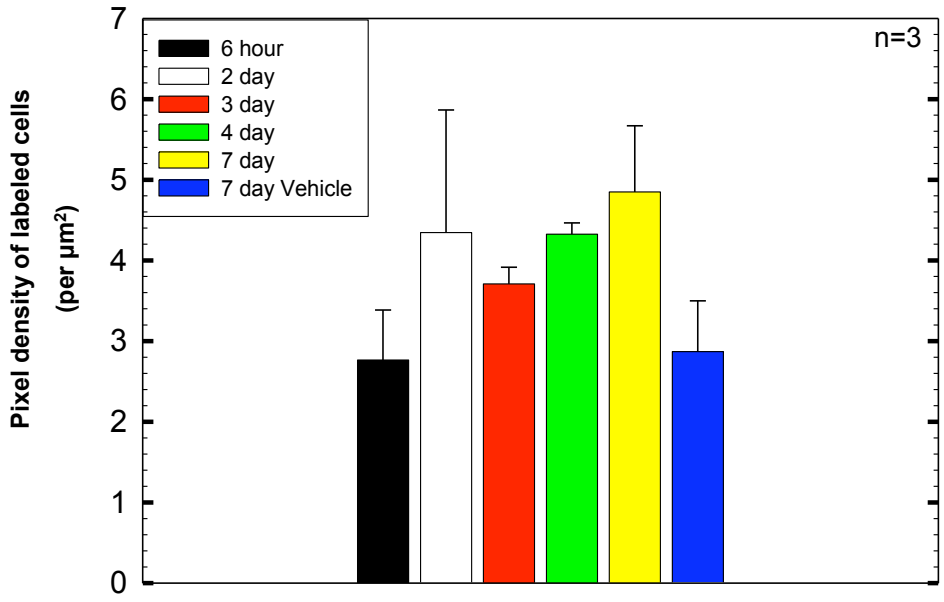

Figure 4.7: BAG1 levels following KU-32 treatment. (A) Representative images from the somatosensory region of BAG1 labeled brains from mice treated with 20 mg/kg of KU-32 or 5% Captisol® starting at 6 hours for up to 7 days. The red arrow indicates positive BAG1 labeling. (B) Quantification of three different mice per treatment day were analyzed and graphed. Statistical analysis was completed using Student's *t* test to compare each of the time points to each other. No statistical differences were observed.

A

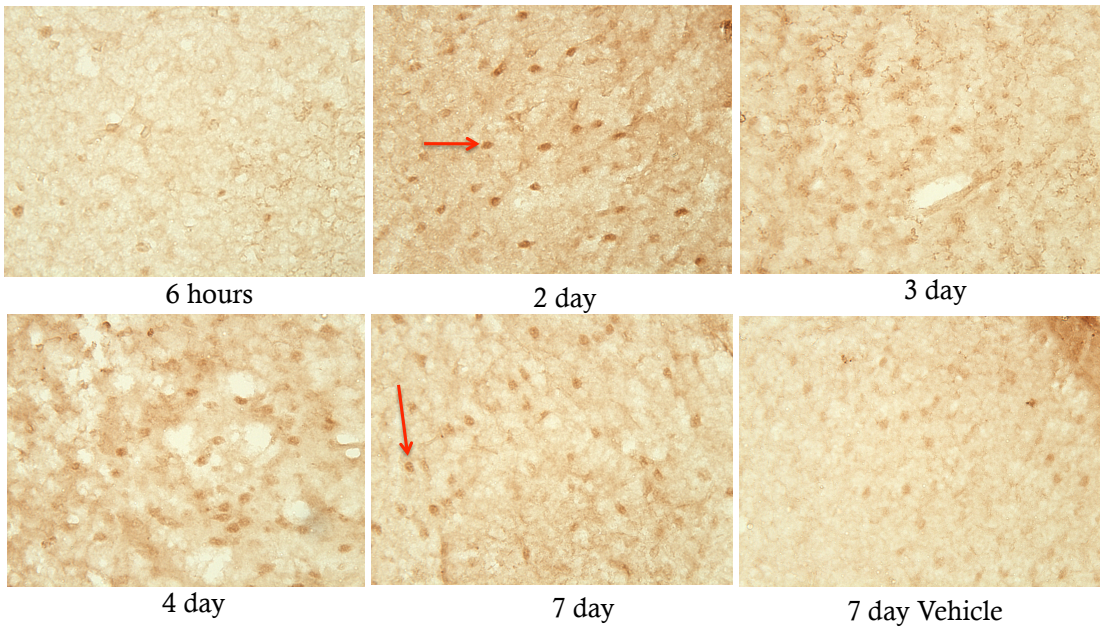

B

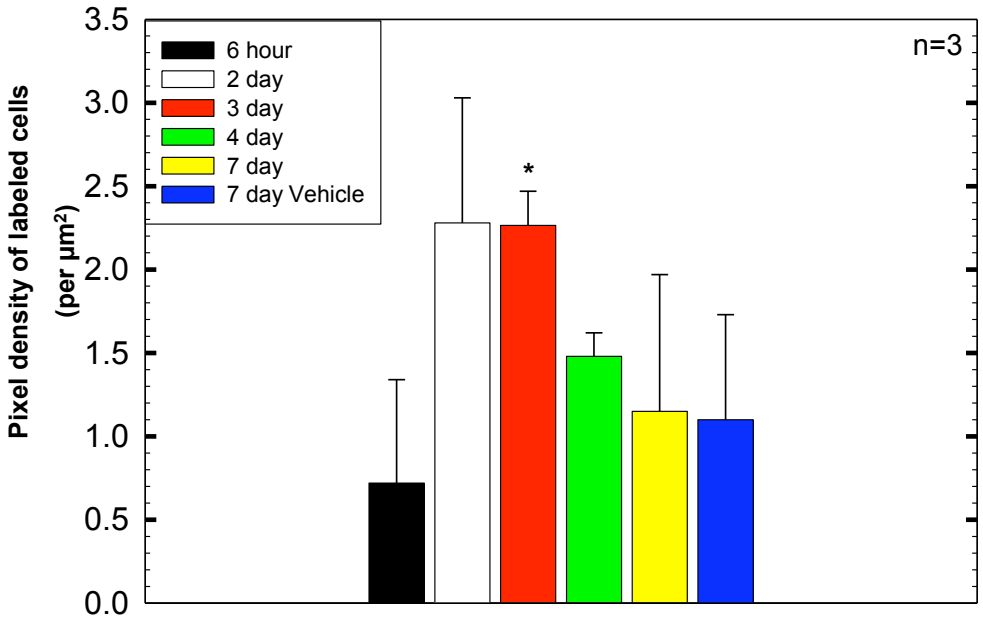

Figure 4.8: BAG2 levels in the somatosensory cortex upon KU-32 administration. (A) Representative images from the somatosensory region of BAG2 labeled mouse brains treated with 20 mg/kg of KU-32 or 5% Captisol® starting at 6 hours for up to 7 days. The red arrow indicates positive BAG2 labeling. (B) Quantification of three different mice per treatment day were analyzed and graphed. Statistical analysis was determined using Student's *t* test to compare each of the time points to each other. Statistical significance is indicated on the graph. * $p<0.027$ vs. 6 hour treatment.

Effects of KU-32 on HSF-1 levels

As previously described, when the heat shock response is activated the transcription factor HSF-1 is trimerized and translocated to the nucleus where it increases transcription of molecular chaperones. We did not observe any changes in Hsp70 levels with immunoblotting techniques; however, it is possible there are increases in other molecular chaperones involved in the heat shock response. As there are various molecular chaperones involved in the heat shock response, we were interested in assessing activation of the heat shock response by looking for changes in the transcriptional factor HSF-1 after administration of KU-32. FVB mice were treated one time with 20 mg/kg of KU-32 or 5% Captisol® and sacrificed 96 hours after treatment. The brains were excised from the mice, the cerebella were removed, and the hippocampus was dissected from the remaining brain tissue. The tissues were homogenized and subjected to centrifugation to separate the cytosol from the nuclear material. These fractions were evaluated using Western blotting. As shown in Figure 4.9, KU-32 did not change levels or location of HSF-1 in the hippocampal or the remaining brain tissue. There was no detectable KU-32 mediated translocation of HSF-1 to the nuclei, although HSF-1 was present in the nuclear fraction. These data further suggest that KU-32 is not acting through a mechanism similar to N-terminal Hsp90 ATPase inhibitors, and does not stimulate translocation of the transcription factor, HSF-1. However, it should be noted that we did not check to see if GA mediated

translocation of HSF-1.

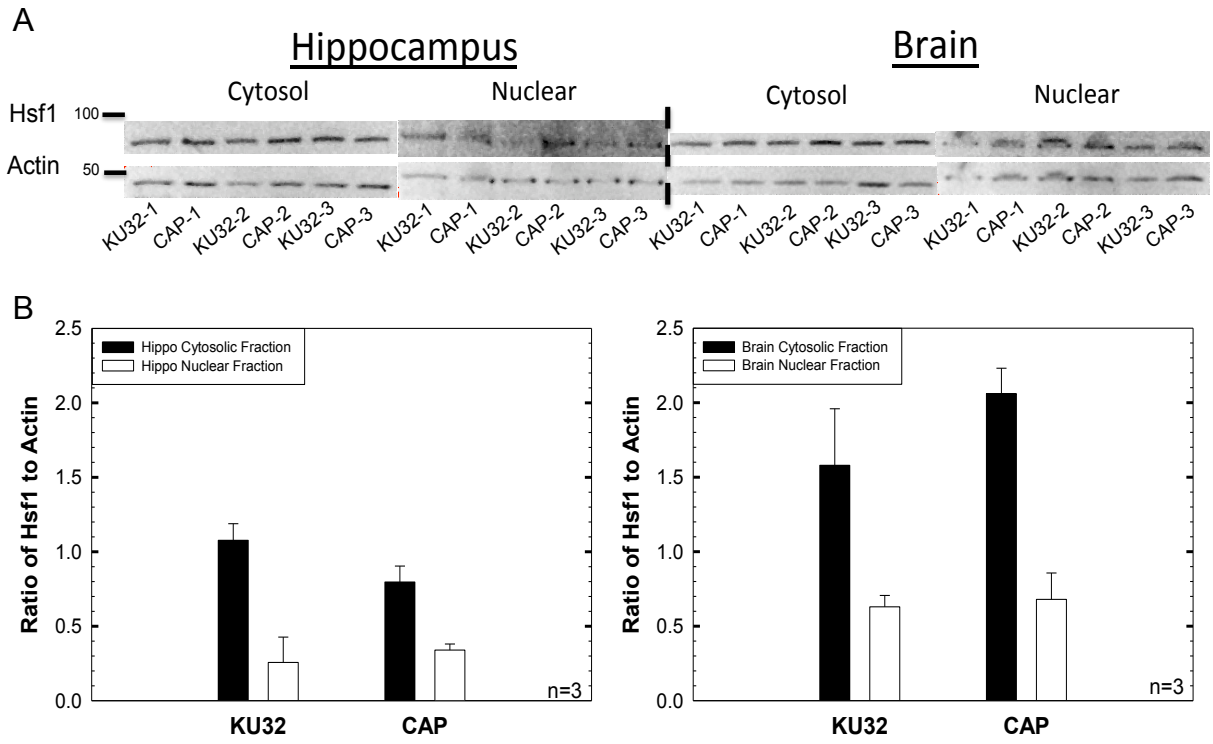

Figure 4.9: KU-32 effects on HSF-1 levels in the nuclear or cytosolic fraction of brain or hippocampal tissue. Three mice per group were treated with 20 mg/kg of KU-32 or 5% Captisol®. (A) Cytosolic and nuclear fractions were separated from brain and hippocampal tissue then analyzed by Western blotting. Representative immunoblots of HSF-1 and Actin (the loading control) labeling from cytosolic and nuclear fractions of hippocampus and brain tissue. (B) Densitometric analyses of the immunoblots were completed using Actin as the loading control, and were graphed as ratio of HSF-1 to Actin labeling. The black bars represent the cytosolic fraction, and the white bars represent the nuclear fraction. The graph on the left is data from hippocampal tissue, and the graph on the right is results from brain tissue. Student's *t* tests were performed and demonstrate no statistically significant changes in HSF-1 levels.

HSF-1 trimerization with KU-32 treatment up to 48 hours

While changes in the protein levels and location of HSF-1 did not change upon KU-32 administration, we set out to determine if KU-32 stimulated detectable trimerization of HSF-1. In order to look at trimerization and translocation of HSF-1 following KU-32 exposure, we treated FVB mice one-time with 20 mg/kg of KU-32 or 5%

Captisol®. Six, 12, 24, and 48 hours post-treatment we sacrificed the mice, extracted the brains, and removed the cerebella. Centrifugation was performed to separate the cytosolic and nuclear fractions. Native Blue gels were used to maintain the intrinsic conformation of the protein complexes, and HSF-1 antibodies were used to visualize the bands after separation. These results revealed that KU-32 did not stimulate trimerization of HSF-1 up to 48 hours post KU-32 administration. In its monomeric form, HSF-1 is about 85 kDa, and the trimeric form is about 270 kDa. As to be expected, the nuclear fraction demonstrates more HSF-1 trimer formation in comparison to the cytosolic HSF-1; however, KU-32 administration does not stimulate an increase in the multimeric formation of HSF-1 in the nucleus or the cytosol. These results suggest that KU-32 administration does not increase translocation or trimerization of HSF-1. Interestingly, we did not expect to observe trimerization of HSF-1 in the no treatment animals, as there was no stimulation applied to the animals to activate the heat shock response. Our controls using no treatment and GA-treated primary cortical lysates demonstrate that HSF-1 was not trimerized with no treatment ,but GA robustly increased the trimerization of the protein. As of now, there are no reports available investigating *in vivo* trimerization of HSF-1. It appears from our studies that there is a basal level of HSF-1 trimerization that occurs *in vivo*, indicating difficulty in studying multimer formation of HSF-1 in animal models.

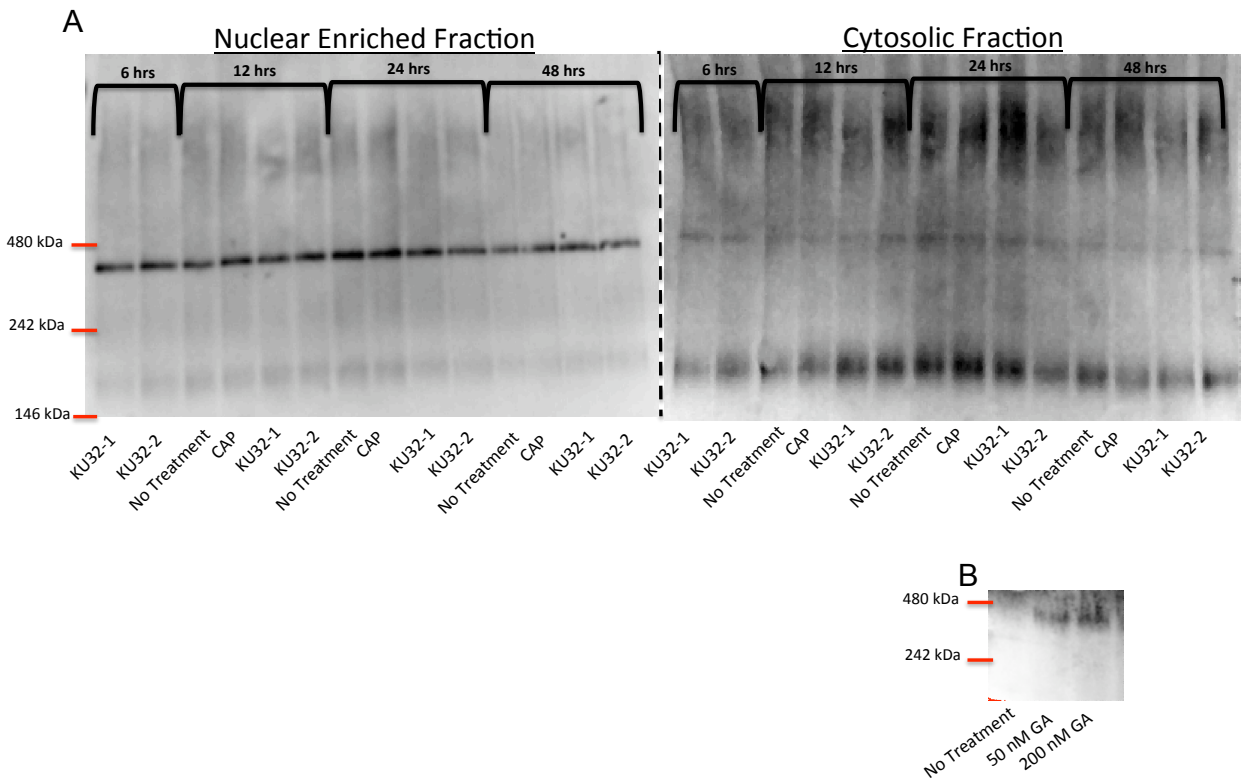

Figure 4.10: KU-32 effects on multimer formation of HSF-1. (A) Mice were given one injection of 20 mg/kg of KU-32 or 5% Captisol®. At 6, 12, 24 and 48 hours following the treatment, the mice were sacrificed. Cytosolic and nuclear fractions from each time point were separated by NativePage gel electrophoresis, and analyzed by Western blotting with HSF-1 antibodies. HSF-1 is about 85 kDa as a monomer. KU-32 treatment did not increase HSF-1 trimerization above the 5% Captisol® or the no treatment condition. (B) Non-treated and GA treated lysates were separated by NativePage and served as the negative and positive controls. The no treatment condition in lysates showed no trimerization, while the positive control, GA, demonstrated trimeric HSF-1.

IV. Discussion

The studies presented in this chapter were completed to determine if KU-32 was acting through a mechanism similar to N-terminal Hsp90 inhibitors. As mentioned earlier, Hsp90 inhibitors directed at the N-terminus lead to dose dependent decreases in p35 and cdk5 activity (Dou et al., 2003) as well as stimulate the heat shock response by increasing levels of molecular chaperones i.e. Hsp70 (Luo et al., 2007). Based on

these previous reports, we undertook to determine if our novel C-terminal Hsp90 inhibitor, KU-32, was acting through a mechanism similar to that known for the N-terminal ATPase Hsp90 inhibitors.

We first tested primary cortical neurons treated with KU-32 and the well-known N-terminal Hsp90 inhibitor, GA. Using this technique, we wanted to determine if the KU-32-mediated decreases in hyperphosphorylated Tau we observed *in vivo* (Chapter 3) were accompanied by decreases in the cdk5 regulatory fragment, p35. It has been demonstrated by Greengard and colleagues that an analog of the N-terminal Hsp90 inhibitor, GA, dose dependently decreased p35 levels and concurrently decreased cdk5 activity (Dou et al., 2003). Unlike the results reported by Greengard, our immunoblot studies showed that no changes in p35 levels (Figure 4.1). Although we did not see decreases in p35 levels, we attempted to measure cdk5 activity to determine if KU-32 directly decreased activity of the kinase as this would lead to decreases in hyperphosphorylated Tau. The experimental results obtained from the cdk5 assay showed no significant changes in cdk5 activity upon KU-32 administration. However, since the cdk5 inhibitor, Roscovitine, did not decrease the activity we were measuring our results cannot directly address the question of the effects of KU-32 administration on the activity of this kinase. Previous work from our lab has demonstrated robust increases in cdk5 activity with the addition of Aβ peptides (Seyb et al., 2007). Unfortunately, similar results with cdk5 activity were not obtained our recent rat cultures. This could be attributed to the differences in experimenters performing the procedure.

Although we did not observe changes with cdk5, there are multiple kinases that phosphorylate Tau and lead to fibril formation. Enzymes such as GSK3β

phosphorylates many of the similar sites on Tau that cdk5 phosphorylates (Wang et al., 1998, Anderton et al., 2001). Therefore, the *in vivo* decreases in Tau hyperphosphorylation may be mediated by GSK3β. Other kinases like MAPK, MARK, or CaMKII could also be responsible for the changes (Pei et al., 2003, Iqbal et al., 2005).

On the other hand, the decreases in phospho-Tau could be mediated by increased phosphatase activity. The activities of protein phosphatase 1 and 2A are decreased in AD brain and could decrease accumulation of hyperphosphorylated Tau (Gong et al., 1995). Perhaps KU-32 is stimulating the activity of one or more of the phosphatases and thereby leading to increased removal of phosphate from Tau.

A second pathway we investigated as a potential mechanism for KU-32 effects *in vivo*, was stimulation of the heat shock response. We used Western blotting to assess Hsp70 levels in primary cortical neurons treated with varying concentrations of KU-32 and the positive control, GA. A representative immunoblot (Figure 4.3) of the Hsp70 treatments demonstrated that KU-32 did not increase Hsp70 protein levels even at concentrations up to 10 μM, while the positive control GA, robustly increased Hsp70 levels above those in non-treated cells. Conversely, previous reports regarding KU-32 demonstrate dose-dependent increases in Hsp70 levels in cells and sciatic nerve (Urban et al., 2010). However, the Hsp70 protein level assessment results by Urban and colleagues were performed in MCF7 cells, while our experiments were performed in primary rat cortical neurons. Overall, these reports may indicate that KU-32 dependent increases in Hsp70 are cell-type specific.

Since we did not observe changes of Hsp70 *in vitro* we set out to determine if different phenomena would be observed *in vivo*. Therefore, we treated mice with KU-32 one time for 96 hours and measured mRNA and protein levels of Hsp70. Our results revealed, once again, that KU-32 did not increase Hsp70 mRNA or protein levels up to 96 hours in mice.

As we only looked at one time point for the *in vivo* assessment of Hsp70 expression and protein levels, we decided to use immunohistochemistry to look for changes in Hsp70 over time as well as to examine whether changes in Hsp70 were region-specific. We administered 20 mg/kg of KU-32 one time, and sacrificed mice at 6 hours, 2, 3, 4, and 7 days post-injection. Immunohistochemical results show that Hsp70 levels were significantly increased on day 2, specifically in the somatosensory cortex of the brain. These results indicate that in the previous experiment, we may have waited too long as Hsp70 levels were measured at 96 hours. The morphometric analyses from the 6 hour to 7 day time treatment studies demonstrated Hsp70 levels were increased at day 2, and then decreased to levels similar to vehicle by day 4. The immunohistochemical results showed that increases in Hsp70 levels are region specific, and these changes in a small region of the brain may have been overshadowed in the immunoblots using whole brain homogenates assessing Hsp70 levels 96 hours post KU-32 injection. This region-focused increase of Hsp70 may be more beneficial for AD treatment, as individuals with AD develop protein aggregates in specific brain regions such as the hippocampus (Selkoe 2001). Therefore, providing a therapeutic to stimulate proper cellular function in areas of the brain that are primarily affected by the aggregated proteins, may prove to be a better alternative.

Since the molecular chaperone machinery has many different players, we decided to look at changes in co-chaperones of the BAG family that have demonstrated promising interactions with Hsp70 and abnormal Tau protein (Takayama et al., 1999, Carrettiero et al., 2009). Immunohistochemical labeling of the somatosensory cortex of the KU-32 treated mouse brains demonstrated that BAG2 levels are significantly increased by day 3, while BAG1 results revealed no significant changes. These results provide a potential mechanism for how KU-32 is acting in this region of the brain. As BAG2 plays a role in Hsp70 mediated ubiquitin-independent degradation of abnormal Tau through the proteasome (Carrettiero et al., 2009), it is possible KU-32 may be mediating increases in processes that efficiently remove proteins from the cell through degradation. Further studies examining ubiquitinated and non-ubiquitinated proteins and proteasomal activity in this brain region might address how these protein increases are improving cellular function.

The heat shock response is controlled by the transcription factor, HSF-1 (Bagatell et al., 2000). Since we did not observe changes in Hsp70 like those observed with N-terminal ATPase Hsp90 inhibitors, we thought that perhaps the protein levels of other heat shock proteins were being changed with KU-32 administration. Instead of focusing on all of the potential heat shock proteins that may have increased, we decided to look upstream in the pathway at HSF-1.

First, we wanted to determine if KU-32 was prompting the translocation of HSF-1. The up-regulation of the proteins involved in the heat shock response requires binding of HSF-1 to promoter sequences in the nucleus (Cotto et al., 1996). So one of the first steps involved in the heat shock response is translocation of HSF-1. Using

immunoblots of brain samples from mice treated for 96 hours with 20 mg/kg of KU-32 or 5% Captisol, we looked at levels of HSF-1 in cytosolic and nuclear fractions. There were no indications that HSF-1 was translocated to the nucleus at 96 hours after KU-32 administration.

The second aspect of HSF-1 we wanted to investigate were changes in multimer formation of the protein. Before HSF-1 translocates to the nucleus in the heat shock response pathway, it is phosphorylated and trimerizes (Bagatell et al., 2000). Therefore, we decided to move further upstream and determine if KU-32 was inducing trimerization of HSF-1. Surprisingly, results demonstrate that brains of mice treated with KU-32, 5% Captisol, or no treatment have trimeric HSF-1 present in the nucleus and cytosol in the absence of any stimulus. As expected, the nuclear fraction had more prominent HSF-1 bands than the cytosolic fraction; however, we did not expect the non-treated brain homogenates to have trimerized HSF-1. Our immunoblot showing the controls with non-treated and GA-treated primary cortical lysates show that trimerization only occurred with GA treatment and not in the absence of treatment. To the best of our knowledge, most groups do not investigate HSF-1 trimerization *in vivo*. Therefore, it is possible that there is a basal level of HSF-1 trimerization occurring to maintain activation of molecular chaperones that has not yet been published in the literature.

Overall, our results demonstrate that KU-32 appears to act through a different mechanism than the N-terminal Hsp90 inhibitors such as GA. We did observe some region specific increases in Hsp70 and BAG2 with KU-32 treatment; however, other experiments revealed no changes in HSF-1 translocation and trimerization suggesting that KU-32 does not activate the heat shock response in the expected way. We also did

not observe changes in the cdk5 regulatory fragment p35 or cdk5 activity upon KU-32 administration. Previous reports using KU-32 demonstrate the therapeutic benefit of KU-32 in diabetic peripheral neuropathy (Urban et al., 2010) as well as in neuronal protection in AD (Chapter 2 of this dissertation; unpublished results). Even though KU-32 does not follow the same pathway as the N-terminal Hsp90 inhibitors, there is still promise for this drug as a therapeutic target. Unfortunately, the mechanism of KU-32 protection is still unknown, and will need further investigation.

V. References

Anderton B, Betts J, Blackstock W, Brion J, Chapman S, Connell J, Dayanandan R, Gallo J, Gibb G, Hanger D, Hutton M, Kardalinou E, Leroy K, Lovestone S, Mack T, Reynolds C, Van Slegtenhorst M (2001) Sites of phosphorylation in Tau and factors affecting their regulation. Biochemical Society Symposia 73-80.

Bagatell R, Paine M, G, Taylor C, Pulcini E, Akinaga S, Benjamin I, Whitesell L (2000) Induction of a heat shock factor 1-dependent stress reponse alters the cytotoxic activity of Hsp90-binding agents. Clinical Cancer Research 6:3312-3318.

Carrettiero D, Hernandez I, Neveu R, Papagiannakopoulos T, Kosik K (2009) The co-chaperone BAG2 sweeps paired helical filament-insoluble Tau from the microtubule. Journal of Neuroscience 29:2151-2161.

Cotto J, Kline M, Morimoto R (1996) Activation of heat shock factor 1 DNA binding precedes stress-induced serine phosphorylation. Journal of Biological Chemistry 271:3355-3358.

Demand J, Alberti S, Patterson C, Hohfeld J (2001) Cooperation of a ubiquitin domain protein and an E3 ligase during chaperone/proteasome coupling. Current Biology 11:1569-1577.

Dickey C, Dunmore J, Lu B, Wang J, Lee W, Kamal A, Burrows F, Eckman CB, Hutton M, Petrucelli L (2006) HSP induction mediates selective clearance of Tau phosphorylated at proline-directed Ser/Thr sites but not KXGS (MARK) sites. The FASEB Journal 20:753-755.

Dickey CA, Kamal A, Lundgren K, Klosak N, Bailey RM, Dunmore J, Ash P, Shoraka S, Zlatkovic J, Eckman CB, Patterson C, Dickson DW, Jr. NSN, Hutton M, Burrows F, Petrucelli L (2007) The high-affinity HSP90-CHIP complex recognizes and selectively degrades phosphorylated Tau client proteins. The Journal of Clinical Investigation 117:648-658.

Dou F, Netzer W, Tanemura K, Li F, Hartl U, Takashima A, Gouras G, Greengard P, Xu H (2003) Chaperones increase association of Tau protein with microtubules. Proceedings of the National Academy of Sciences 100:721-726.

Gamerdinger M, Carra S, Behl C (2011) Emerging roles of molecular chaperones and co-chaperones in selective autophagy: focus on BAG proteins. Journal of Molecular Medicine 89:1175-1182.

Gong C, Shaikh S, Wang J, Zaidi T, Grundke-Iqbal I, Iqbal K (1995) Phosphatase activity toward abnormally phosphorylated Tau: decrease in Alzheimer disease brain. Journal of Neurochemistry 65:732-738.

Hartl F, Hayer-Hartl M (2002) Molecular chaperones in the cytosol; from nascent chain to folded protein. Science 295:1852-1858.

Iqbal K, Alonso A, Chen S, Chohan M, El-Akkad E, Gong C, Khatoon S, Li B, Liu F, Rahman A, Tanimukai H, Grundke-Iqbal I (2005) Tau pathology in Alzheimer disease and other Tauopathies. Biochimica et Biophysica Acta 1739:198-210.

Kampinga H, Craig E (2010) The HSP70 chaperone machinery: J proteins as drivers of functional specificity. Nature Reviews Molecular Cell Biology 11:579-592.

Kushakawa G, Saito T, Onuki R, Ishiguro K, Kishimoto T, Hisanaga S (2000) Calpain-dependent proteolytic cleavage of the p35 cyclin-dependent kinase 5 activator to p25. Journal of Biological Chemistry 275:17166-17172.

Lee M, Kwon Y, Li M, Peng J, Friedlander R, Tsai L (2000) Neurotoxicity induces cleavage of p35-p25 by calpain. Nature 405:360-364.

Luders J, Demand J, Hohfeld J (2000) The ubiquitin-related BAG1 provides a link between molecular chaperones Hsc70/Hsp70 and the proteasome. The Journal of Biological Chemistry 275:4613-4617.

Lukiw WJ (2007) Micro-RNA speciation in fetal, adult and Alzheimer's disease hippocampus. Neuroreport 18:297-300.

Luo W, Dou F, Rodina A, Chip S, Joungnam K, Zhao Q, Moulick K, Aguirre J, Wu N, Greengard P, Chiosis G (2007) Roles of heat-shock protein 90 in maintaining and facilitating the neurodegenerative phenotype in Tauopathies. Proceedings of the National Academy of Sciences 104:9511-9516.

Luo W, Rodina A, Chiosis G (2008) Heat shock protein 90: translation from cancer to Alzheimer's disease treatment? BMC Neuroscience 9:S7.

Michaelis M, Ansar S, Chen Y, Reiff E, Seyb K, Himes R, Audus K, Georg G (2005) Beta-Amyloid-induced neurodegeneration and protection by structurally diverse

microtuble-stabilizing agents. Journal of Pharmacology and Experimental Therapeutics 312:659-668.

Michaelis M, Ranciat N, Chen Y, Bechtel M, Ragan R, Hepperle M, Liu Y, Georg G (1998) Protection against beta-amyloid toxicity in primary neurons by paclitaxel (Taxol). Journal of Neurochemistry 70:1623-1627.

Michaelis M, Walsh J, Pal R, Hurlbert M, Hoel G, Bland K, Foye J, Kwong W (1994) Immunologic localization and kinetic characterization of a Na+/Ca2+ exchanger in neuronal and non-neuronal cells. Brain Research 661:104-116.

Muchowski P (2002) Protein misfolding, amyloid formation, and neurodegeneration: a critical role for molecular chaperones? Neuron 35:9-12.

Muchowski P, Wacker J (2005) Modulation of neurodegeneration by molecular chaperones. Nature Reviews Neuroscience 6:11-22.

Nijtmans L, Henderson N, Holt I (2002) Blue Native electrophoresis to study mitochondrial and other protein complexes. Methods 26:327-334.

Pei J, Gong C, An W, Winblad B, Cowburn R, Grundke-Iqbal I, Iqbal K (2003) Okadaic-acid-induced inhibition of protein phosphatase 2A produces activation of mitogen-activated protien kinases ERK1/2, MEK1/2, and p70 S6, similar to that in Alzheimer's disease. American Journal of Pathology 163:845-858.

Selkoe D (2001) Alzheimer's disease: genes, proteins and therapy. Journal of Physiological Reviews, 81:741-766.

Seyb K, Ansar S, Li G, Bean J, Michaelis ML, Dobrowsky R (2007) p35/Cyclin-dependent kinase 5 is required for protection against beta-amyloid-induced cell

death but not Tau phosphorylation by ceramide. Journal of Molecular Neuroscience 31:23-35.

Sittler A, Lurz R, Lueder G, Priller J, Hayer-Hartl M, Hartl F, Lehrach H, Wanker E (2001) Geldanamycin activates a heat shock response and inhibits huntingtin aggregation in a cell culture model of Huntington's disease. Human Molecular Genetics 10:1307-1315.

Sonderman H, Scheufler C, Schneider C, Hohfeld J, Hartl F, Moarefi I (2001) Stucture of Bag/Hsc70 complex: convergent functional evolution of Hsp70 nucleotide exchange factors. Science 291:1552-1557.

Takahashi S, Ohshima T, Cho A, Sreenath T, Iadorola M, Pant H, Kim Y, Nairn A, Brady R, Greengard P, Kulkarni A (2005) Increased activity of cyclin-dependent kinase 5 leads to attenuation of cocaine-mediated dopamine signaling. Proceedings of the National Academy of Sciences 102:1737-1742.

Takayama S, Reed J (2001) Molecular chaperone targeting and regulation by BAG family proteins. Nature Cell Biology 3:E237-E241.

Takayama S, Xie Z, Reed JC (1999) An evolutionarily conserved family of Hsp70/Hsc70 molecular chaperone regulators. The Journal of Biological Chemistry 274:781-786.

Urban M, Li C, Yu C, Lu Y, Krise J, McIntosh M, Rajewski R, Blagg BS, Dobrowsky R (2010) Inhibiting heat-shock protien 90 reverses sensory hypoalgesia in diabetic mice. ASN Neuro 2:189-199.

Wang J, Wu Q, Smith A, Grundke-Iqbal I, Iqbal K (1998) Tau is phosphorylated by GSK-3 at several sites found in Alzheimer disease and its biological activity

markedly inhibitied only after it is prephosphorylated by A-kinase. FEBS Letters 436:28-34.

CHAPTER FIVE: Exploration of Potential Mechanisms of C-terminal Hsp90 Modulation using an Unbiased Approach

I. Introduction

The preceding chapters of this dissertation have demonstrated the neuroprotective properties of the novel C-terminal Hsp90 modulator, KU32 (Chapters 1 and 2; unpublished results); however, the mechanisms of KU-32 protection have yet to be fully elucidated. In order to assess what is happening with KU-32 administration, we wanted to use an unbiased approach to look at changes in multiple genes. One way to examine potential changes in the 39,000 genes in the mouse genome without prejudice is microarray analysis.

We treated mice with 20 mg/kg of KU-32 and vehicle (5% Captisol) to determine which changes in a multitude of genes upon drug administration. We discovered 731 different probe-sets with significant changes. Of the 731 genes that significantly changed, 293 probe-sets were up-regulated and 431 genes were down-regulated. In this final chapter, six genes that were significantly changed with KU-32 treatment will be discussed in their relation to maintaining the quality of cellular protein machinery. These findings may point the way for future studies.

II. Materials and Methods

Microarray Analysis using GeneChip

Four-month old SVJ129S6 mice were treated intraperitoneally with 20 mg/kg KU-32 or 5% Captisol®. Three mice were used per treatment group. All mice were

sacrificed four days following injection. Upon sacrificing, the hippocampi were removed and flash frozen in liquid N_2, then placed at -80°C. RNA was extracted using the RNeasy mini kit from Qiagen (Valencia, CA), and nucleic acid concentration was estimated with NanoDrop instrument. Total RNA (1 µg) was used for hybridization onto the Affymetrix Mouse Genome 430 2.0 GeneChip (Affymetrix, Santa Clara, CA), which contains probes for over 39,000 gene transcripts from the mouse genome. This process was carried out in the University of Kansas Genomics Facility by Dr. Xinkun Wang. The data were analyzed as described in a previous publication by Dr. Wang (Wang et al., 2010). Overall, statistical significance was based on a Bayesian *P* value ≤ 0.05, a fold change ≥ 1.3, and a false discovery rate (FDR) ≤ 1%.

III. Results

The microarray results demonstrated that 731 genes were significantly changed, exhibiting at least a 1.3-fold change. Of these significant changes 431 genes were down-regulated and 293 were up-regulated. A scatter plot (Figure 5.1) demonstrates the 731 probe-sets that significantly changed.

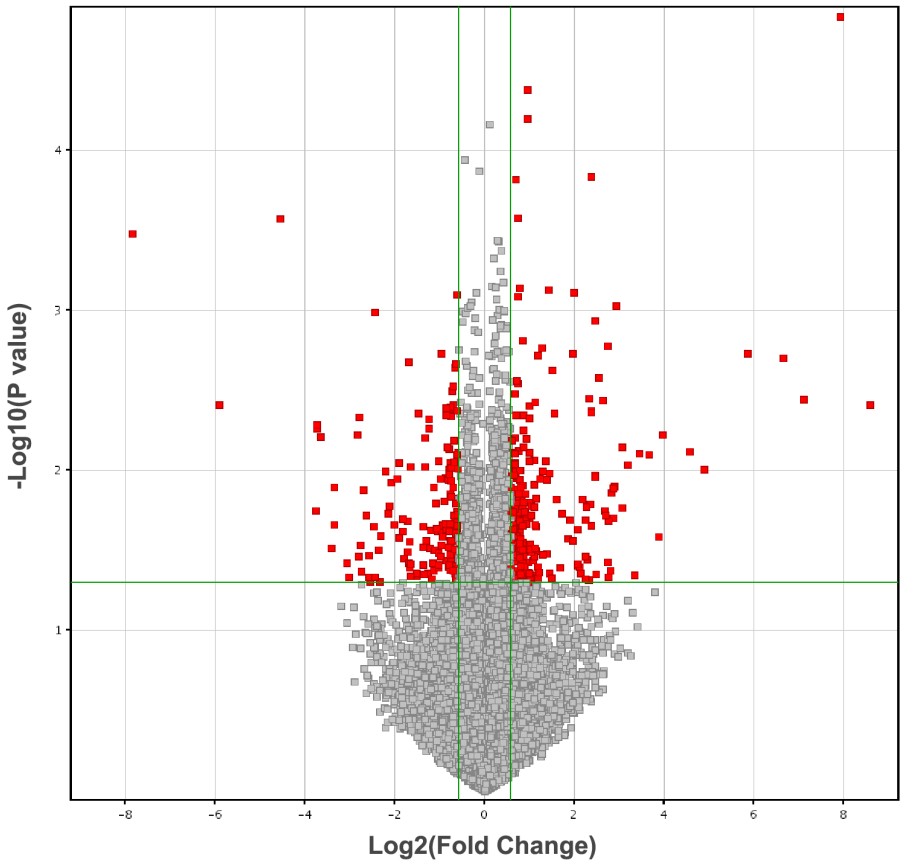

Figure 5.1: Identification of differentially expressed genes. The Mouse Genome 430 2.0 Affymetrix GeneChip was hybridized to RNA extracted from KU-32 and 5% Captisol®-treated 129S6 mice. Results from over 39,000 genes on the GeneChip demonstrate that 731 probe-sets were significantly changed (1.3-fold above or below 5% Captisol®-treated mice). The grey circles represent genes that did not significantly change, and the red circles are genes that significantly changed.

As a large number of genes were significantly changed with KU-32 administration, we analyzed the data to select genes primarily involved in cellular maintenance. These genes are outlined in Table 5.1. It should be noted that some genes that were significantly altered with KU-32 treatment are not well understood in terms of their gene ontology categories and their functions in cells. Therefore, we decided to investigate probe-sets that have been previously published in the literature. The genes found in Table 5.1 will be considered in detail in the discussion section.

Genes	Fold Change	Title	Function
Rhoh	13-fold down	Ras homolog gene family, member H, mRNA	GTPase
Dnajc13	1.75-fold down	Hsp40 protein	Endosomal trafficking
Mtap9	6.43-fold up	Microtubule-associated protein 9	Cell cycle maintenance
Nos1	4.75-fold up	Nitric oxide synthase 1	Synthesizes nitric oxide from L-arginine
Hdac10	2.00-fold up	Histone deacetylase 10	Deacetylates lysine residues on histones
Stub1	1.61-fold up	Carboxy terminus of Hsc70 interacting protein	E3 ligase and mediates degradation

Table 5.1: Genes involved in cellular maintenance with significant fold changes. The various genes selected that have significantly changed with KU-32 administration are outlined, as well as their fold change, gene name and protein function.

IV. Discussion

Rhoh

The hematopoietic-specific Rhoh protein is a Rho GTPase essential in T cell development (Dallery et al., 1995). Rhoh is a member of the RhoE/Rnd3 subfamily.

Members of this family remain in the constitutively active GTP-bound state and have no intrinsic GTPase activity (Aspenstrom et al., 2007). Rhoh has demonstrated inhibitory capabilities by negatively regulating other Rho GTPases i.e. Rac (Li et al., 2002). Overall, RhoH has major implications in the T cell maturation and T cell receptor signaling (Gu et al., 2006, Chae et al., 2010).

Dnajc13

The Dnajc13 gene codes for a Hsp40, J-domain protein in mammals called receptor-mediated endocytosis-8 (RME-8) (Zhang et al., 2001). RME-8 is broadly distributed in tissues with cellular localization on endosomal membranes (Girard et al., 2005). This J-domain-containing protein is a major binding partner of the constitutively active Hsp70 isoform, Hsc70, and RME-8 assists Hsc70 in endocytosis (Chang et al., 2004).

Mapt9

The Mapt9 gene codes for a microtubule associated protein call Aster-associated protein (ASAP) or MAP9 (Saffin et al., 2005). Mapt9 expression is most prominent in areas where microtubules are highly concentrated including the brain, particularly growing neurites (Venoux et al., 2008b). The MAP9 protein plays an essential role in the cell cycle, where it localizes to microtubules during interphase to assist mitotic spindles during mitosis (Saffin et al., 2005).

Interestingly, MAP9 is a substrate of Aurora-A, an oncogenic mitotic kinase. When MAP9 is phosphorylated, it is active to assist in mitosis; however, when Aurora-A

levels are decreased, MAP9 is targeted for degradation leading to defects in mitotic progression. Therefore, MAP9 is critical for proper mitosis, indicating a potential target for cancer therapies (Venoux et al., 2008a).

Also, as mentioned previously, MAP9 is highly concentrated in growing neurites. Although, neurons of the CNS are post-mitotic, it has been suggested that these cells need to have proper cell cycle regulation in order to avoid initiating an altered cell cycle state (Herrup and Yang, 2007). Loss of cell cycle control has been demonstrated in several neurodegenerative diseases, including AD (Yang and Herrup, 2007). Overall, these data suggest a potential role for MAP9 in keeping the cell cycle in check, particularly in aging neurons.

Nos1

The family of enzyme proteins called the nitric oxide synthases (NOSs) is responsible for the conversion of L-arginine to citrulline and forming nitric oxide through NADH mediated catalysis. It has been suggested that regulation of neuronal NOS (nNOS) occurs through Hsp90-based chaperone machinery. In the presence of an Hsp90 inhibitor, there is increased proteasomal degradation of nNOS (Bender et al., 1999). Further, it has been demonstrated that the E3 ligase, carboxy-terminus of Hsc70 interacting protein (CHIP) ubiquitinates nNOS through interactions with Hsp40 and Hsp70 (Peng et al., 2004).

Hdac10

Histone deacetylase-10 (HDAC10) belongs to the Class IIa family of HDACs with HDAC6. The proteins in this class differ from other HDACs in that they have two catalytic sites that deacetylate lysine residues on the N-terminal end of core histones (Dokmanovic et al., 2007). HDAC10 and HDAC6 are binding proteins of Hsp90, and play pivotal roles in proteasomal degradation of Hsp90 client proteins (Park et al., 2008). Recent evidence suggests that decreases in HDAC6 lead to clearance of abnormal Tau in a cellular model of AD (Cook et al., 2012).

Stub1

Stub1 is the gene that codes for the carboxy terminus of Hsc70-binding protein (CHIP). This protein has a tetratricopeptide repeat (TPR) domain that associates with Hsp70 protein (Ballinger et al., 1999) and a U-box domain that has E3, or ubiquitin-ligase activity. The E3 enzymes catalyze the third and final step of substrate recognition by the proteasome (Hatakeyama et al., 2004).

As discussed previously in the Introduction of this dissertation, CHIP has been implicated in the fate of protein aggregates in AD. CHIP interacts with Hsp70, Hsp90, and Tau, although its most prominent effect is observed through Hsp70 (Grelle et al., 2006). CHIP binding to Hsp70 abrogates the ATPase refolding activity of HSP70 (Ballinger et al., 1999). CHIP levels are elevated in human Alzheimer's disease tissue (Sahara et al., 2005), suggesting that CHIP plays a part in the formation of Tau tangles. This ubiquitin-ligase protein mediates ubiquitination of Tau and increases Tau

aggregation in AD, where proteasomal degradation is compromised (Petrucelli et al., 2004).

Many of the genes that were significantly changed in the microarray analysis upon KU-32 administration were unexpected. The only expected gene that was significantly up-regulated with KU-32 treatment was Stub1, or CHIP. Overall, the results from the microarray analysis demonstrate that there are a multitude of genes changing with KU-32 administration, leaving many avenues for future investigations.

V. References

Aspenstrom P, Ruusala A, Pacholsky D (2007) Taking Rho GTPases to the next level: the cellular functions of atypical Rho GTPases. Experimental Cellular Research 313:3673-3679.

Ballinger C, Connell P, Wu Y, Hu Z, Thompson L, Yin L, Patterson C (1999) Identification of CHIP, a novel tetratricopeptide repeat-containing protein that interacts with heat shock proteins and negatively regulates chaperone functions. Molecular and Cellular Biology 19:4535-4545.

Bender A, Silverstein A, Demandy D, Kanelakis K, Noguchi S, Pratt W, Osawa Y (1999) Neuronal nitric-oxide synthase is regulated by the Hsp90-based chaperone system in vivo. Journal of Biological Chemistry 274:1472-1478.

Chae H, Siefring J, Hildeman D, Gu Y, Williams D (2010) RhoH regulates subcellular localization of ZAP-70 and Lck in T cell receptor signaling. PLoS One 5:1-11.

Chang H, Hull M, Mellman I (2004) The J-domain protein Rme-8 interacts with Hsc70 to control clathrin-dependent endocytosis in Drosophila. Journal of Cellular Biology 164:1055-1064.

Cook C, Gendron T, Scheffel K, Carlomagno Y, Dunmore J, Denture M, Petrucelli L (2012) Loss of HDAC6, a novel CHIP substrate, alleviates abnormal Tau accumulation. Human Molecular Genetics Epub ahead of print.

Dallery E, Galiegue-Zouitina S, Collyn-d'Hooghe M, Quief S, Denis C, Hildebrand M, Lantoine D, Deweindt C, Tilly H, Bastard C (1995) TTF, a gene encoding a novel small G protein, fuses to the lymphoma-associated LAZ3 gene by t(3;4) chromosomal translocation. Oncogene 10:2171-2178.

Dokmanovic M, Clarke C, Marks P (2007) Histone deacetylase inhibitors: overview and perspective. Molecular Cancer Research 5:981-989.

Girard M, Poupon V, Blondeau F, McPherson P (2005) The DnaJ-domain protein RME-8 funtions in endosomal trafficking. Journal of Biological Chemistry 280:40135-40143.

Grelle G, Kostka S, Otto A, Kersten B, Genser K, Muller E, Walter S, Boddrich A, Stelzl U, Hanig C, Volker-Engert R, Landgraf C, Alberti S, Hohfeld J, Strodicke M, Wanker E (2006) Identification of VCP/p97, carboxyl terminus of Hsp70-interacting protein (CHIP), and amphiphysin II interaction partners using membrane-based human proteome arrays. Molecular and Cellular Proteomics 5:234-244.

Gu Y, Chae H, Siefring J, Jast I, Hildeman D, Williams D (2006) RhoH, a GTPase recruits and activates Zap70 required for T cell receptor signaling and thymocyte development. Nature Immunology 7:1182-1190.

Hatakeyama S, Matsumoto M, Kamura T, Murayama M, Chui D-H, Planel E, Takahashi R, Nakayama KI, Takashima A (2004) U-box protein carboxyl terminus of Hsc70-interacting protein (CHIP) mediates poly-ubiquitination preferentially on four-repeat Tau and is involved in neurodegeneration of Tauopathy. Journal of Neurochemistry 91:299-307.

Herrup K, Yang Y (2007) Cell cycle regulation in the postmitotic neurons: oxymoron or new biology? Nature Review Neuroscience 8:368-378.

Li X, Bu X, Lu B, Avraham H, Flavell R, Lim B (2002) The hematopoiesis-specific GTP-binding protein RhoH is GTPase deficient and modulates activities of other Rho GTPases by an inhibitory function. Molecular and Cellular Biology 22:1158-1171.

Park J, Kim S, Choi M, Lee J, Oh D, Im S, Bang Y, Kim T (2008) Class II histone deacetylases play pivotal roles in heat shock protein 90-mediated proteasomal degradation of vascular endothelial growth factor receptors. Biochemical and Biophysical Research Communications 368:318-322.

Peng H, Morishima Y, Jenkins G, Dunbar A, Lau M, Patterson C, Pratt W, Osawa Y (2004) Ubiquitylation of neuronal nitric-oxide synthase by CHIP, a chaperone-dependent E3 ligase. Journal of Biological Chemistry 279:52970-52977.

Petrucelli L, Dickson D, Kehoe K, Taylor J, Snyder H, Grover A, Lucia MD, McGowan E, Lewis J, Prihar G, Kim J, Dillmann WH, Browne SE, Hall A, Voellmy R, Tsuboi Y, Dawson TM, Wolozin B, Hardy J, Hutton M (2004) CHIP and Hsp70 regulate Tau

ubiquitintation, degradation, and aggregation. Human Molecular Genetics 13:703-714.

Saffin J, Venoux M, Prigent C, Espeut J, Poulat F, Giorgi D, Abrieu A, Rouquier S (2005) ASAP, a human microtubule-associated protein required for bipolar spindle assembly and cytokinesis. Proceedings of the American Association of Cancer Research 102:11302-11307.

Sahara N, Murayama M, Mizoroki T, Urushitani M, Imai Y, Takahashi R, Murata S, Tanaka K, Takashima A (2005) In vivo evidence of CHIP up-regulation attenuating Tau aggregation. Journal of Neurochemistry 94:1254-1263.

Venoux M, Basbous J, Berthenet C, Prigent C, Fernandez A, Lamb N, Rouquier S (2008a) ASAP is a novel substrate of the oncogenic mitotic kinase Aurora-A: phosphorylation on Ser625 is essential to spindle formation and mitosis. Human Molecular Genetics 17:215-224.

Venoux M, Delmouly K, Milhavet O, Vidal-Eychenie S, Giorgi D, Rouquier S (2008b) Gene organization, evolution and expression of the microtubule-associated protein ASAP (MAP9). BMC Genomics 9:1-22.

Wang X, Bao X, Pal R, Abdulbaki A, Michaelis E (2010) Transcriptomic responses in mouse brain exposed to chronic excess of the neurotransmitter glutamate. BMC Genomics 11:1-19.

Yang Y, Herrup K (2007) Cell division in the CNS: protective response or lethal events in post-mitotic neurons? Biochimica et Biophysica Acta 1772:457-466.

Zhang Y, Grant B, Hirsh D (2001) RME-8, a conserved J-domain protein, is required for endocytosis in *Caenorhabditis elegans*. Molecular and Cellular Biology 12:2011-2021.

Summary of the Protective Qualities of the Novel C-terminal Hsp90 Modulator, KU-32

The chapters in this dissertation have focused on the novel C-terminal Hsp90 modulator, KU-32. First, we demonstrated that KU-32 and other novobiocin analogs i.e. KU-426, KU-430, and KU-433 are significantly protective against various cellular toxins such as $A\beta_{1-42}$, $A\beta_{25-35}$, and Thapsigargin (Tg). KU-32 and KU-430 demonstrated similar protection in primary neuronal culture, where these were they only analogs tested that protected against $A\beta_{1-42}$, $A\beta_{25-35}$, Tg. When both KU-32 and KU-430 were used in the same experiment to test for protection against Aβ peptides, it was discovered that KU-32 provided better protection than KU-430.

After demonstrating significant protection of KU-32 in primary neuronal cultures, we decided to test the effects of KU-32 *in vivo*. We treated two AD mouse models containing P301L mutant Tau, the JNPL3 and the rTg4510 mice. In the JNPL3 mice, we showed that chronic KU-32 treatment significantly decreased CP-13 and AT8-labeled Tau in the premotor cortex. The more robust Tau pathology model, the rTg4510 mice, also demonstrated significant decreases in the CP-13 labeled Tau in the premotor cortical region. As the rTg4510 mouse model also demonstrated neurodegenerative qualities in the brain, we assessed the effect of KU-32 on three different markers of neuroprotection: synaptophysin for synaptic damage; MAP2 labeling for neuritic dystrophy; and NeuN for neuronal loss. Synaptophysin labeling demonstrated that KU-32 significantly protected against synaptic damage in the premotor cortex and hippocampus. MAP2 antibody labeling exhibited significant protection of KU-32 against

neuritic dystrophy in premotor cortical and hippocampal regions of the brain. KU-32 also significantly protected against neuronal loss, as measured by NeuN labeling in the premotor cortex and hippocampus. Overall, KU-32 demonstrated robust protection in cellular and animal models of AD.

The elucidation of potential mechanisms of KU-32 has been difficult. We demonstrated time and region specific statistically significant increases in the somatosensory cortex of Hsp70 and the co-chaperone, BAG2-labeled mouse brain sections. Unfortunately, when using lysate or brain homogenate we did not observe changes in Hsp70 or the transcription factor, HSF-1. These results suggest that in order to fully elucidate the mechanism of KU-32 neuroprotection, more experimental work needs to be completed.

Taken as a whole, the results presented in this dissertation demonstrate that KU-32 is consistently statistically neuroprotective in cellular and animal models of AD; however, the mechanism responsible for this neuroprotection is still unknown. Since this compound exhibits beneficial effects in multiple models, it warrants further investigation as a potential therapeutic agent for AD.